Advances in barycentric rational interpolation of a function and its derivatives

Doctoral Dissertation submitted to the
Faculty of Informatics of the Università della Svizzera Italiana
in partial fulfillment of the requirements for the degree of
Doctor of Philosophy

presented by
Emiliano Cirillo

under the supervision of
Kai Hormann

March 2019

Dissertation Committee

Kai Hormann	Università della Svizzera italiana, Lugano, Switzerland
Igor Pivkin	Università della Svizzera italiana, Lugano, Switzerland
Stefan Wolf	Università della Svizzera italiana, Lugano, Switzerland
Jean-Paul Berrut	Université de Fribourg, Switzerland
Stefano De Marchi	Università di Padova, Italy

Dissertation accepted on 15 March 2019

Research Advisor	PhD Program Director
Kai Hormann	**Walter Binder**

I certify that except where due acknowledgement has been given, the work presented in this thesis is that of the author alone; the work has not been submitted previously, in whole or in part, to qualify for any other academic award; and the content of the thesis is the result of work which has been carried out since the official commencement date of the approved research program.

Emiliano Cirillo
Lugano, 15 March 2019

...entre deux vérités du domaine réel, le chemin le plus facile et le plus court passe bien souvent par le domaine complexe.

[...between two truths of the real domain, the easiest and shortest path quite often passes through the complex domain.]

Paul Painlevé, 1900

Abstract

Linear barycentric rational interpolants are a particular kind of rational interpolants, defined by weights that are independent of the function f. Such interpolants have recently proved to be a viable alternative to more classical interpolation methods, such as global polynomial interpolants and splines, especially in the equispaced setting. Other kinds of interpolants might indeed suffer from the use of floating point arithmetic, while the particular form of barycentric rational interpolants guarantees that the interpolation of data is achieved even if rounding errors affect the computation of the weights, as long as they are non zero.

This dissertation is mainly concerned with the analysis of the convergence of a particular family of barycentric rational interpolants, the so-called Floater–Hormann family. Such functions are based on the blend of local polynomial interpolants of fixed degree d with rational blending functions, and we investigate their behavior in the interpolation of the derivatives of a function f.

In the first part we focus on the approximation of the k-th derivative of the function f with classical Floater–Hormann interpolants. We first introduce the Floater–Hormann interpolation scheme and present the main advantages and disadvantages of these functions compared to polynomial and classical rational interpolants. We then proceed by recalling some previous result regarding the convergence rate of the k-th derivatives of these interpolants and extend these results. In particular, we prove that the k-th derivative of the Floater–Hormann interpolant converges to $f^{(k)}$ at the rate of $O(h_j^{d+1-k})$, for any $k \geq 0$ and any set of well-spaced nodes, where h_j is the local mesh size.

In the second part we instead focus on the interpolation of the derivatives of a function up to some order m. We first present several theorems regarding this kind of interpolation, both for polynomials and barycentric rational functions, and then we introduce a new iterative approach that allows us to generalise the Floater–Hormann family to this new setting. The resulting rational Hermite interpolants have numerator and denominator of degree at most $(m+1)(n+1)-1$ and $(m+1)(n-d)$, respectively, and converge to the function at the

rate of $O(h^{(m+1)(d+1)})$ as the mesh size h converges to zero.

Next, we focus on the conditioning of the interpolants, presenting some classical results regarding polynomials and showing the reasons that make these functions unsuited to fit any kind of equispaced data. We then compare these results with the ones regarding Floater–Hormann interpolants at equispaced nodes, showing again the advantages of this interpolation scheme in this setting. Finally, we extend these conclusions to the Hermite setting, first introducing the generalisation of the results presented for polynomial Lagrange interpolants and then bounding the condition number of our Hermite interpolant at equispaced nodes by a constant independent of n. The comparison between this result and the equivalent for polynomials shows that our barycentric rational interpolants should be in many cases preferred to polynomials.

Acknowledgements

First of all, I would like to thank my advisor, Professor Kai Hormann, for his precious help and the priceless advice received during my PhD. His mentorship and care for the details were fundamental to transform the old master student that I was at the beginning of this journey into the young researcher that I am nowadays.

I would also say thank you to all the members of the committee, Professor Jean-Paul Berrut, Professor Stefano De Marchi, Professor Igor Pivkin and Professor Stefan Wolf, for reading and evaluating this rather long thesis. Without your availability, I would have never found a suitable date for this defense. It is all your merit if setting this date has been way less painful than I was told from my colleagues!

I would also like to express my gratitude to the Swiss National Science Foundation, for the support received during the first three years of my PhD and for allowing me to attend all the conferences I have been to during this period. This really helped me to get to know new researchers all over the world, a priceless experience in this career.

I could never thank enough my Master thesis advisor, Professor Francesco Dell'Accio, for passing on the passion for this work to me. I will never forget the long evenings discussing math and experiences, while tasting Russian vodka in his office.

I also want to thank my former colleagues, Elena and Dima, for creating a nice atmosphere in our otherwise isolated office. Without all the coffees and the chatting together, this would have been much harder. A special thanks goes to Teseo, for his priceless help when I was lost in the code and for involving me in many activities during free time. My first period in Lugano would have been completely different without him and his family.

Finally a special thanks goes to my family and especially my mother, for always encouraging me to pursue my own career, even in the darkest moments and even if this brought me far away from them.

Contents

List of Symbols

h	global mesh size 12
ℓ_i	Lagrange basis function 10
$g(x)$	general solution of the interpolation problem 9
f_i	data sample 9
b_i	barycentric basis function 19
β_i	general Lagrange barycentric weight 20
$\mathscr{P}_d$	space of polynomials of degree at most d 10
$\delta_{i,j}$	Kronecker's delta 10
$\ell(x)$	nodal polynomial 11
d	degree of the local polynomial interpolants in Floater–Hormann interpolation 26
I	index set, $\{0, 1, \ldots, n-d\}$ 26
I_j	index set, $\{i \in I \colon j - d \leq i \leq j\}$ 29
ω_i	barycentric weight Lagrange polynomial interpolant 12
w_j	Floater–Hormann barycentric weight 29
X	family of interpolation nodes 9
X_n	set of interpolation nodes 9
g_m	Hermite interpolant of order m 51
$\beta_{i,j}^{[m]}$	general Hermite barycentric weight of order m 59
$\omega_{i,j}^{[m]}$	barycentric weight Hermite polynomial interpolant of order m 55
L_n	Lagrange polynomial interpolation operator 97
$\lambda_n(x)$	Lebesgue function for Lagrange interpolation 98
Λ_n	Lagrange polynomial interpolation operator 98
$e(x)$	error function 9
p_m	Hermite polynomial interpolant of order m 52

e_m	error function Hermite interpolation 51
$\ell_{i,j}$	Hermite basis functions 52

Chapter 1

Introduction

1.1 Motivation

This thesis is mainly concerned with the interpolation of data, either defined as samples of a known function f or as a finite set of values $f_0, \ldots, f_n$. In the former case interpolation can simplify the evaluation of certain special functions, providing an approximation of f which can be evaluated in a finite number of arithmetic operations. The second case often arises in natural sciences, where the data are the result of experimental procedures and one wishes to approximate the underlying, unknown function. In both cases it is important to be able to approximate the function with arbitrary accuracy, in order for the forthcoming results to be reliable. This certainly requires some tool to be able to judge the approximation quality of the interpolant or, in other words, to 'measure' the distance between the function f and its approximation, g. In this work we always consider the absolute value of the difference of the function and the approximant, and we define the norm as

$$\|f - g\| = \max_{x \in [a,b]} |f(x) - g(x)|,$$

where $[a, b]$ is the interval in which we want to interpolate the function f.

Before the spread of computers, the global polynomial interpolant, that is the unique polynomial passing through the data set, was considered a valuable tool for interpolation. Since each computation was performed by hand, it was practically impossible to handle polynomials of high degree and the approximation quality achieved with polynomials of low degree was considered perfectly reasonable. With the spread of computers it was natural to ask for higher accuracy in order to better describe functions and physical phenomena. On the other hand, computers also allowed the computations of polynomial

interpolants of much higher degree. Assuming that the data set is given at certain locations, or *interpolation nodes*, the polynomials can still lead to very accurate results. This is the case when the data are given at the *Chebyshev points of the first kind* (Brutman [1997]),

$$x_i = -\cos\left(\frac{(2i+1)\pi}{2n+2}\right), \qquad i = 0, \dots, n \tag{1.1}$$

or at the *Chebyshev points of the second kind* (Brutman [1997])

$$x_i = -\cos\left(\frac{i\pi}{n}\right), \qquad i = 0, \dots, n. \tag{1.2}$$

Depending on the smoothness of the function f, if the $n+1$ data are sampled at these nodes, polynomial interpolation converges algebraically as n increases, that is (Trefethen [2013])

$$\|f - r\| \leq Cn^{-j}$$

where C is a constant and $j \in \mathbb{N}$ depends on the differentiability of the function f. If furthermore f is analytic and bounded in an ellipse in the complex plane containing $[a, b]$, the convergence is exponential, that is (Trefethen [2013])

$$\|f - r\| \leq C\rho^n,$$

for some $\rho < 1$ depending on the size of the ellipse.

Unfortunately, in most applications, it is not possible to specify the location of the data but one still has to deal with the interpolation problem and these are the cases where polynomials have shown their limitations. An important example is given by the *equispaced* interpolation nodes,

$$x_i = -1 + \frac{2i}{n}, \qquad i = 0, \dots, n,$$

where polynomial interpolation is often assumed to converge in theory but diverges in machine-precision arithmetic because of the amplifications of the rounding errors. There are moreover several examples in which the quality of polynomial approximation worsens with the increase in the number of data, even if the function f is analytic in a domain containing the interpolation interval. In general the convergence of the sequence of polynomials interpolants is strongly influenced by the analyticity of f not only in the interpolation interval but also in a neighborhood of $[a, b]$ in the complex plane.

Furthermore, in many practical applications it is not sufficient to interpolate a simple data set but it is required to impose further conditions on the

shape of the interpolating curve. Such a result can be achieved by imposing certain values to the derivative of the interpolant. These values can be sampled again from a function f, or imposed separately, in order to satisfy physical requirements. A similar demand can involve also second and higher order derivatives, and there are cases in which it is simply not possible to satisfy these requirements using polynomial interpolants with minimal degree. As an example, given the function

$$f(x) = \frac{25(x-1)(x+1)}{x-5}, \qquad x \in [-1, 1],$$

there is no quadratic polynomial p_2 satisfying

$$p_2(x_0) = f(x_0), \qquad p_2'(x_1) = f'(x_1), \qquad p_2(x_2) = f(x_2)$$

at the equispaced nodes $x_i = i - 1$, $i = 0, 1, 2$.

There are several alternative methods for approximating a function and most of them represent huge advantages over classical polynomial interpolation in the equispaced setting. Here we recall the following.

- *Splines.* Consist of piecewise polynomial interpolants, where each polynomial interpolates two consecutive samples and the remaining degrees of freedom are used to ensure some order of continuity. The main advantage is that it is not necessary to use polynomials of high degree to achieve good approximation results and then the drawbacks of classical polynomial interpolation do not show up. On the other hand, using piecewise polynomials of degree k, the resulting interpolant is only C^{k-1} and higher smoothness cannot be achieved.

- *Interpolatory subdivision schemes.* Introduced initially for curves and surface design, they soon became key ingredients for both computational science and image processing. The idea is to recursively define the interpolant, starting from the data samples by applying a refinement scheme to get a smoother result. There are several subdivision schemes that can be divided into *stationary* and *non-stationary*, depending on whether the refinement scheme is always the same or changes at every recursion step. An example is the *4-point subdivision scheme* defined by Dyn et al. [1987], where the sequence of refined curves has been proved to converge to a $C^1[a, b]$ curve.

- *Radial basis functions.* These interpolants are widely used in higher dimensions, in particular for scattered data sets. The interpolant is defined

as a linear combination of $n+1$ basis functions, one for each interpolation point, whose value at x depends on its distance from the corresponding node. This method offers high accuracy and geometric flexibility. Its smoothness depends on the continuity of the basis functions involved.

- *Classical rational interpolation.* These interpolants use rational polynomials and have been observed to give better results than polynomials (Bulirsch and Rutishauser [1968]). Unfortunately they suffer from problems that are not easy to overcome. We give more details on these interpolants in the following chapters.

A more exhaustive list of available interpolation methods is presented by Platte et al. [2011].

In this work we concentrate on *barycentric rational functions* and in particular on the *Floater–Hormann family* of interpolants. Such interpolants have been proved to be analytic on the whole real line and to have high rates of approximation. Moreover, as we show in the following chapters, Floater–Hormann interpolants are perfectly suited for interpolation of equispaced samples and thus represent one of the best alternative methods for interpolation of univariate data.

1.2 Overview

This dissertation represents an overview of the work I have carried out as a PhD student at *Università della Svizzera italiana*, divided by arguments and basically in chronological order.

In Chapter 2 we begin by giving more insights about the problems that affect polynomial interpolation. We present some classical result by Runge [1901] and Faber [1914] and we emphasize the dependence of the convergence of the polynomial interpolation scheme on the continuity of the function f. Then we introduce classical rational interpolation and explain the two main drawbacks that affect this kind of approximants, the occurrence of poles and unattainable points. In Section 2.2, we introduce the barycentric approach and the barycentric form, presenting the advantages of writing a rational interpolant in this particular way. Some theorems and lemmas that shall be useful in the rest of the thesis are presented in this section. They are mainly related to the location of poles, unattainable points, and to the computation of the derivatives of a rational interpolant in barycentric form. In Section 2.3, we focus on barycentric rational interpolation, presenting Berrut's first and second interpolants (Berrut

[1988]), and their generalization by Floater and Hormann [2007]. We moreover define some basic constants and index sets that will be used in the rest of the work.

In Chapter 3 we focus on a more general problem, in which the interpolation of the values of the derivatives of f up to order m is required. After introducing the polynomial solution, we review some classical results about the convergence of the sequence of polynomial interpolants to the function f in this new setting. We remark how equispaced nodes still represent an insurmountable problem for such a solution and therefore we generalise the barycentric approach to this more general setting. In Section 3.2 we give an overview of the previous results in the field, by presenting the generalisations by Schneider and Werner [1991] of the theorems in Chapter 2. Some of these results shall come in handy in the next sections. Finally we discuss the advantages of barycentric rational interpolants over polynomials and review some specific method by Schneider and Werner [1991], Floater and Schulz [2009] and Jing et al. [2015].

Chapter 4 goes deeper into the whole interpolation process, as we present a theoretical result that shows how polynomial interpolation is basically useless for large sets of equispaced nodes. In this chapter we present the concept of interpolation as the result of operators that act on the function f, and we show how the norms of these operators give important information on the quality of the obtained interpolant. We first introduce the theory behind the interpolation operator and present several classical results by Bernstein [1931], Erdős [1961], Rivlin [1974] and Brutman [1984] in the polynomial setting. Then we review some recent result regarding the Berrut and Floater–Hormann interpolation scheme by Bos et al. [2011], Bos et al. [2012], Bos et al. [2013] and Zhang [2014], emphasizing again the advantages of these interpolants over polynomials in the equispaced case. We then generalise the same theory to the interpolation of the derivative of the function f, showing that, also in this case, the situation is often not favorable to polynomials.

1.3 Contributions

The main focus of this dissertation is on barycentric rational interpolation of a function f and its derivatives. Since polynomial interpolants suffer from problems impossible to overcome at equispaced nodes, our aim is to show that Floater–Hormann interpolants represent the state-of-the-art tool to solve this kind of problems.

In Chapter 2, we analyse in detail the behavior of the k-th derivative of the

error produced by the Floater–Hormann interpolants. We first present some previous result by Berrut et al. [2011] and Klein and Berrut [2012] and then we provide a local bound in which the error does not depend on the mesh size of the interpolation nodes, but on the length of the subinterval $[x_j, x_{j+1}]$ in which we are evaluating it. Namely we prove that the k-th derivative of the error at $x \in [x_j, x_{j+1}]$ converges to zero as $O(h_j^{d+1-k})$ for any set of well-spaced nodes, where $h_j = x_{j+1} - x_j$. To this end we split our proof in two parts, one related to the value of the error at the nodes and one at the intermediate points. Several numerical examples conclude Chapter 2. This part is mainly based on our work

Cirillo, E., Hormann, K. and Sidon, J. [2017]. Convergence rates of derivatives of Floater–Hormann interpolants for well-spaced nodes, Applied Numerical Mathematics 116:108–118.

After the analysis of the behavior of the derivatives of Floater–Hormann interpolants, we focus on the interpolation of the derivatives of a function f, up to a certain order m. The main goal of Chapter 3 is to generalise this family of barycentric rational interpolants to the Hermite setting and, to this end, we present a general, iterative approach that allows us to generalise any sufficiently continuous Lagrange interpolant to the new setting. The application of this iterative method to the Floater–Hormann interpolants leads to the definition of an infinitely smooth family of barycentric rational Hermite interpolants with no poles in $\mathbb{R}$. We first find a closed form for the barycentric weights of the new interpolants and then, in Section 3.4, we provide a bound for the error. This section is divided into two parts. In the first we focus on the cases $m = 1$ and $m = 2$ and prove that the interpolants converge as $O(h^{2(d+1)})$ and $O(h^{3(d+1)})$, respectively, as the mesh size h converges to zero. This proof relies on the closed form of the barycentric weights found previously, but does not allow an easy generalisation to the general case. In the second part, we generalise these results for any $m \geq 0$, proving that our iterative Hermite interpolant converges to the function as $O(h^{(m+1)(d+1)})$ as $h \to 0$. This proof, valid also for the first two cases, uses completely different techniques and it is therefore my opinion that both versions deserve to be included here. Several numerical examples conclude this chapter. This part of the thesis is based on the following works.

Cirillo, E. and Hormann, K. [2018]. An iterative approach to barycentric rational Hermite interpolation, Numerische Mathematik 140(4):939–962;

Cirillo, E., Hormann, K. and Sidon, J. [2019]. Convergence rates of iterative

rational Hermite interpolants. Submitted.

In the last part of the thesis we further analyse the iterative Hermite interpolant proposed in Chapter 3. Inspired by the unfavorable growth of the condition number of polynomial Hermite interpolants at equispaced nodes, Section 4.4 is devoted to the application of the theory presented in the first part of the chapter to the interpolant introduced in Chapter 3. In particular we prove that the condition number of our interpolant is bounded from above by a constant independent of n. Some numerical experiments show that the same quantity grows exponentially with d, a behavior that recalls the one experienced by classical Floater–Hormann interpolants in the Lagrange setting. This final part of the thesis is mainly based on our work

Cirillo, E. and Hormann, K. [2019]. On the Lebesgue constant of barycentric rational Hermite interpolants at equidistant nodes, Journal of Computational and Applied Mathematics 349:292–301.

Chapter 2

Barycentric rational interpolation

Given a real valued function $f \in C^0[a,b]$ and the set of $n+1$ nodes

$$X_n = \{x_0^{(n)}, x_1^{(n)}, \ldots, x_n^{(n)}\}, \tag{2.1}$$

such that $a = x_0^{(n)} < x_1^{(n)} < \cdots < x_n^{(n)} = b$, the *Lagrange interpolation problem* consists in finding a function g such that

$$g(x_i^{(n)}) = f_i = f(x_i^{(n)}), \qquad i = 0, \ldots, n. \tag{2.2}$$

We are mainly interested in studying the behavior of

$$e(x) = f(x) - g(x), \tag{2.3}$$

as the number of nodes n increases, that is, given a triangular array $X = (X_n)_{n\in\mathbb{N}}$ of nodes in $[a,b]$,

$$\begin{array}{ccccccc} x_0^{(0)} & & & & & & \\ x_0^{(1)} & x_1^{(1)} & & & & & \\ x_0^{(2)} & x_1^{(2)} & x_2^{(2)} & & & & \\ \vdots & \vdots & & \ddots & & & \\ x_0^{(n)} & x_1^{(n)} & & \cdots & x_n^{(n)} & & \\ \vdots & \vdots & & & & \ddots & \end{array} \tag{2.4}$$

we analyse the behavior of $e(x)$ as $n \to \infty$. Each X_n is called a *set of nodes*, while we refer to X as a *system of interpolation nodes*. When no confusion is likely to arise, we omit the superscript that refers to the number of nodes, $x_i = x_i^{(n)}$.

We emphasize that the interpolant g clearly depends on the number of interpolation nodes and on the function f and therefore we should more formally write $g = g_n = g_n[f]$. Nevertheless, we assume this to be clear to the reader and we omit the dependance of g on n and f, when it is not strictly necessary.

We finally denote the couple (x_i, f_i) as the i-th *support point* of the interpolant g (Stoer and Bulirsch [1993]).

In the next section, we introduce the polynomial solution of the Lagrange interpolation problem (2.2) and give more details regarding polynomial interpolation. Then we present classical rational interpolants and the linearised interpolation conditions and we point out the main issues that affect this kind of interpolants. In Section 2.2, we introduce the barycentric approach and present some of the theorems that will be used later on. In Section 2.3 we focus on Berrut's rational interpolants and their generalisation by Floater and Hormann, together with some result regarding the main properties of these interpolants. After presenting some previous results about the convergence of the derivatives of the Floater–Hormann interpolants, in Section 2.4, we extend them to a more general case.

2.1 Polynomial and classical rational interpolation

Let us denote with $\mathscr{P}_d$ the space of polynomials of degree at most d. Given the $n+1$ nodes in (2.1), there exists a unique set of $n+1$ polynomials in $\mathscr{P}_n$

$$\ell_i(x) = \prod_{j=0, j\neq i}^{n} \frac{x - x_j}{x_i - x_j}, \qquad i = 0, \dots, n, \tag{2.5}$$

that satisfies the *Lagrange property*

$$\ell_i(x_j) = \delta_{i,j}, \tag{2.6}$$

where $\delta_{i,j}$ is the *Kronecker delta*

$$\delta_{i,j} = \begin{cases} 0, & \text{if } i \neq j, \\ 1, & \text{if } i = j. \end{cases}$$

Such polynomials are called *Lagrange basis functions*, since, in a moment, we shall show that they are a basis for the $(n+1)$-dimensional vector space $\mathscr{P}_n$.

Definition 2.1. Let Φ be a vector space of dimension d. A set of d elements $\{\phi_1, \dots, \phi_d\}$ is called a basis for Φ if its elements are linearly independent. In this case we write

$$\Phi = \operatorname{span}\{\phi_1, \dots, \phi_d\}.$$

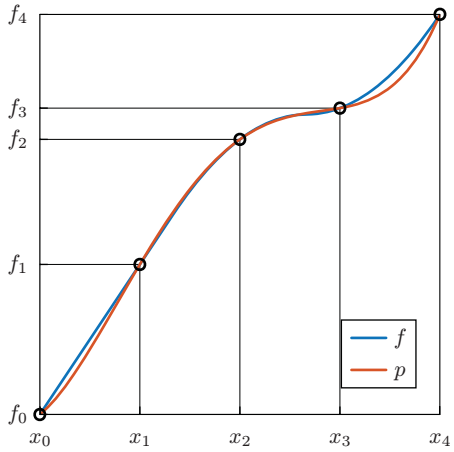

Figure 2.1. The Lagrange polynomial p (in red) interpolating the function f (in blue) at 5 equispaced nodes.

Given a function $f \in C^0[a,b]$, let

$$p(x) = p_n[f](x) = \sum_{i=0}^{n} \ell_i(x) f_i. \tag{2.7}$$

By the Lagrange property of the Lagrange functions, p is the unique polynomial solution of minimal degree for the Lagrange interpolation problem (2.2), see Figure 2.1.

For any choice of n, such a polynomial satisfies the following, see Davis [1975].

Theorem 2.1. Let $f \in C^n[a,b]$ and suppose that $f^{(n+1)}$ exists at each point of (a,b). Then the polynomial interpolant (2.7) satisfies

$$e(x) = \ell(x) \frac{f^{(n+1)}(\xi)}{(n+1)!},$$

where ξ is in the convex hull of $x, x_0, x_1, \ldots, x_n$ and depends on f and

$$\ell(x) = \prod_{i=0}^{n} (x - x_i) \tag{2.8}$$

is the *nodal polynomial* associated to the nodes $x_0, \ldots, x_n$.

Letting $A_n(x) = \|f^{(n+1)}\| \ell(x)$, the previous theorem states that we have convergence as long as

$$\lim_{n\to\infty} \frac{\|A_n\|}{(n+1)!} = 0, \tag{2.9}$$

and, in this case, p converges to f as $O(h^{n+1})$, where

$$h = \max_{i=1,\dots,n} (x_i - x_{i-1}). \tag{2.10}$$

From Theorem 2.1 moreover descends the fact that the Lagrange functions are a basis for the linear space $\mathscr{P}_n$, since, if $f \in \mathscr{P}_n$, it can be written as a linear combination of the ℓ_i's with coefficients given by the samples of f at the nodes.

As pointed out by Berrut and Trefethen [2004], Equation (2.7) requires $O(n^2)$ operations for each evaluation of p and the insertion of a new node x_{n+1} with a corresponding value f_{n+1} requires a new computation from scratch. However p can be rearranged in a computationally less expensive form. By considering the nodal polynomial (2.8), we rewrite each ℓ_i as

$$\ell_i(x) = \frac{\ell(x)}{(x - x_i)\ell'(x_i)} = \ell(x)\frac{\omega_i}{x - x_i} \tag{2.11}$$

with

$$\omega_i = 1/\ell'(x_i) \tag{2.12}$$

and the corresponding interpolant as

$$p(x) = \ell(x) \sum_{i=0}^{n} \frac{\omega_i}{(x - x_i)} f_i. \tag{2.13}$$

This form is called the *first form of the barycentric interpolation formula* (Rutishauser [1990]). The computation of each ω_i requires $O(n^2)$ operations but, since these values do not depend on the function f, they can be precomputed to approximate several functions on the same set of nodes. Once this is done the evaluation of the polynomial itself requires $O(n)$ operations. Moreover the insertion of a new node requires only to update ω_i, $i = 0, \dots, n$, and to compute ω_{n+1}, and both operations can be done in $O(n)$ steps. This form of the polynomial interpolant has been shown by Higham [2004] to be *backward* and *forward stable*.

Definition 2.2. The evaluation method $\tilde{f}$ used to evaluate a function f is backward stable if, for any $x \in \mathbb{R}$,

$$\tilde{f}(x) = f(x + \delta x)$$

for some small *backward error* $|\delta x|$. Moreover if

$$\frac{\|\tilde{f} - f\|}{\|f\|} = \delta y$$

for some small *forward error* $|\delta y|$, $\tilde{f}$ is said to be forward stable.

In practice, a backward stable evaluation method provides the right value of f at the almost right value of x, while a forward stable evaluation method outputs a value that is 'close enough' to the right answer. The difference between the two notions is substantial. Suppose for example that $x = \pi/2 - 10^{-2}$, and $f(x) = \tan(x)$. An evaluation method $\tilde{f}$ with a backward error $|\delta x| = 2 \cdot 10^{-3}$ can still result in a relatively big forward error $|\delta y| \approx 0.25$. Conversely, if f is very flat around x, a pretty big backward error δx can still result in a small forward error δy.

If we denote with u the unit roundoff, the first barycentric form satisfies the following.

Theorem 2.2 (Higham [2004])**.** The value $\tilde{p}(x)$ of the polynomial interpolant as computed with the first barycentric form (2.13) satisfies

$$\tilde{p}(x) = \ell(x) \sum_{i=0}^{n} \frac{\omega_i}{x - x_i} f_i \langle 5n + 5 \rangle_i,$$

where

$$\langle k \rangle = \prod_{i=1}^{k} (1 + \delta_i)^{\rho_i}, \qquad \rho_i = \pm 1$$

and $\delta_i \leq u$.

This result states that the value computed using the first barycentric form can be interpreted as the exact solution of the Lagrange interpolation problem for the slightly perturbed data values

$$\tilde{f}_i = f_i \langle 5n + 5 \rangle_i, \qquad i = 0, \ldots, n.$$

As for the forward stability, we need to introduce the *condition number* of p at x with respect to f.

Definition 2.3 (Higham [2004])**.** The condition number of p at x with respect to f is

$$\operatorname{cond}(x, n, f) = \lim_{\delta \to 0} \sup \left\{ \left| \frac{p_n[f](x) - p_n[f + \Delta f](x)}{\delta p_n[f](x)} \right| : |\Delta f(x)| \leq \delta |f(x)| \right\}.$$

The condition number of p can be thought of as the maximum relative error of p produced by a slight perturbation of the function f.

Theorem 2.3 (Higham [2004])**.** The value $\tilde{p}(x)$ of the polynomial interpolant as computed with the first barycentric form (2.13) satisfies

$$\left| \frac{p(x) - \tilde{p}(x)}{p(x)} \right| \leq \frac{(5n + 5)u}{1 - (5n + 5)u} \operatorname{cond}(x, n, f).$$

The first barycentric formula it is not the end of the story, as, by Theorem 2.1, the Lagrange basis functions satisfy the *partition of unity property*

$$\ell(x)\sum_{i=0}^{n}\frac{\omega_i}{x-x_i}=1.$$

Therefore, dividing (2.13) by 1 and simplifying the common factors, we get

$$p(x)=\sum_{i=0}^{n}\frac{\omega_i}{x-x_i}f_i\Bigg/\sum_{i=0}^{n}\frac{\omega_i}{x-x_i}. \tag{2.14}$$

This new form has been called by Rutishauser [1990] the *second form of the barycentric formula* and has been shown to be forward stable.

Theorem 2.4 (Higham [2004])**.** The polynomial interpolant $\tilde{p}(x)$ as computed with the second barycentric form satisfies

$$\left|\frac{p(x)-\tilde{p}(x)}{p(x)}\right|\leq(3n+4)u\,\mathrm{cond}(x,n,f)+(3n+2)u\Lambda_n+O(u^2),$$

where

$$\Lambda_n=\max_{x\in[a,b]}\sum_{i=0}^{n}|\ell_i(x)|.$$

This result shows that the second barycentric form is forward stable as long as the constant Λ_n is not too large. We give more details about this important quantity in Chapter 4, where we also specify favorable choices for the interpolation nodes, that guarantee a slow growth of Λ_n.

Higham [2004] concludes his work by specifying that the second barycentric formula is in general not backward stable, while Mascarenhas and de Camargo [2014] make this observation more precise, specifying that (2.14) is backward stable as long as the constant Λ_n remains small.

Despite the restriction on Λ_n, the second barycentric form has a practical benefit over the first one, as noted by Berrut and Trefethen [2004]. Since the weights ω_i appears linearly in the numerator and the denominator of p, all their common factors can be factored out to avoid overflows and underflows. There exist several simple expressions for the weights for particular systems of nodes. For example, if the nodes are equispaced, Henrici [1982] proves that

$$\omega_i=(-1)^i\binom{n}{i},$$

no matter the length of the interval $[a, b]$. For the Chebyshev nodes of the first kind (1.1), Henrici [1982] finds

$$\omega_i = (-1)^i \sin \frac{(2i+1)\pi}{2n+2}, \qquad i = 0, \dots, n$$

while, for the Chebyshev nodes of the second kind (1.2), Salzer [1972] finds

$$\omega_0 = \frac{1}{2}, \qquad \omega_i = (-1)^i, \quad i = 1, \dots, n-1, \qquad \omega_n = \frac{(-1)^n}{2}. \tag{2.15}$$

For general distributions of nodes, instead, Berrut and Trefethen [2004] suggest to multiply all the factors in $\ell'(x_i)$ by $4/(b-a)$, in order to avoid overflows and underflows in the weights (2.12).

Comparing the weights for Chebyshev and equispaced nodes we can notice a huge difference. While with the former the weights vary as $O(n)$, in the equispaced case the weights vary exponentially as $O(2^n)$. In this latter case it is clear that, for large n, we cannot prevent overflows or underflows with a rescaling of the weights. Berrut and Trefethen [2004] remark that this fact is not strictly correlated with the barycentric form but with the polynomial interpolation per se, as we will illustrate in the following lines.

From Theorem 2.1, it is clear that the convergence of the polynomial p as $n \to \infty$ is strongly influenced by the behavior of the nodal polynomial (2.8) and thus by the location of the nodes. If the nodes are equally spaced, Runge [1901] proves that the sequence of polynomial interpolants may diverge as n increases, even when the function f is analytic. An example in which the polynomial interpolant diverges as $n \to \infty$ is displayed in Figure 2.2, left. The Lagrange polynomials for $n = 5, 10, 15$ converge to the *Runge function*

$$f(x) = \frac{1}{1+25x^2}, \qquad x \in [-1, 1] \tag{2.16}$$

exponentially in the middle of the interpolation interval, while they diverge as x approaches the endpoints of $[-1, 1]$. The reason for this divergence is the location of the poles of the Runge function in the complex plane. As noticed by Runge, indeed, the convergence of the sequence of polynomial interpolants $(p_n)_{n\in\mathbb{N}}$ is strongly influenced by the location of these poles in the neighborhood of the interpolation interval. Runge [1901] understands that it is not sufficient for f to be analytic in $[a, b]$ but it must be analytic in a larger *Runge region* (Trefethen [2013]). Since (2.16) is not analytic inside this area, the polynomial interpolants fail to converge as $n \to \infty$, see Figure 2.2, right. Similarly, functions which have poles near the boundary of this region, will tend

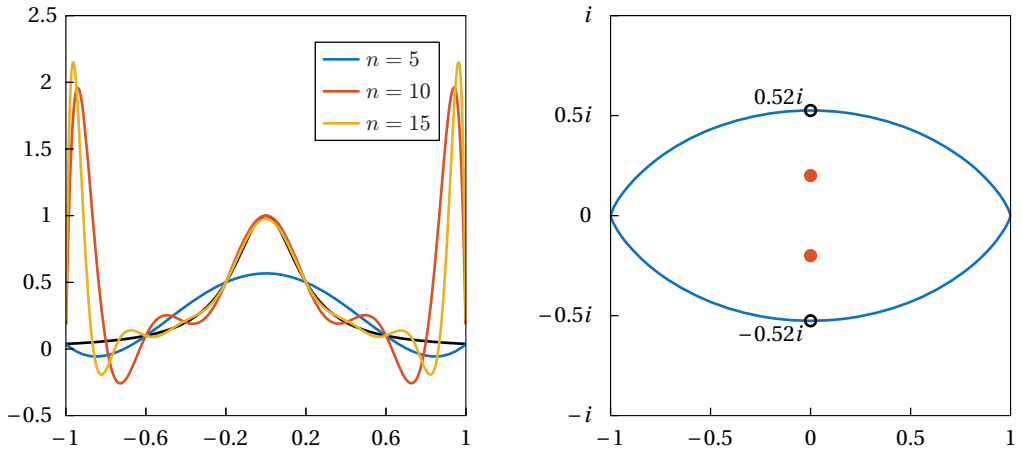

Figure 2.2. Left: the Lagrange polynomials interpolating the Runge function in (2.16) (in black), for $n = 5, 10, 15$, at equispaced nodes. Right: the Runge region for the interval $[-1, 1]$ (in blue) and the poles of the Runge function (in red).

to converge or diverge slowly. For example, consider the functions

$$f_1(x) = \frac{9}{100x^2 + 9}, \qquad \text{and} \qquad f_2 = \frac{49}{100x^2 + 49}, \tag{2.17}$$

with poles in $\pm 0.3i$ and $\pm 0.7i$, respectively. In Figure 2.3 we represent the behavior of the errors $e_1 = \|f_1 - p\|$ and $e_2 = \|f_2 - p\|$, for $n = 5, 10, \ldots, 40$. We notice a slow divergence for the function f_1 and a slow convergence for f_2. The farthest the poles are away from the boundary of the Runge region, the most these trends are visible.

Faber [1914] extends Runge's observation, by proving that, no matter how the points are distributed, polynomial interpolation cannot converge for all continuous functions.

Despite this last discouraging result, Trefethen [2011] notices that, if the nodes x_i are nicely distributed (e.g. Chebyshev nodes), the polynomial interpolants are guaranteed to converge, as long as the function f is at least Lipschitz continuous, i.e. if

$$|f(x) - f(y)| \leq L|x - y|, \qquad x, y \in [a, b]$$

for some constant $L > 0$, a condition that is easily met (see also Grünwald [1942]). Moreover the following important result holds.

Theorem 2.5 (Rivlin [1981])**.** For any $f \in C^0[a, b]$ there exists a system of nodes X such that p converges uniformly to f in $[a, b]$ as $n \to \infty$.

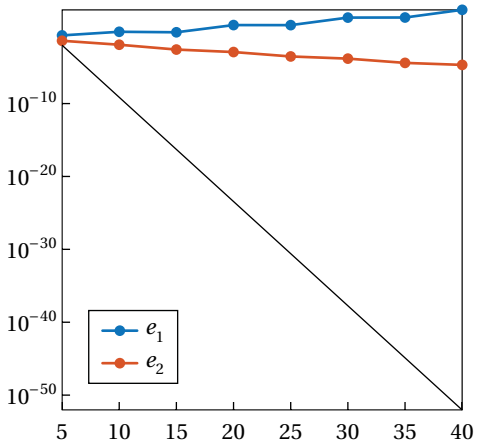

Figure 2.3. Behavior of the errors $e_1 = \|f_1 - p\|$ (in blue) and $e_2 = \|f_2 - p\|$ (in red) for the functions f_1 and f_2 in (2.17) and $n = 5, 10, \ldots, 40$ at equispaced nodes. The straight reference line (in black) represents the $O(h^{n+1})$ behavior.

Anyway in most applications one cannot choose the interpolation points and has somehow to deal with the prescribed distribution of nodes. It is therefore necessary to look for interpolants different from polynomials.

One suitable alternative to polynomial interpolation is the use of rational functions

$$r(x) = \frac{p(x)}{q(x)}, \qquad p \in \mathscr{P}_l, \quad q \in \mathscr{P}_m,$$

with $l + m = n$[1]., to solve the *linearised interpolation conditions*

$$p(x_i) = f_i q(x_i), \qquad i = 0, \ldots, n. \tag{2.18}$$

As Bulirsch and Rutishauser [1968] notice, classical rational interpolants often give better results than polynomials, especially when we want to approximate a function f close to its poles and discontinuities. As an example they consider the function $f(x) = \cot(x)$ sampled at the equispaced nodes $x_i = i + 1$, $i = 0, \ldots, 4$. In Figure 2.4 we interpolate the function using a polynomial of degree 4 and a rational function with $l = m = 2$. Since polynomials are smooth, they are not well suited for interpolation of functions close to points of discontinuity. On the other hand, rational functions are flexible enough to interpolate f in a neighborhood of a pole, as shown in this particular example. The corresponding

[1]The rational interpolant r is determined only up to a common factor of the $l + m + 2$ coefficients of p and q. Therefore we can freely fix one of those coefficients, so as to normalise r

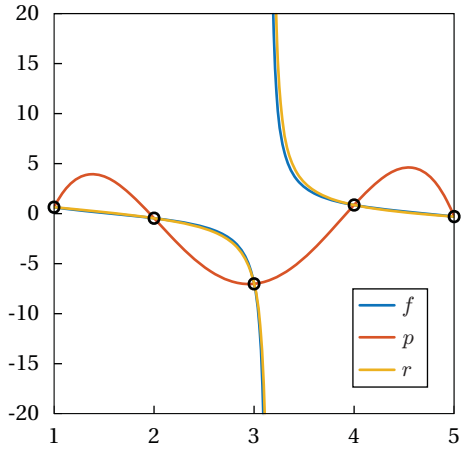

Figure 2.4. Interpolation of $\cot(x)$ (in blue) at 5 equispaced nodes with a polynomial p (in red) and a rational function r (in yellow).

rational function r has a pole in the interpolation interval at $x \approx 3.1635$, that nicely approximates the pole of $\cot(x)$ at π already for $n = 4$.

The situation is completely different if the function f is continuous in the whole interpolation interval. In this case, the lack of tools to control the occurrence and the position of poles makes it impossible to handle such kind of interpolants, see Figure 2.5, left. The other big disadvantage of classical rational interpolants is the occurrence of *unattainable (support) points*, a problem that has been pointed out by Claessens [1978] and that is due to the use of the linearised interpolation conditions. Indeed, the node x_i may be a zero of both polynomials p and q, making the i-th support point unattainable, see Figure 2.5, right. As an example, Stoer and Bulirsch [1993] consider the nodes

$$x_i = i, \qquad i = 0, 1, 2$$

with function values

$$f_0 = 1, \qquad f_1 = f_2 = 2.$$

The use of the linearised interpolation conditions (2.18) with $l = m = 1$ gives

$$p(x) = 2x, \qquad q(x) = x$$

and the support point corresponding to x_0 is unattainable for the rational interpolant

$$r(x) = \frac{p(x)}{q(x)} = 2.$$

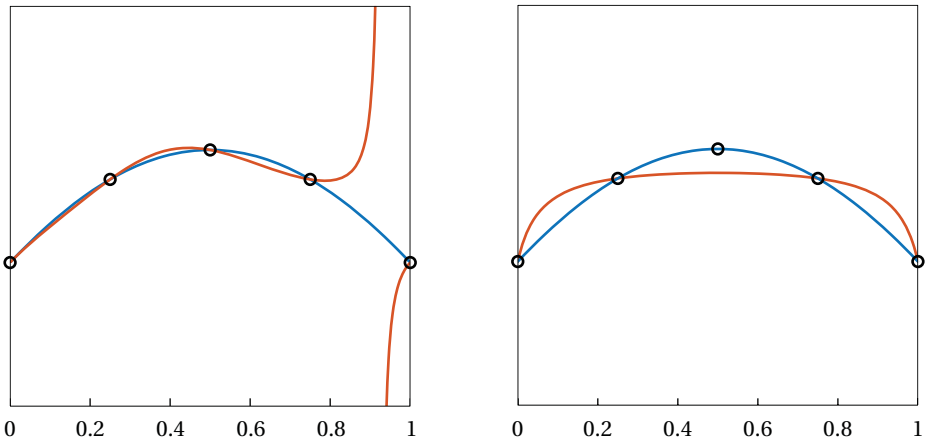

Figure 2.5. Left: a rational interpolant (in red) of a function (in blue) at 5 equispaced nodes with a pole. Right: a different rational interpolant (in red) of the same function at the same nodes with an unattainable point.

The main goal of this thesis is to explore a third, more promising approach and to investigate the properties of the obtained interpolants. In particular we deal with an alternative kind of solutions to the Lagrange interpolation problem, the so-called barycentric rational interpolants, which has recently proved to compare favorably with more classical methods such as polynomials, splines and rational functions in the equispaced setting.

2.2 The barycentric approach

Barycentric interpolants are a special kind of interpolants of the form

$$g(x) = \sum_{i=0}^{n} b_i(x) f_i \tag{2.19}$$

where the *barycentric basis functions* b_i, $i = 0, \ldots, n$, satisfy the three properties

$$\textit{Lagrange property}: \qquad b_i(x_j) = \delta_{ij}, \tag{2.20a}$$

$$\textit{Partition of unity}: \qquad \sum_{i=0}^{n} b_i(x) = 1, \tag{2.20b}$$

$$\textit{Barycentric property}: \qquad \sum_{i=0}^{n} b_i(x) x_i = x. \tag{2.20c}$$

It is clear that any interpolant g that reproduces linear functions stems from a set of basis functions that satisfy all the three barycentric properties. Anyway, Hormann [2014] remarks that it is common use to name an interpolant as barycentric only if there exists an explicit closed form for b_i and g reproduces linear functions.

Berrut and Mittelmann [1997] prove that any rational interpolant with a certain degree can be written in a form that is similar to (2.19).

Theorem 2.6 (Berrut and Mittelmann [1997])**.** Let (x_i, f_i), $i = 0, \dots, n$ be $n+1$ distinct support points. Then any rational function r of degree at most n satisfying (2.2) can be written in linear form as

$$r(x) = \sum_{i=0}^{n} b_i(x) f_i, \tag{2.21}$$

with

$$b_i(x) = \frac{\beta_i}{x - x_i} \Bigg/ \sum_{j=0}^{n} \frac{\beta_j}{x - x_j}, \tag{2.22}$$

for some $\boldsymbol{\beta} = (\beta_0, \dots, \beta_n) \in \mathbb{R}^n$.

Any interpolant as in (2.21) is said to be expressed in *barycentric form*, while the quantities $\beta_0, \dots, \beta_n$ are called *barycentric weights* and, in order to retrieve their form, we give a sketch of the proof of the theorem. Let

$$r(x) = \frac{p(x)}{q(x)}, \qquad p \in \mathscr{P}_l, \quad q \in \mathscr{P}_m$$

with $l, m \leq n$. Since the Lagrange basis functions are a basis for $\mathscr{P}_n$, we resort to (2.11) and rewrite p and q as

$$p(x) = \ell(x) \sum_{i=0}^{n} \frac{\omega_i}{x - x_i} p(x_i) \qquad \text{and} \qquad q(x) = \ell(x) \sum_{i=0}^{n} \frac{\omega_i}{x - x_i} q(x_i).$$

Then, using the linearised interpolation conditions (2.18),

$$r(x) = \sum_{i=0}^{n} \frac{\beta_i}{x - x_i} f_i \Bigg/ \sum_{i=0}^{n} \frac{\beta_i}{x - x_i},$$

with $\beta_i = \omega_i q(x_i)$, $i = 0, \dots, n$. We notice in particular that the barycentric weights depend only on the denominator of r, and therefore, once this is specified, the interpolant is completely determined.

The similarity between the barycentric form and (2.19) might bring us to conclude that any choice of barycentric weights guarantees r to be a barycentric interpolant but, despite each b_i in (2.22) satisfies (2.20b) and (2.20a), the answer is in general negative. The following proposition gives the last characterisation.

Proposition 2.1. A rational interpolant in barycentric form (2.21) satisfies the barycentric property (2.20c) if and only if

$$\sum_{i=0}^{n} \beta_i = 0.$$

Proof. In Proposition 3, Hormann [2014] proves that if

$$\sum_{i=0}^{n} \beta_i = 0$$

then the corresponding interpolant satisfies the barycentric property. The other implication is trivial. □

We remark that, since the functions in (2.22) satisfy the Lagrange property, they are actually a basis of some linear subspace of rational functions

$$\mathscr{R}_{\boldsymbol{\beta}} = \operatorname{span}\{b_0, \ldots, b_n\},$$

where the subscript $\boldsymbol{\beta}$ emphasises the dependence of the subspace on the barycentric weights $\boldsymbol{\beta} = \{\beta_0, \ldots, \beta_n\}$. As an example, if we consider $\beta_i = \omega_i$, $i = 0, \ldots, n$ from (2.12), then the function r is a polynomial of degree at most n and therefore $\mathscr{R}_{\boldsymbol{\omega}} = \mathscr{P}_n$.

The big advantage of the barycentric form is that we can replace each weight β_i with some other non-zero weight, being sure that the interpolation property is still preserved. This property stems from the following result.

Lemma 2.1 (Berrut et al. [2005])**.** Let (x_i, f_i), $i = 0, \ldots, n$, be $n + 1$ distinct support points. Then if $\beta_i \neq 0$, the interpolant r in (2.21) interpolates f_i at x_i, that is

$$\lim_{x \to x_i} r(x) = f_i.$$

To prove this result it is sufficient to multiply both numerator and denominator in (2.21) by the nodal polynomial $\ell(x)$ and to compute the limit as $x \to x_i$.

This represents a great advantage from a computational point of view since, even if rounding errors in the computation of the weights occur, the

function does not lose its interpolation property. Moreover, by the similarity of (2.14) and (2.21), any interpolant in barycentric form inherits all the properties regarding the precomputation and storage of the weights we already noticed in the previous section. We observe that, by Lemma 2.1, the choice $\beta_i = \omega_i$, $i = 0, \ldots, n$, is the only way to get a polynomial from the barycentric form (2.21), while any other choice results in a proper rational function for any f.

The barycentric weights provide the tools that in classical rational interpolation lacks. Indeed, Schneider and Werner [1986] prove the following results for barycentric rational interpolants in reduced form, regarding occurrence of poles and unattainable points.

Proposition 2.2 (Schneider and Werner [1986])**.** The support point (x_i, f_i) is unattainable for an interpolant r in barycentric form if and only if $\beta_i = 0$.

Proposition 2.3 (Schneider and Werner [1986])**.** If an interpolant r in barycentric form has no poles in $[a, b]$, then

$$\text{sign } \beta_i = -\text{sign } \beta_{i+1}, \qquad i = 0, \ldots, n-1.$$

If sign β_i = sign β_{i+1} for some $i = 0, \ldots, n-1$ then r has an odd number of poles in the i-th subinterval (x_j, x_{j+1}), with multiplicities taken into account.

Figure 2.6 represents all the possible cases described by the previous propositions. The function in blue is being interpolated at 6 equispaced nodes. In (a), the signs of the weights are alternating and the interpolant has neither poles nor unattainable points. In (b), we set the first weight to 0 obtaining an unattainable point as described by Proposition 2.2. The last two examples are related to Proposition 2.3. In (c) we represent an interpolant with

$$\text{sign } \beta_1 = \text{sign } \beta_2 = \text{sign } \beta_3.$$

As predicted by Proposition 2.3, it has an odd number of poles in both subintervals (x_1, x_2) and (x_2, x_3). Unfortunately, the condition on the alternating sign is not sufficient. In (d) we show the interpolant corresponding to the weights

$$\beta_0 = -\beta_5 = 441, \quad \beta_1 = -\beta_4 = -125, \quad \beta_2 = -\beta_3 = 90.$$

Even if the weights alternate in sign, the corresponding interpolant still has poles in $[a, b]$. By Proposition 2.3, this interpolant must have an even number

of poles in each subinterval and this is confirmed by looking at the denominator of the corresponding interpolant,

$$q(x) = 24000\left(x - \frac{3}{10}\right)^2\left(x - \frac{7}{10}\right)^2,$$

which has two roots with double multiplicity at $x = \frac{3}{10}, \frac{7}{10}$.

We finally would like to recall another proposition by Schneider and Werner [1986], regarding the differentiation of rational interpolants in barycentric form. Such functions are easy to differentiate both at the nodes and at the intermediate points $x \in (x_i, x_{i+1})$. Before stating the result, let us recall the definition of *divided differences*.

Definition 2.4. Given $n+1$ support points (x_i, f_i), $i = 0, \dots, n$, the divided differences of f are defined as

$$\begin{aligned} f[x_j] &= f_j, \qquad j = 0, \dots, n, \\ f[x_j, \dots, x_{j+k}] &= \frac{f[x_{j+1}, \dots, x_{j+k}] - f[x_j, \dots, x_{j+k-1}]}{x_{j+k} - x_j}, \qquad j = 0, \dots, n-k, \end{aligned}$$

for any $k = 1, \dots, n$.

We shall often use the k-fold notation

$$f[(x)^k, \dots] = f[\underbrace{x, \dots, x}_{k \text{ times}}, \dots].$$

Proposition 2.4 (Schneider and Werner [1986])**.** Let r be an interpolant in barycentric form. Then

- If $x \in \mathbb{R} \setminus \{x_0, \dots, x_n\}$ and x is not a pole of r,

$$r^{(k)}(x) = k! \sum_{i=0}^{n} \frac{\beta_i}{x - x_i} r[(x)^k, x_i] \Bigg/ \sum_{i=0}^{n} \frac{\beta_i}{x - x_i}, \qquad k \geq 0.$$

- If $x = x_j$ for some $j = 0, \dots, n$, we get

$$r^{(k)}(x_j) = -\frac{k!}{\beta_j} \sum_{i=0, i \neq j}^{n} \beta_j r[(x_j)^k, x_i].$$

This proposition will come in handy in Section 2.4.3 and in the next chapter, where we treat the Hermite interpolation problem.

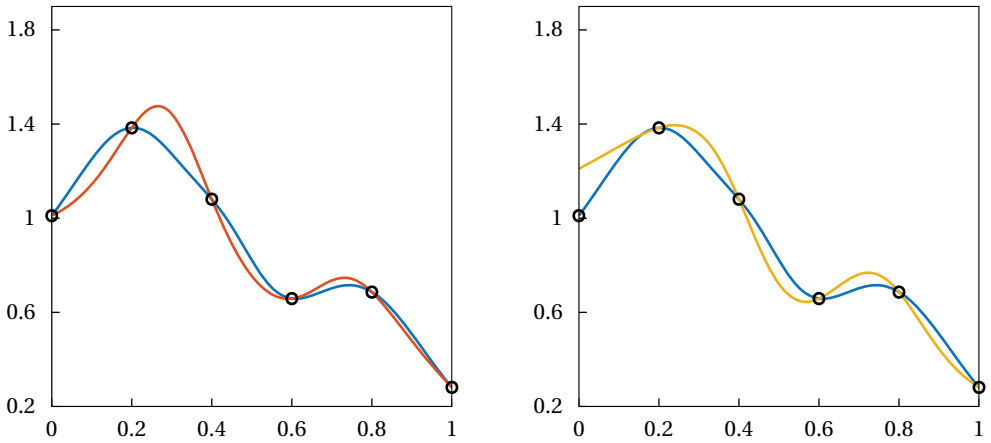

(a) $\beta = (1, -1, 1, -1, 1, -1)$ *(b)* $\beta = (0, -1, 1, -1, 1, -1)$

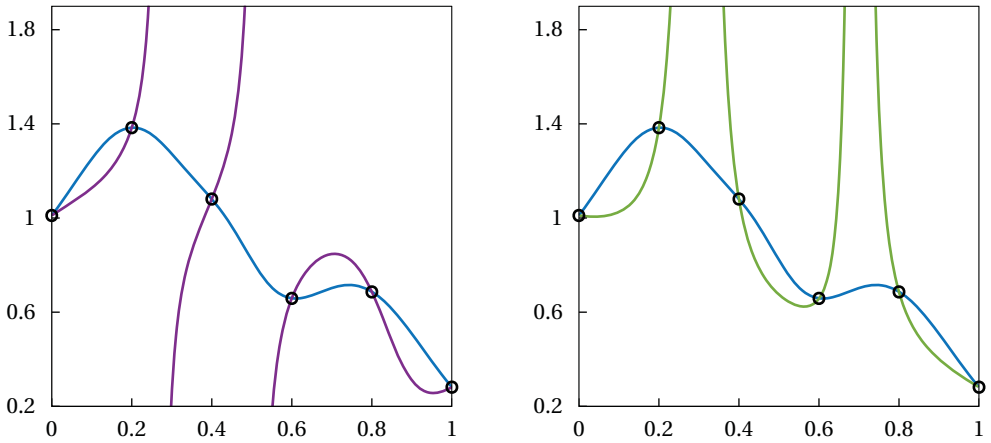

(c) $\beta = (1, -1, -1, -1, 1, -1)$ *(d)* $\beta = (441, -125, 90, -90, 125, -441)$

Figure 2.6. Some example illustrating all possible cases in Propositions 2.2 and 2.3 for 4 different interpolants of the same function (in blue) at 6 equispaced nodes: (a) An interpolant (in red) with neither poles nor unattainable points; (b) an interpolant (in yellow) with an unattainable point; (c) an interpolant (in purple) with an odd number of poles in the subintervals (x_1, x_2) and (x_2, x_3); (d) an interpolant (in green) in barycentric form with weights with alternating sign and an even number of poles in the subintervals (x_1, x_2) and (x_3, x_4).

Therefore, barycentric rational interpolants are natural candidates for the solution of the Lagrange interpolation problem at equispaced nodes, since they enjoy the best properties of both polynomial and classical rational interpolation, without inheriting any of their disadvantages. Indeed, a suitable choice of barycentric weights can guarantee that the corresponding interpolant does not suffer from divergence problems as polynomials do, and, on the other hand, can solve the two main issues of classical rational interpolation, i.e., the difficulty of handling poles and unattainable points. In the next section we review a particular choice of barycentric weights β_i, $i = 0, \dots, n$, that guarantees the absence of poles and unattainable points and a favorable convergence rate of the corresponding interpolant to the function f.

2.3 Barycentric rational interpolation

While Schneider and Werner investigate the rational interpolants in barycentric form (2.21) in depth for any choice of the barycentric weights, Berrut [1988] is the first author who proposes an accurate analysis of the interpolant for a particular choice of the values β_i. His strategy is very simple. Since the weights ω_i in (2.12) are the only non-zero weights for which the interpolant (2.21) is a polynomial, any different choice is guaranteed to give a rational interpolant. Between all the possible choices of weights β_i, we search for the ones that guarantee the interpolant to have no poles.

In order to introduce his rational interpolant, let us consider the unique polynomial interpolant of the function f at the nodes $x_0 = a$ and $x_1 = b$. By recalling the weights (2.12) we get

$$-\ell'(x_0) = \ell'(x_1) = b - a$$

and, after rescaling,

$$\omega_i = (-1)^i, \qquad i = 0, 1.$$

These weights clearly correspond to an interpolant with no poles in $\mathbb{R}$, no matter how the two nodes x_0, x_1 are placed. Inspired by this fact, Berrut [1988] suggests to use the weights

$$\beta_i = (-1)^i, \qquad i = 0, \dots, n,$$

and proves the following result.

Lemma 2.2 (Berrut [1988])**.** For any $x \in \mathbb{R}$,

$$q(x) = \ell(x) \sum_{i=0}^{n} \frac{(-1)^i}{x - x_i} \neq 0.$$

Therefore the rational function corresponding to this choice of barycentric weights has no real poles for any distribution of nodes. We refer to this rational interpolant as *Berrut's first interpolant*. Supported by some numerical tests, Berrut [1988] conjectures that this interpolant converges to the function as $O(h)$ as $h \to 0$, where h is the global mesh-size (2.10).

We can immediately see from Proposition 2.1 that Berrut's first interpolant is not barycentric for even n but Berrut [1988] also proposes a different choice of the β_i's that corresponds to a barycentric interpolant, that is

$$\beta_i = (-1)^i \kappa_i, \qquad \kappa_i = \begin{cases} 1, & \text{if } j = 0 \text{ or } j = n, \\ 2, & \text{otherwise.} \end{cases}$$

We refer to this interpolant as *Berrut's second interpolant* and Baltensperger et al. [1999] conjecture a faster convergence $O(h^2)$ in this case.

Berrut's first interpolant can be understood in a completely different manner. If we consider the values $f_0, \ldots, f_n$ as $n+1$ constant polynomial interpolants, we can see Berrut's rational function as a blend of these local interpolants with rational blending functions

$$\frac{(-1)^i}{x - x_i} \Bigg/ \sum_{j=0}^{n} \frac{(-1)^j}{x - x_j}, \qquad i = 0, \ldots, n,$$

see Figures 2.7, left, and 2.9.

This consideration leads Floater and Hormann [2007] to generalise Berrut's approach by using local polynomial interpolants of degree d, with $0 < d \leq n$. Namely, let us denote by I the index set

$$I = \{0, 1, \ldots, n - d\}.$$

Then for every $i \in I$, let p_i be the unique polynomial interpolant of degree at most d for the support points (x_j, f_j), $j = i, \ldots, i + d$ and let

$$\lambda_i(x) = \frac{(-1)^i}{(x - x_i) \ldots (x - x_{i+d})}; \tag{2.23}$$

see Figure 2.8. Then the Floater–Hormann interpolant is defined as

$$r(x) = \sum_{i=0}^{n-d} \lambda_i(x) p_i(x) \Bigg/ \sum_{i=0}^{n-d} \lambda_i(x), \tag{2.24}$$

see Figure 2.9, right. This construction reproduces Berrut's first interpolant

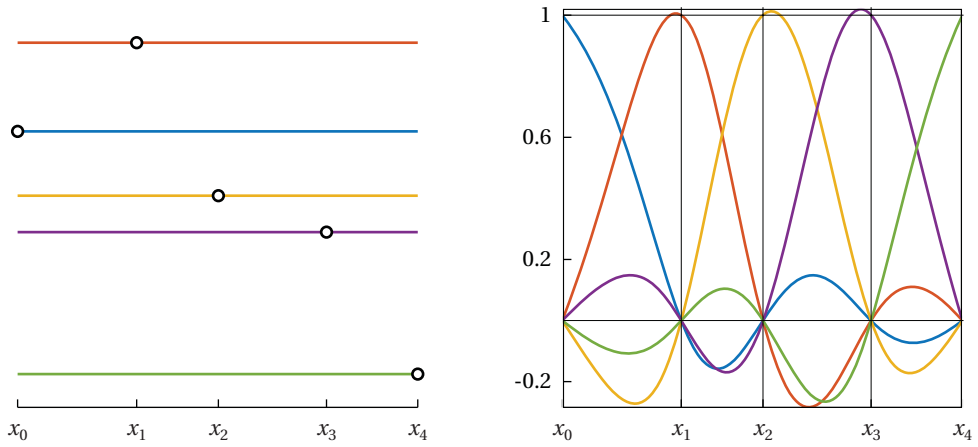

Figure 2.7. Left: local constant polynomial interpolants for Berrut's first interpolant in Figure 2.9, left. Right: the corresponding weighting functions $\frac{(-1)^i/(x-x_i)}{\sum_{j=0}^{n}(-1)^j/(x-x_j)}$, $i = 0, \ldots, n$

.

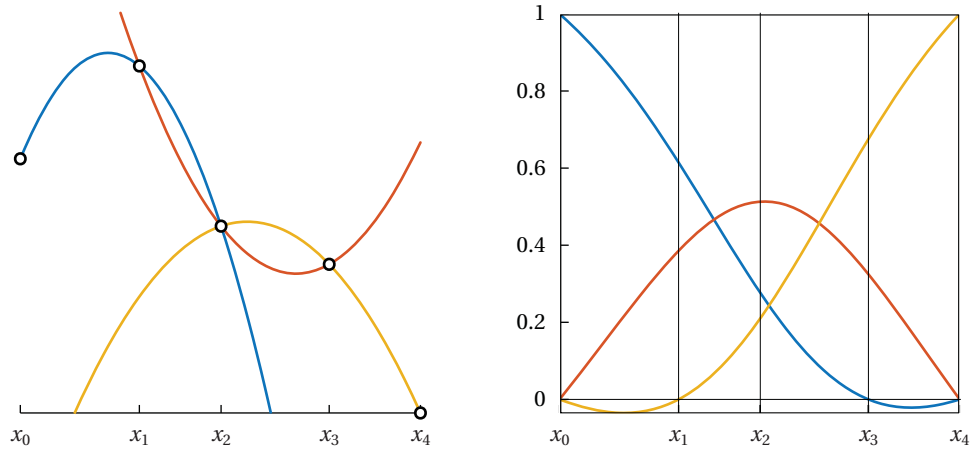

Figure 2.8. Left: the local quadratic polynomial interpolants for the Floater–Hormann interpolant in Figure 2.9, right. Right: the corresponding weighting functions $\lambda_i(x)/\sum_{i=0}^{n-2}\lambda_i(x)$, $i = 0, \ldots, n-2$.

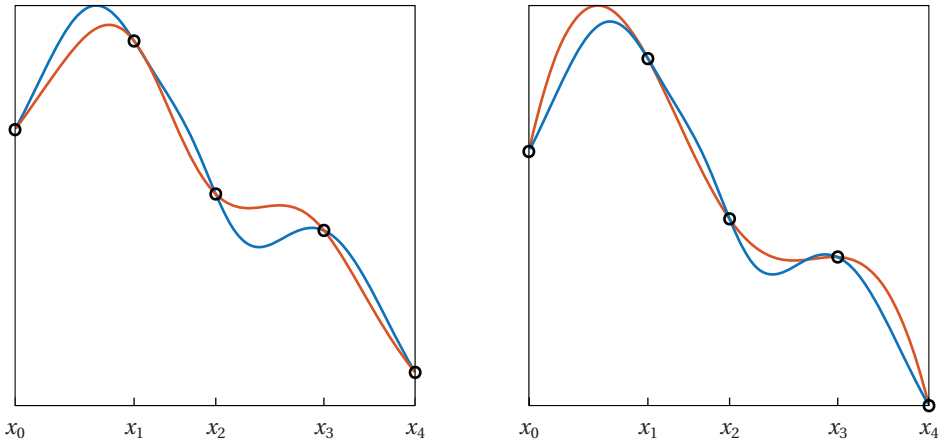

Figure 2.9. Left: Berrut's first interpolant (in red) of the function (in blue) at 5 randomly distributed nodes. Right: Floater–Hormann interpolant for $d = 2$ (in red) of the same function at the same nodes.

for $d = 0$ but additionally defines n different interpolants, one for each choice of $d \leq n$. We refer to these rational functions as the *Floater–Hormann family of interpolants*. Floater and Hormann [2007] confirm Berrut's conjecture about his first interpolant and prove the following result regarding the convergence rate of the interpolant (2.24).

Theorem 2.7 (Floater and Hormann [2007])**.** Suppose $d \geq 0$ and $f \in C^{d+2}[a, b]$, and let h be as in (2.10). Then the Floater–Hormann interpolant satisfies

$$|e(x)| \leq Ch^{d+1},$$

where the constant C depends only on d, the derivatives of f, the interval length $b - a$, and, only in the case $d = 0$, on the local mesh ratio

$$\beta = \max_{1 \leq i \leq n-2} \min\left\{ \frac{x_{i+1} - x_i}{x_i - x_{i-1}}, \frac{x_{i+1} - x_i}{x_{i+2} - x_{i+1}} \right\}. \tag{2.25}$$

The local mesh ratio β emphasizes the dependence of this construction on the distribution of the nodes, and will appear also in the following chapters.

Since the Floater–Hormann interpolants are defined as a blend of polynomials, it is reasonable to expect the Runge phenomenon to arise for a large number of equispaced nodes. In practice this happens only if the degree d increases together with the number of nodes n, while, if d is fixed, the Runge phenomenon does not show up. In his PhD thesis, Klein [2012] gives a detailed

analysis of the underlying reasons for this fact and the following intuitive explanation. Since the error of the Floater–Hormann interpolant can be expressed as

$$f(x) - r(x) = \sum_{i=0}^{n-d} \lambda_i(x)(f(x) - p_i(x)) \Big/ \sum_{i=0}^{n-d} \lambda_i(x),$$

it is strongly influenced by the error of the $n-d+1$ polynomials $p_i \in \mathscr{P}_d$. Each of them interpolates the function f in $[x_i, x_{i+d}]$, and the size of this subinterval tends to zero as $n \to \infty$. Therefore, the Runge region corresponding to $[x_i, x_{i+d}]$ shrinks as n increases, excluding the poles of f that are potentially close to the interpolation interval $[a, b]$.

Since (2.24) is a generalisation of Berrut's first interpolant it is natural to expect that r has no poles for any d and this is confirmed by the following.

Theorem 2.8 (Floater and Hormann [2007])**.** For any d, $0 \leq d \leq n$, the rational function in (2.24) has numerator and denominator of degree at most n and $n-d$, respectively, and has no poles in $\mathbb{R}$.

Therefore, by Theorem 2.6, the Floater–Hormann interpolants can be written in barycentric form with barycentric weights (Floater and Hormann [2007])

$$w_j = (-1)^{j-d} \sum_{i \in I_j} \prod_{\substack{k=i \\ k \neq j}}^{i+d} \frac{1}{|x_j - x_k|}, \qquad j = 0, \ldots, n, \tag{2.26}$$

where I_j is the index set defined by

$$I_j = \{i \in I : j - d \leq i \leq j\}. \tag{2.27}$$

In order to avoid confusion we remark that, here and in the rest of this dissertation, we denote with w_i, the *Floater–Hormann weights* defined in (2.26), with ω_i the weights corresponding to the polynomial interpolant in barycentric form (2.12) and with β_i a general set of barycentric weights.

Floater and Hormann [2007] notice that the weights (2.26) simplify to

$$w_j = (-1)^{j-d} \sum_{i \in I_j} \binom{d}{j-i}. \tag{2.28}$$

if the nodes are equispaced. Explicitly writing the first values of $|w_j|$ for dif-

ferent d's we get

$$\begin{aligned} &1,1,\dots,1,1, && d=0,\\ &1,2,2,\dots,2,2,1, && d=1,\\ &1,3,4,4,\dots,4,4,3,1, && d=2,\\ &1,4,7,8,8,\dots,8,8,7,4,1, && d=3,\\ &1,5,11,15,16,16,\dots,16,16,15,11,5,1, && d=4. \end{aligned} \tag{2.29}$$

This shows a pattern, that appears clearly by having a more careful look at (2.27). The sum in (2.28) contains at most $d+1$ terms of the type

$$\binom{d}{0}, \binom{d}{1}, \dots, \binom{d}{d-1}, \binom{d}{d}$$

and therefore $|w_j| \leq 2^d$, a property that will come in handy in Chapter 4. This observation is made more precise by Bos et al. [2012] for $n \geq 2d$, who note that

$$w_j = (-1)^j \sum_{k=d}^{n} \binom{d}{k-j} = \begin{cases} \sum_{k=0}^{j} \binom{d}{k}, & \text{if } j \leq d,\\ 2^d, & \text{if } d \leq j \leq n-d,\\ w_{n-j}, & \text{if } j \geq n-d. \end{cases} \tag{2.30}$$

We point out that, if the nodes are equispaced, the case $d = 1$ in (2.29) corresponds to Berrut's second interpolant and therefore its convergence rate conjectured by Baltensperger et al. [1999] is also confirmed by Theorem 2.7.

Instead of resorting to Proposition 2.1 to prove that the Floater–Hormann interpolant is barycentric for any $d \geq 2$, Floater and Hormann [2007] show that r reproduces polynomials up to degree d. If $f_i = q(x_i)$ for some polynomial $q \in \mathscr{P}_d$, indeed, by the uniqueness of the local polynomial interpolant we get that $p_i(x) = q(x)$, $i = 0, \dots, n-d$ and therefore

$$r(x) = \frac{\sum_{i=0}^{n-d} \lambda_i(x) p_i(x)}{\sum_{i=0}^{n-d} \lambda_i(x)} = \frac{q(x) \sum_{i=0}^{n-d} \lambda_i(x)}{\sum_{i=0}^{n-d} \lambda_i(x)} = q(x).$$

In particular, r reproduces linear functions and we can conclude that it is barycentric with barycentric basis functions

$$b_i(x) = \frac{w_i}{x - x_i} \Bigg/ \sum_{j=0}^{n} \frac{w_j}{x - x_j}. \tag{2.31}$$

The functions b_i, $i = 0, \dots, n$, clearly depend on d and we refer to them as the *Floater–Hormann basis functions*.

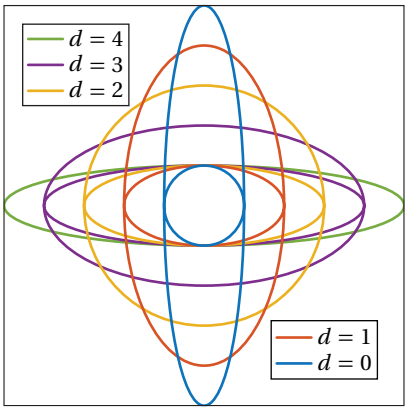

Figure 2.10. The inclusion chain of the linear spaces $\mathscr{R}_{\boldsymbol{w}_d}$ (vertical ellipses) and $\mathscr{P}_d$ (horizontal ellipses) for $n = 4$ and $d = 0, \ldots, 4$.

Now, let us fix n and denote by

$$\mathscr{R}_{\boldsymbol{w}_d} = \operatorname{span}\{b_0, \ldots, b_n\} \tag{2.32}$$

the linear space spanned by these basis functions. For any d, with $0 \leq d < n$, $r \in \mathscr{R}_{n,n-d}$, where $\mathscr{R}_{l,m}$ denotes the space of rational functions with numerator and denominator of degree at most l and m, respectively. Therefore $\mathscr{R}_{\boldsymbol{w}_d} \subset \mathscr{R}_{n,n-d}$, where the inclusion is strict, as $\mathscr{R}_{\boldsymbol{w}_d}$ is a linear space, while $\mathscr{R}_{n,n-d}$ is not. Moreover, by the reproduction property of the Floater–Hormann interpolant, we have $\mathscr{P}_d \subseteq \mathscr{R}_{\boldsymbol{w}_d}$, and then

$$\mathscr{P}_d \subseteq \mathscr{R}_{\boldsymbol{w}_d} \subset \mathscr{R}_{n,n-d},$$

with

$$\dim \mathscr{P}_d \leq \dim \mathscr{R}_{\boldsymbol{w}_d} < \dim \mathscr{R}_{n,n-d}.$$

Hence, $\mathscr{R}_{\boldsymbol{w}_d}$ is an $(n+1)$-dimensional linear space that contains a space of increasing dimension, $\mathscr{P}_d$, and, at the same time, is contained in a space whose dimension is decreasing, $\mathscr{R}_{n,n-d}$. We may imagine $\mathscr{R}_{\boldsymbol{w}_d}$ as a linear space of fixed dimension, embedded in $\mathscr{R}_{n,n}$, that 'squeezes' on $\mathscr{P}_{n-1}$ as $d \to n-1$, see Figure 2.10. For $d = n$ both $\mathscr{P}_n$ and $\mathscr{R}_{n,0}$ have the same dimension as $\mathscr{R}_{\boldsymbol{w}_n}$ and therefore $\mathscr{R}_{\boldsymbol{w}_n} = \mathscr{P}_n$. For that reason, the corresponding Floater–Hormann interpolant coincides with the unique polynomial interpolant of degree at most n.

The next section is devoted to the analysis of the derivatives of the error e produced by the Floater–Hormann interpolant. We start by presenting some result by Berrut et al. [2011] regarding e' and e'', valid for any system of nodes.

Then we proceed with the analysis by Klein and Berrut [2012] of $e^{(k)}$, $k \geq 3$, at *quasi-equispaced* nodes. In the last part of this section we generalise these previous results to any $k = 0, \ldots, d$ for a more general system of nodes, in what is the main contribution of this chapter.

2.4 Convergence rates of derivatives for well-spaced nodes

Since Floater–Hormann interpolants are infinitely smooth, the interest of the community has recently moved towards the investigation of the convergence rate of their derivatives to the corresponding derivatives of f.

Since r is a blend of local polynomial interpolants of degree at most d, it is reasonable to expect that $e^{(k)}$ converges to 0 at a rate of $O(h^{d+1-k})$, for any $k \leq d$.

This initial conjecture is supported by the following theorem, regarding the behavior of the first derivative of $e(x)$.

Theorem 2.9 (Berrut et al. [2011])**.** If $d \geq 1$ and $f \in C^{d+3}[a,b]$, then

$$|e'(x)| \leq Ch^d, \qquad x \in [a,b]$$

with h as in (2.10) and where the constant C depends only on d, the derivatives of f, the interval length $b-a$ and, only if x is not a node and $d = 1$, on the quantity

$$\mu = \max\left\{ \max_{1\leq i\leq n-1} \frac{x_{i+1}-x_i}{x_i - x_{i-1}}, \max_{0\leq i\leq n-2} \frac{x_{i+1}-x_i}{x_{i+2}-x_{i+1}} \right\}. \tag{2.33}$$

If $x = x_j$, Berrut et al. [2011] prove a similar bound also for $d = 0$, under less stringent conditions on the continuity of the function f.

They also provide a similar bound for e''.

Theorem 2.10 (Berrut et al. [2011])**.** If $d \geq 2$ and $f \in C^{d+4}[a,b]$, then

$$|e''(x)| \leq Ch^{d-1}, \qquad x \in [a,b],$$

with h as in (2.10) and where the constant C depends only on d, the derivatives of f, the interval length $b-a$ and, only if x is not a node, on the quantity μ in (2.33).

In the same work, a similar bound is proved also for the case $d = 1$, if x is a node and, also in this case, the condition on the continuity of f is less requiring.

The previous theorems make our observation on the expected rate of $|e^{(k)}|$ more precise about the continuity of the function f. In particular it seems that, in order to have a convergence rate of $O(h^{d+1-k})$ in $[a, b]$, it is necessary for the function f to be $C^{d+k+2}[a, b]$.

As for the generalisation of the previous results to $k \geq 3$, a straightforward recursive approach turned out to be too complicated to be carried out. More recently Klein and Berrut [2012] establish this convergence rate for $k \geq 3$, but at the cost of restricting themselves in two ways. On the one hand they study the behavior of the k-th derivative of the error only at the nodes and not at the intermediate points $x \in (x_j, x_{j+1})$, $j = 0, \ldots, n-1$, while, on the other, they considered the nodes to be quasi-equispaced.

Definition 2.5. A system of interpolation nodes $X = (X_n)_{n\in\mathbb{N}}$ is said to be quasi-equispaced, if

$$\frac{h}{h_{\min}} \leq c \tag{2.34}$$

with $c \geq 1$,

$$h_{\min} = \min_{i=1,\ldots,n} (x_i - x_{i-1})$$

and h as in (2.10), holds for every set X_n.

Under these assumptions on the distribution of the nodes, it is possible to prove the following result.

Theorem 2.11 (Klein and Berrut [2012])**.** Let X be a system of quasi-equispaced nodes, $k \leq d$, and $f \in C^{d+1+k}[a, b]$. Then

$$|e^{(k)}(x_j)| \leq Ch^{d+1-k}, \qquad j = 0, \ldots, n,$$

with h as in (2.10) and where C is a constant depending only on c, d, k, and derivatives of f.

Definition 2.5 characterises a set of nodes that does not let any subinterval decrease too fast with respect to h, as $n \to \infty$. This is a strong requirement which, de facto, excludes many important systems of nodes such as the Chebyshev nodes of first (1.1) and second kind (1.2). The latter, for example, can be seen as the projection of $n + 1$ uniformly sampled points on the upper half of the unit circle

$$c_i = \left(\cos\frac{i\pi}{n}, \sin\frac{i\pi}{n}\right)$$

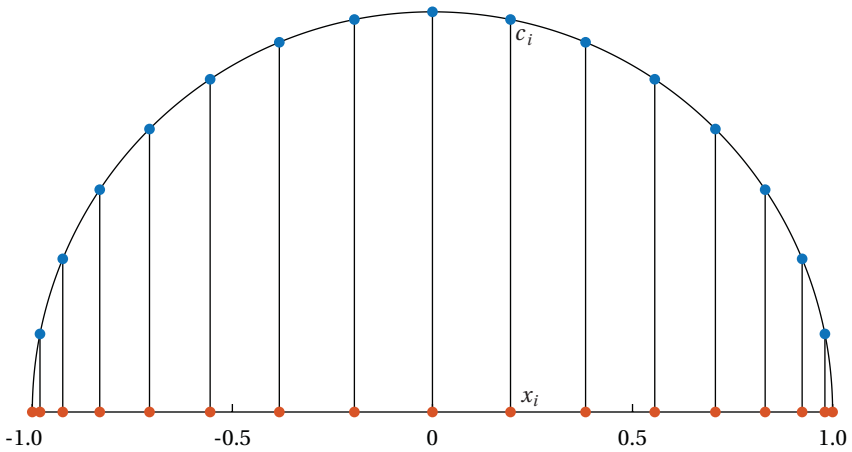

Figure 2.11. Chebyshev points of the second kind in $[-1, 1]$.

on the x-axis, see Figure 2.11. Therefore, for even n,

$$h_{\min} = 1 - \cos\left(\frac{\pi}{n}\right), \qquad h = \cos\left(\frac{\pi}{2} - \frac{\pi}{n}\right) = \sin\left(\frac{\pi}{n}\right),$$

and hence,

$$\lim_{n\to\infty} \frac{h}{h_{\min}} = \lim_{n\to\infty} \frac{\sin\left(\frac{\pi}{n}\right)}{1 - \cos\left(\frac{\pi}{n}\right)} = \lim_{n\to\infty} \frac{1 + \cos\left(\frac{\pi}{n}\right)}{\sin\left(\frac{\pi}{n}\right)} = +\infty.$$

For odd values of n and Chebyshev nodes of the first kind, the result can be proved along similar lines. The goal of this chapter is to generalise these results about $r^{(k)}$ in two directions.

We first show that the convergence rate of $e^{(k)}(x)$ is $O(h^{d+1-k})$ for any $k \geq 1$ under the assumption of using *well-spaced* interpolation nodes. If we denote with

$$h_i = h_{i+1,i}, \qquad h_{i,j} = |x_i - x_j|$$

such interpolation nodes are defined by the following.

Definition 2.6 (Bos et al. [2013])**.** A system of interpolation nodes $X = (X_n)_{n\in\mathbb{N}}$ is *well-spaced*, if there exist constants $R_1, R_2 \geq 1$, independent of n, such that the two conditions

$$\frac{1}{R_1} \leq \frac{h_i}{h_{i-1}} \leq R_1, \qquad i = 1, \ldots, n-1, \tag{2.35}$$

and

$$\begin{aligned} \frac{h_i}{h_{i+1,j}} &\leq \frac{R_2}{i+1-j}, \qquad j = 0, \dots, i, \quad i = 0, \dots, n-1, \\ \frac{h_i}{h_{j,i}} &\leq \frac{R_2}{j-i}, \qquad j = i+1, \dots, n, \quad i = 0, \dots, n-1, \end{aligned} \tag{2.36}$$

hold for every set X_n.

While condition (2.35) bounds the mesh ratio locally, (2.36) is a global condition that limits the factor by which the length h_i of an interval can be larger than the average lengths

$$\frac{h_{i-k} + h_{i-k+1} + \cdots + h_i}{k+1} \qquad \text{and} \qquad \frac{h_i + h_{i+1} + \cdots + h_{i+k}}{k+1}$$

of neighboring intervals to the left and to the right for all valid k.

Bos et al. [2013] prove that the previous definition includes not only equispaced and quasi-equispaced nodes, but also *extended Chebyshev nodes*[2] to obtain interpolation at the endpoints. (Brutman [1997]). Using similar arguments as in their proof, it is possible to show that the same is valid also for Chebyshev nodes of the first kind.

For a general characterisation of well-spaced nodes, Bos et al. [2013] prove that they are strictly correlated with *regular distribution functions*.

Definition 2.7. A function $G \in C^1[0,1]$ is a regular distribution function if it is a strictly increasing bijection on the interval $[0,1]$ and G' has at most a finite number of zeros, all of which have a finite multiplicity.

Then, if we define the nodes as an equispaced sample of a regular distribution function, that is

$$x_i = G(i/n), \qquad i = 0, \dots, n, \tag{2.37}$$

the following holds.

Theorem 2.12 (Bos et al. [2013])**.** Let G be a regular distribution function and X_n be the set defined by (2.37) for any $n \in \mathbb{N}$. Then, the system $X = (X_n)_{n\in\mathbb{N}}$ is well-spaced.

[2]Extended Chebyshev nodes are obtained from the Chebyshev nodes of the first kind by mapping them to the interval $[a, b]$, in order

This last result shows that well-spaced nodes include also Chebyshev nodes of the second kind, since (1.2) shows that they are generated by the regular distribution function

$$G(x) = -\cos(\pi x).$$

Despite being very general, Definition 2.6 does not include all possible systems and some customary example of points do not satisfy relations (2.35) and (2.36). An example of a set satisfying only (2.35) are nodes in geometric progression,

$$x_i = \frac{\mu^i - 1}{\mu^n - 1}, \qquad i = 0, \dots, n, \tag{2.38}$$

for any $\mu > 1$. This set is characterised by nodes that tend to cluster at the beginning of the interval while they tend to form subintervals of uniform size

$$\lim_{n\to\infty} \frac{\mu^{n-1} - 1}{\mu^n - 1} = \frac{1}{\mu},$$

near its end, see Figure 2.12, left. Similarly the set

$$\begin{aligned} x_0 &= 0, \\ x_i &= \frac{2}{a_n} \begin{cases} x_{i-1} + 1, & i \text{ odd}, \\ x_{i-1} + n, & i \text{ even}, \end{cases} \end{aligned} \tag{2.39}$$

with

$$a_n = \begin{cases} n^2 + 1, & \text{if } n \text{ is odd}, \\ n(n+1), & \text{if } n \text{ is even}, \end{cases}$$

satisfies only (2.36). Indeed, if i is odd,

$$\frac{h_i}{h_{i-1}} = n,$$

and therefore this set tends to produce couples of nodes, separated by larger subintervals, see Figure 2.12, right.

The other direction in which we generalise the results by Berrut et al. [2011] and Klein and Berrut [2012] is the localization of the behavior of the error, by showing that it depends on the local mesh size rather than on the global mesh size. More precisely, we establish the following upper bounds on the error and its derivatives.

Theorem 2.13. For any set of well-spaced nodes, any k with $0 \le k \le d$, and $f \in C^{d+k+2}[a, b]$,

$$|e^{(k)}(x)| \le Ch^{d+1-k}, \qquad x \in [a, b],$$

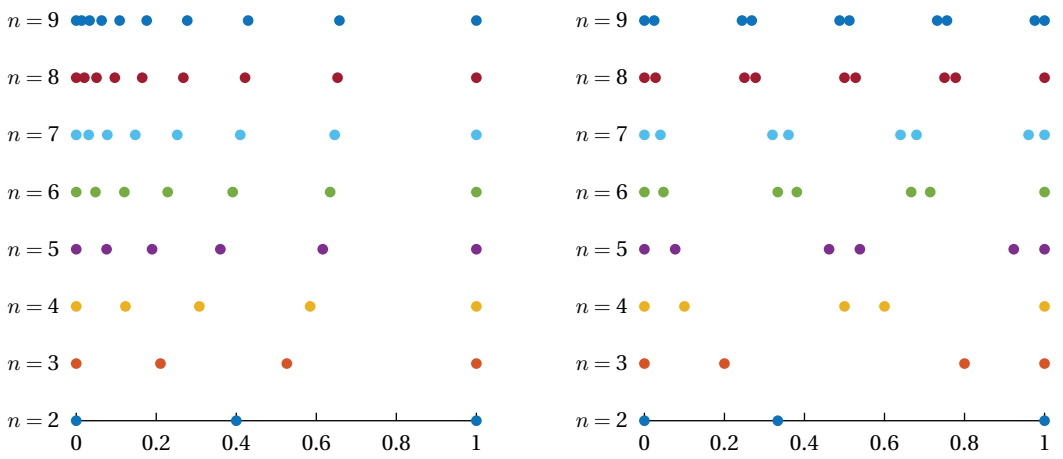

Figure 2.12. Two sets of non well-spaced nodes for $n = 2, \ldots, 9$. Left: the set defined by (2.38) for $\mu = 3/2$. Right: the set defined by (2.39).

and more specifically,

$$|e^{(k)}(x)| \leq C h_j^{d+1-k}, \qquad x \in [x_j, x_{j+1}], \qquad j = 0, \ldots, n-1. \tag{2.40}$$

Note that in Theorem 2.13 and throughout the rest of the chapter we denote by C a generic constant depending only on k, d, the derivatives of f, the interval length $b - a$, and the constants R_1 and R_2 from Definition 2.6. To establish the bounds in Theorem 2.13, we first analyse the error at the nodes x_j (Subsection 2.4.1) and then at intermediate points $x \in (x_j, x_{j+1})$ (Subsection 2.4.2). We conclude this chapter with several numerical examples which confirm the bound in (2.40) and highlight the dependence on the local mesh size h_j (Subsection 2.4.3).

2.4.1 Error at the nodes

In what follows, it helps to remember that Floater and Hormann [2007] write the error (2.3) of their interpolant as

$$e(x) = \frac{A(x)}{B(x)} \tag{2.41}$$

where

$$A(x) = \sum_{i=0}^{n-d} (-1)^i f[x_i, x_{i+1}, \ldots, x_{i+d}, x]$$

and

$$B(x) = \sum_{i=0}^{n-d} \lambda_i(x).$$

Let us now study the convergence rate of the derivatives of e at the interpolation nodes.

Lemma 2.3. For any set of well-spaced interpolation nodes, any k with $1 \leq k \leq d$, and $f \in C^{d+k+2}[a,b]$,

$$|e^{(k)}(x_j)| \leq Ch_j^{d+1-k}, \qquad j = 0, \ldots, n-1$$

and

$$|e^{(k)}(x_j)| \leq Ch_{j-1}^{d+1-k}, \qquad j = 1, \ldots, n.$$

Proof. Throughout this proof we consider only the first statement, since the second can be established analogously by taking into account that $h_j \leq R_1 h_{j-1}$, according to (2.35). We also point out that the proof is largely inspired by the proof of Theorem 2.1 by Klein and Berrut [2012], except that we utilize (2.35) and (2.36) to derive local error bounds in h_j instead of the global error bounds in h that were considered by those authors. Moreover, we resort to Hoppe's formula in (2.42) as a generalization of the chain rule to higher derivatives instead of Faà di Bruno's formula, which was used by Klein and Berrut [2012] for the same purpose, because the latter does not lead to our local error bounds.

We start by fixing the index j and expressing the error in (2.41) as

$$e(x) = \phi(x)\hat{e}(x),$$

where

$$\phi(x) = x - x_j, \qquad \hat{e}(x) = \frac{A(x)}{D(x)}, \qquad D(x) = \phi(x)B(x).$$

By the Leibniz rule, we have

$$e^{(k)}(x) = \phi(x)\hat{e}^{(k)}(x) + k\phi'(x)\hat{e}^{(k-1)}(x)$$

and

$$e^{(k)}(x_j) = k\hat{e}^{(k-1)}(x_j).$$

Again, we use the Leibniz rule to obtain

$$\hat{e}^{(k-1)}(x_j) = \sum_{l=0}^{k-1} \binom{k-1}{l} A^{(k-1-l)}(x_j)(D^{-1})^{(l)}(x_j).$$

Since Lemma 2 by Berrut et al. [2011] guarantees that the absolute values of A and its derivatives are bounded by some constant over $[a,b]$ for $f \in C^{d+1+k}[a,b]$, it remains to show that

$$|(D^{-1})^{(l)}(x_j)| \leq Ch_j^{d-l}, \qquad l = 0, \ldots, d-1.$$

Using Hoppe's formula (see the works by Hoppe [1845] and Johnson [2002]) we obtain

$$(D^{-1})^{(l)}(x) = \sum_{p=0}^{l} \frac{(-1)^p}{D^{p+1}(x)} \sum_{m=0}^{p} \binom{p}{m} (-1)^{p-m} D^{p-m}(x) (D^m)^{(l)}(x), \tag{2.42}$$

so that

$$|(D^{-1})^{(l)}(x_j)| \leq \sum_{p=0}^{l} \sum_{m=0}^{p} \binom{p}{m} \frac{|(D^m)^{(l)}(x_j)|}{|D^{m+1}(x_j)|},$$

and the final step now is to prove by induction over m that

$$\frac{|(D^m)^{(l)}(x_j)|}{|D^{m+1}(x_j)|} \leq C h_j^{d-l}, \qquad l = 0, \ldots, d-1 \tag{2.43}$$

for any $m \geq 0$.

We obtain this result by first deriving a lower bound for $|D(x_j)|$ and an upper bound for $|D^{(l)}(x_j)|$, and to this end it helps to write $D(x)$ as

$$D(x) = E(x) + \phi(x) F(x)$$

with

$$E(x) = \sum_{i \in I_j} (-1)^i \prod_{k=i, k \neq j}^{i+d} \frac{1}{x - x_k},$$

$$F(x) = \sum_{i \in I \setminus I_j} (-1)^i \prod_{k=i}^{i+d} \frac{1}{x - x_k},$$

and I_j as in (2.27). Berrut et al. [2011] show that

$$|D(x_j)| = |E(x_j)| \geq \prod_{k=i, k \neq j}^{i+d} h_{j,k}^{-1}, \qquad i \in I_j \tag{2.44}$$

and continue to bound the right hand side from below by Ch^{-d}. Instead, we use (2.35) to conclude

$$h_{j,k} \leq \sum_{m=\max(0, j-d)}^{\min(n-1, j+d-1)} h_m \leq \sum_{m=\max(0, j-d)}^{\min(n-1, j+d-1)} R_1^{|j-m|} h_j \leq 2 d R_1^d h_j \tag{2.45}$$

for all $h_{j,k}$ in (2.44), which leads to the lower bound

$$|D(x_j)| \geq C h_j^{-d}. \tag{2.46}$$

For the upper bounds on the derivatives of D at x_j, we assume $l \geq 1$ for the moment, follow Klein and Berrut [2012], and use the relation

$$D^{(l)}(x_j) = E^{(l)}(x_j) + lF^{(l-1)}(x_j)$$

and the Leibniz rule to get

$$E^{(l)}(x) = \sum_{i \in I_j} (-1)^{i+l} l! \sum_{|\boldsymbol{\alpha}_{i,j}|=l} \prod_{k=i, k\neq j}^{i+d} \frac{1}{(x-x_k)^{1+\alpha_k}},$$

where the second sum ranges over all d-dimensional multi-indices $\boldsymbol{\alpha}_{i,j} = (\alpha_i, \ldots, \alpha_{j-1}, \alpha_{j+1}, \ldots, \alpha_{i+d})$ whose non-negative integer components add up to l. By (2.35) and (2.36),

$$\begin{aligned} |E^{(l)}(x_j)| &\leq \sum_{i \in I_j} l! \sum_{|\boldsymbol{\alpha}_{i,j}|=l} \prod_{k=i, k\neq j}^{i+d} \frac{1}{h_{j,k}^{1+\alpha_k}} \\ &\leq \sum_{i \in I_j} l! \sum_{|\boldsymbol{\alpha}_{i,j}|=l} \prod_{k=i, k\neq j}^{i+d} \left(\frac{R_1 R_2}{h_j |j-k|} \right)^{1+\alpha_k} \\ &\leq C h_j^{-(d+l)}, \end{aligned} \tag{2.47}$$

and the same upper bound can be derived analogously for $|F^{(l-1)}(x_j)|$, so that overall

$$|D^{(l)}(x_j)| \leq C h_j^{-(d+l)}, \qquad l = 1, \ldots, d-1. \tag{2.48}$$

Let us now return to (2.43) and observe that the base case $m = 0$ and the special case $l = 0$ follow directly from (2.46). For the induction step assume that (2.43) holds for an arbitrary value of $m \geq 0$ and apply again the Leibniz rule to get

$$\frac{(D^{m+1})^{(l)}(x)}{D^{m+2}(x)} = \frac{\sum_{k=0}^{l} \binom{l}{k} (D^m)^{(l-k)}(x) D^{(k)}(x)}{D^{m+1}(x) D(x)}.$$

Using the induction hypothesis as well as the bounds in (2.46) and (2.48), we then have

$$\begin{aligned} \frac{|(D^{m+1})^{(l)}(x_j)|}{|D^{m+2}(x_j)|} &\leq \frac{\sum_{p=0}^{l} \binom{l}{p} |(D^m)^{(l-p)}(x_j)| |D^{(p)}(x_j)|}{|D^{m+1}(x_j)| |D(x_j)|} \\ &= \frac{|(D^m)^{(l)}(x_j)|}{|D^{m+1}(x_j)|} + \sum_{p=1}^{l} \binom{l}{p} \frac{|(D^m)^{(l-p)}(x_j)|}{|D^{m+1}(x_j)|} \frac{|D^{(p)}(x_j)|}{|D(x_j)|} \\ &\leq C_1 h_j^{d-l} + \sum_{p=1}^{l} \binom{l}{p} C_1 h_j^{d-l+p} \frac{C_2 h_j^{-(d+p)}}{C_3 h_j^{-d}} \\ &\leq C h_j^{d-l} \end{aligned}$$

for $l = 1, \dots, d-1$. □

Lemma 2.3 generalises Theorem 2.11 by Klein and Berrut [2012] in two ways. On the one hand, it covers well-spaced interpolation nodes, which includes equidistant and quasi-equidistant nodes as special cases. On the other hand, it provides an error bound in terms of the local mesh size h_j instead of the global mesh size h. The special cases $k = 1$ and $k = 2$ also appear as Theorems 2.9 and 2.10 by Berrut et al. [2011], which are more general than Lemma 2.3 in the sense that they do not require the nodes to be well-spaced, but, as in the work of Klein and Berrut [2012], the error bound is given in terms of the global mesh size only.

2.4.2 Error at intermediate points

We now consider the convergence rate of the derivatives of e at the intermediate points between the interpolation nodes.

Lemma 2.4. For any set of well-spaced interpolation nodes, any k with $0 \leq k \leq d$, and $f \in C^{d+k+2}[a, b]$,

$$|e^{(k)}(x)| \leq C h_j^{d+1-k}, \qquad x \in (x_j, x_{j+1}), \qquad j = 0, \dots, n-1.$$

Proof. The proof of this lemma is largely inspired by Theorem 5 by Berrut et al. [2011] and roughly follows the same reasoning as the proof of Lemma 2.3. Hence, we expect the reader to already be familiar with the main arguments and keep the exposition brief.

We start by fixing the index j and writing the error in (2.41) as

$$e(x) = \psi(x)\tilde{e}(x),$$

where

$$\psi(x) = (x - x_j)(x - x_{j+1}), \qquad \tilde{e}(x) = \frac{A(x)}{D(x)}, \qquad D(x) = \psi(x)B(x).$$

By the Leibniz rule, we have

$$e^{(k)}(x) = \psi(x)\tilde{e}^{(k)}(x) + k\psi'(x)\tilde{e}^{(k-1)}(x) + \frac{k(k-1)}{2}\psi''(x)\tilde{e}^{(k-2)}(x),$$

and since it follows from the definition of ψ that

$$|\psi(x)| \leq h_j^2, \qquad |\psi'(x)| \leq 2h_j, \qquad |\psi''(x)| \leq 2, \tag{2.49}$$

it remains to show that $|\tilde{e}^{(k)}(x)| \le Ch_j^{d-1-k}$. As in the proof of Lemma 2.3, we use the Leibniz rule to obtain

$$\tilde{e}^{(k)}(x) = \sum_{l=0}^{k} \binom{k}{l} A^{(k-l)}(x)(D^{-1})^{(l)}(x)$$

and since the absolute values of A and its derivatives are bounded by some constant over $[a,b]$ for $f \in C^{d+2+k}$, it is sufficient to prove

$$|(D^{-1})^{(l)}(x)| \le Ch_j^{d-1-l}, \qquad l = 0, \dots, d.$$

Using again Hoppe's formula and the same reasoning as in the previous proof, the final step now is to prove by induction over m that

$$\frac{|(D^m)^{(l)}(x)|}{|D^{m+1}(x)|} \le Ch_j^{d-1-l}, \qquad l = 0, \dots, d \tag{2.50}$$

for any $m \ge 0$, and the crucial ingredients are a lower bound for $|D(x)|$ and an upper bound for $|D^{(l)}(x)|$.

For the lower bound, we recall from Berrut et al. [2011] that

$$|D(x)| \ge \prod_{\substack{k=i \\ k \ne j, j+1}}^{i+d} \frac{1}{|x - x_k|}, \qquad i \in I_j \setminus \{j-d\},$$

but instead of further bounding this from below by $Ch^{-(d-1)}$, we use (2.45) to obtain

$$|D(x)| \ge \prod_{k=i}^{j-1} h_{j+1,k}^{-1} \prod_{k=j+2}^{i+d} h_{j,k}^{-1} \ge Ch_j^{-(d-1)}. \tag{2.51}$$

For the upper bounds on the derivatives of D, we assume $l \ge 1$ for the moment, split $D^{(l)}(x)$ into five parts as in Berrut et al. [2011],

$$D^{(l)}(x) = E_1^{(l)}(x) + E_2^{(l)}(x) + E_3^{(l)}(x) + E_4^{(l)}(x) + E_5^{(l)}(x),$$

where

$$E_1(x) = \psi(x) \sum_{i=0}^{j-d-1} \lambda_i(x), \qquad E_2(x) = \psi(x)\lambda_{j-d}(x),$$

$$E_3(x) = \psi(x) \sum_{i=j-d+1}^{j} \lambda_i(x), \qquad E_4(x) = \psi(x)\lambda_{j+1}(x),$$

$$E_5(x) = \psi(x) \sum_{i=j+2}^{n-d} \lambda_i(x),$$

and derive separate upper bounds for each of the terms $E_i^{(l)}(x)$.

For $E_1^{(l)}(x)$, we let

$$F_1(x) = \sum_{i=0}^{j-d-1} \lambda_i(x) = \sum_{i=0}^{j-d-1} (-1)^i \prod_{k=i}^{i+d} \frac{1}{x - x_k}$$

and use the Leibniz rule to get

$$E_1^{(l)}(x) = \psi(x)F_1^{(l)}(x) + l\psi'(x)F_1^{(l-1)}(x) + \frac{l(l-1)}{2}\psi''(x)F_1^{(l-2)}(x).$$

Using the Leibniz rule again we further find that

$$F_1^{(l)}(x) = \sum_{i=0}^{j-d-1} (-1)^{i+l} l! \sum_{|\boldsymbol{\beta}_i|=l} \prod_{k=i}^{i+d} \frac{1}{(x - x_k)^{1+\beta_k}},$$

where the second sum ranges over all $(d+1)$-dimensional multi-indices $\boldsymbol{\beta}_i = (\beta_i, \ldots, \beta_{i+d})$ whose non-negative integer components sum up to l. Since $x \in (x_j, x_{j+1})$, the terms of the first sum alternate in sign and increase in absolute value, so that $|F_1^{(l)}(x)|$ is bounded from above by the absolute value of the last term. With the same reasoning as in (2.47) we then have

$$\begin{aligned} |F_1^{(l)}(x)| &\leq l! \sum_{|\boldsymbol{\beta}_{j-d-1}|=l} \prod_{k=j-d-1}^{j-1} \frac{1}{|x - x_k|^{1+\beta_k}} \\ &\leq l! \sum_{|\boldsymbol{\beta}_{j-d-1}|=l} \prod_{k=j-d-1}^{j-1} \frac{1}{h_{j,k}^{1+\beta_k}} \\ &\leq C h_j^{-(d+1+l)}, \end{aligned}$$

and together with (2.49) we conclude

$$|E_1^{(l)}(x)| \leq C h_j^{-(d-1+l)}, \qquad l = 1, \ldots, d. \tag{2.52}$$

For $E_2^{(l)}(x)$, we let

$$F_2(x) = (x - x_j)\lambda_{j-d}(x) = (-1)^{j-d} \prod_{k=j-d}^{j-1} \frac{1}{x - x_k},$$

so that

$$E_2^{(l)}(x) = (x - x_{j+1})F_2^{(l)}(x) + lF_2^{(l-1)}(x)$$

and

$$F_2^{(l)}(x) = (-1)^{j-d+l} l! \sum_{|\boldsymbol{\beta}_{j-d}|=l} \prod_{k=j-d}^{j-1} \frac{1}{(x-x_k)^{1+\beta_k}},$$

with $\boldsymbol{\beta}_{j-d}$ defined as before. Therefore,

$$|F_2^{(l)}(x)| \le l! \sum_{|\boldsymbol{\beta}_{j-d}|=l} \prod_{k=j-d}^{j-1} \frac{1}{h_{j,k}^{1+\beta_k}} \le C h_j^{-(d+l)}$$

and

$$|E_2^{(l)}(x)| \le C h_j^{-(d-1+l)}, \qquad l = 1, \dots, d. \tag{2.53}$$

For $E_3^{(l)}(x)$, we notice that

$$E_3(x) = \sum_{i=j-d+1}^{j} (-1)^i \prod_{\substack{k=i \\ k\neq j,j+1}}^{i+d} \frac{1}{x-x_k},$$

hence

$$E_3^{(l)}(x) = \sum_{i=j-d+1}^{j} (-1)^{i+l} l! \sum_{|\boldsymbol{\beta}_i|=l} \prod_{\substack{k=i \\ k\neq j,j+1}}^{i+d} \frac{1}{(x-x_k)^{1+\beta_k}}$$

and

$$|E_3^{(l)}(x)| \le \sum_{i=j-d+1}^{j} l! \sum_{|\boldsymbol{\beta}_i|=l} \prod_{\substack{k=i \\ k\neq j,j+1}}^{i+d} \frac{1}{h_{j,k}^{1+\beta_k}} \le C h_j^{-(d-1+l)}, \qquad l = 1, \dots, d. \tag{2.54}$$

Combining (2.52), (2.53), (2.54), and noting that the error bounds for $E_4^{(l)}(x)$ and $E_5^{(l)}(x)$ can be derived similarly as the bounds for $E_2^{(l)}(x)$ and $E_1^{(l)}(x)$, respectively, we finally conclude

$$|D^{(l)}(x)| \le C h_j^{-(d-1+l)}, \qquad l = 1, \dots, d. \tag{2.55}$$

We now observe that the base case $m = 0$ of (2.50) and the special case $l = 0$ follow directly from (2.51) and the induction step follows from (2.51) and (2.55) with the same arguments as in the proof of Lemma 2.3. □

While the special cases $k = 0, 1, 2$ were already covered by Floater and Hormann [2007] and Berrut et al. [2011], Lemma 2.4 generalises the result to general $0 \le k \le d$ and provides a local instead of a global error bound. However, this comes at the cost of having to assume that the interpolation nodes are well-spaced. Theorem 2.7 by Floater and Hormann [2007] and Theorem 2.9 by Berrut et al. [2011] hold for any nodes and, only in the cases $k = 0 = d$, $k = 1 = d$, $k = 2 < d$, and $k = 2 = d$, require that the mesh ratio is bounded, which is basically the first condition (2.35) of well-spaced nodes.

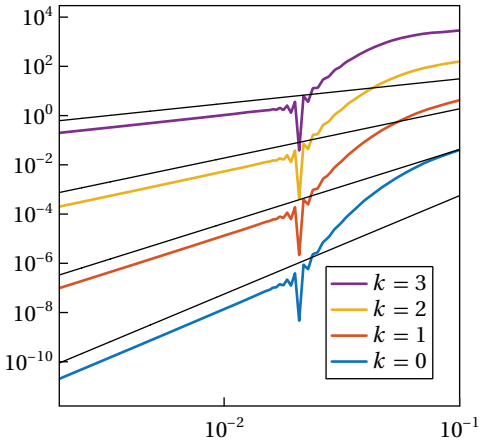

Figure 2.13. Log-log plot of $\|e^{(k)}\|$ over h for f_1 in (2.56), using equidistant nodes and $d = 3$. The straight reference lines represent the expected $O(h^{d+1-k})$ behavior.

n	$\|e\|$	order	$\|e'\|$	order	$\|e''\|$	order	$\|e'''\|$	order
10	4.03e−02		4.22e+00		1.57e+02		2.88e+03	
20	1.81e−03	4.48	3.59e−01	3.56	2.80e+01	2.49	1.01e+03	1.51
40	2.85e−06	9.31	1.11e−03	8.34	1.77e−01	7.30	1.34e+01	6.23
80	3.43e−08	6.38	2.66e−05	5.38	8.60e−03	4.37	1.33e+00	3.33
160	2.03e−09	4.08	3.14e−06	3.08	2.04e−03	2.08	6.40e−01	1.06
320	1.23e−10	4.04	3.81e−07	3.04	4.97e−04	2.04	3.14e−01	1.03
640	7.58e−12	4.02	4.69e−08	3.02	1.23e−04	2.02	1.55e−01	1.01

Table 2.1. Norm and approximation order of the error and its derivatives for f_1 in (2.56), using equidistant nodes and $d = 3$. Compare Figure 2.13.

2.4.3 Numerical examples

To confirm our theoretical results, we prepared four numerical examples, using Proposition 2.4 by Schneider and Werner [1986] for evaluating the derivatives of the rational interpolant r both at the nodes and at intermediate points. In the first two examples we investigated the behavior of the norm $\|e^{(k)}\|$ of the error and its derivatives in dependence of the global mesh size h. For both examples we used *MATLAB* with double precision (about 16 digits precision) and approximated $\|e^{(k)}\|$ by evaluating $|e^{(k)}(x)|$ at 100 equidistant points in each interval $[x_j, x_{j+1}]$, $j = 0, \ldots, n-1$. Instead, the last two examples were prepared with *MAPLE* using a precision of 30 digits and illustrate the pointwise values $|e^{(k)}(x)|$ for various x and k with respect to the local mesh size.

In our first example we study the Floater–Hormann interpolant with $d = 3$

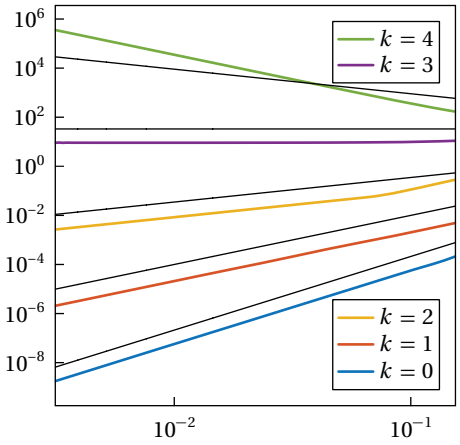

Figure 2.14. Log-log plot of $\|e^{(k)}\|$ over h for f_2 in (2.57), using Chebyshev nodes and $d = 2$. The straight reference lines represent the expected $O(h^{d+1-k})$ behavior.

n	$\|e\|_\infty$	order	$\|e'\|_\infty$	order	$\|e''\|_\infty$	order	$\|e'''\|_\infty$	order
10	2.13e−04		4.90e−03		2.85e−01		1.10e+01	
20	2.71e−05	3.03	1.27e−03	1.98	6.87e−02	2.09	9.58e+00	0.20
40	3.44e−06	2.99	3.22e−04	1.99	3.31e−02	1.06	9.24e+00	0.05
80	4.30e−07	3.00	8.10e−05	1.99	1.65e−02	1.00	9.15e+00	0.01
160	5.39e−08	3.00	2.03e−05	2.00	8.27e−03	1.00	9.13e+00	0.00
320	6.74e−09	3.00	5.07e−06	2.00	4.14e−03	1.00	9.17e+00	−0.01
640	8.42e−10	3.00	1.27e−06	2.00	2.07e−03	1.00	9.25e+00	−0.01

Table 2.2. Norm and approximation order of the error and its derivatives for f_2 in (2.57), using Chebyshev nodes and $d = 2$. Compare with Figure 2.14.

for Runge's function in the interval $[0, 1]$,

$$f_1(x) = \frac{1}{1 + 25(2x - 1)^2}, \qquad x \in [0, 1], \tag{2.56}$$

sampled at $n+1$ equidistant nodes. Table 2.1 reports the maximum norm and estimated approximation order of the error and its derivatives for several values of n. Figure 2.13 shows the maximum norm of the error and its derivatives in dependence of h for all even n from $n = 10$ to $n = 500$. We did not include the values for odd n in the plot, because they follow the same trend, but are always a bit smaller, so that including them would have resulted in slightly confusing zigzag curves. The data clearly support the first bound in Theorem 2.13.

In our second example we consider the Floater–Hormann interpolant with

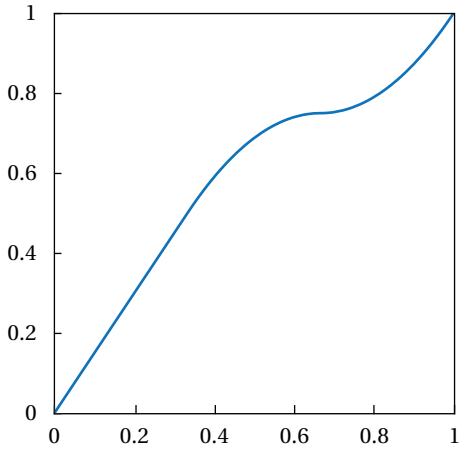

Figure 2.15. Plot of the regular distribution function G in (2.59).

$d = 2$ for the function

$$f_2(x) = \sin(\pi x), \quad x \in [0, 1], \tag{2.57}$$

sampled at the Chebyshev nodes of the second kind.[3] Table 2.2 and Figure 2.14 are similar to those of the first example. Again, the data supports our theoretical results, and the case $k = 3$ shows that the expected bound also holds for $k = d + 1$. But since we only get boundedness and not convergence in this case, we did not include it in the statement of Theorem 2.13.

In our third example we sample the function

$$f_3(x) = \exp(x^2), \quad x \in [0, 1], \tag{2.58}$$

at the interpolation nodes generated as in (2.37) with the regular distribution function

$$G(x) = \begin{cases} \frac{3}{2}x, & x \in \left[0, \frac{1}{3}\right), \\ -\frac{9}{4}x^2 + 3x - \frac{1}{4}, & x \in \left[\frac{1}{3}, \frac{2}{3}\right), \\ \frac{9}{4}x^2 - 3x + \frac{7}{4}, & x \in \left[\frac{2}{3}, 1\right], \end{cases} \tag{2.59}$$

see Figure 2.15. The obtained family of interpolation nodes is well-spaced by Theorem 2.12 by Bos et al. [2013]. For this function, the local mesh size h_j around $x = 1/4$ and $x = 3/4$ behaves differently, namely like $O(h)$ and $O(h^2)$, respectively. Therefore, the expected convergence rates of $e^{(k)}(1/4)$

[3] Note that this example is for illustration purposes only. We do not advocate the use of Floater–Hormann interpolation for these nodes, for which polynomial interpolation is better in every respect, see [Trefethen, 2013, Chpts. 7–8].

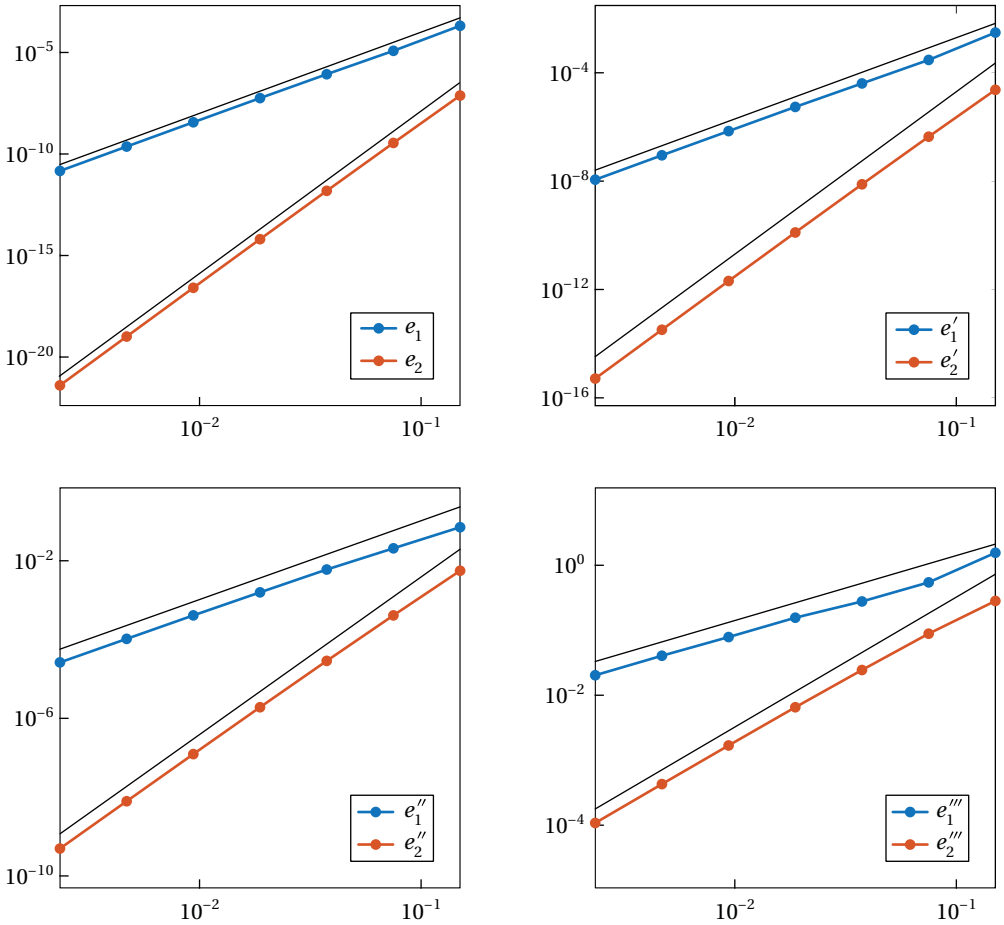

Figure 2.16. From top left to bottom right: log-log plot of $e_1^{(k)} = |e^{(k)}(1/4)|$ (in blue) and $e_2^{(k)} = |e^{(k)}(3/4)|$ (in red) over h for f_3 in (2.58), for the well-spaced nodes generated by the regular distribution function G in (2.59), $d = 3$ and $k = 0, 1, 2, 3$. The straight reference lines (in black) represent the expected $O(h^{d+1-k})$ and $O(h^{2(d+1-k)})$ behaviors.

and $e^{(k)}(3/4)$, according to Theorem 2.13, are $O(h^{d+1-k})$ and $O(h^{2(d+1-k)})$, respectively. This is confirmed by the plots in Figure 2.16 for the case $d = 3$.

In our last example we go back to Chebyshev nodes, consider the Floater–Hormann interpolant with $d = 1$ for the function

$$f_4(x) = \tfrac{3}{4}e^{-(9x-2)^2/4} + \tfrac{3}{4}e^{-(9x+1)^2/49} + \tfrac{1}{2}e^{-(9x-7)^2/4} + \tfrac{1}{5}e^{-(9x-4)^2}, \quad x \in [0,1], \tag{2.60}$$

and study the convergence rate of $e'(x)$ at the start and the center of the interpolation interval. According to Theorem 4 in Klein and Berrut [2012],

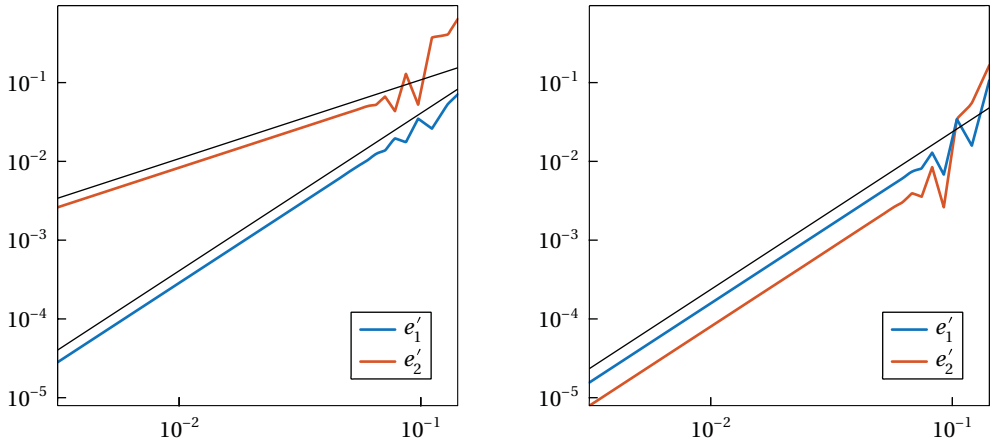

Figure 2.17. Left: log-log plot of $e_1' = |e'(0)|$ (in blue) and $e_2' = |e'(1/2)|$ (in red) over h for f_4 in (2.60), for Chebyshev nodes of the second kind, $d = 1$ and even n. The straight reference lines (in black) represent the $O(h)$ and the $O(h^2)$ behavior. Right: the same quantity for odd n. The straight reference line (in black) represents the $O(h^2)$ behavior.

the expected convergence rates of $e'(0)$ and $e'(1/2)$ with respect to the global mesh size are both $O(h)$, but while the left plot in Figure 2.17 confirms this rate for $e'(1/2)$, it also illustrates that $e'(0)$ converges at the rate of $O(h^2)$. Theorem 2.13 explains this result, because the local mesh size at $x = 0$ behaves like $O(h^2)$, while the local mesh size at $x = 1/2$ behaves like $O(h)$. However, the right plot in Figure 2.17 shows that $e'(1/2)$ converges at the rate of $O(h^2)$, too, if restricted to odd n, so that $x = 1/2$ is not an interpolation node, and it remains future work to better understand the underlying reason.

Chapter 3

A Hermite generalisation

Given a real valued function $f \in C^m[a,b]$, a set of $n+1$ interpolation nodes as in (2.1) and $m \in \mathbb{N}$, the Hermite interpolation problem consists in finding a function $g_m \colon \mathbb{R} \to \mathbb{R}$, such that

$$g_m^{(k)}(x_i) = f_i^{(k)} = f^{(k)}(x_i), \qquad i = 0, \dots, n, \quad k = 0, \dots, m. \tag{3.1}$$

We remark that, in its original form, m might not be the same at each node but, in order to keep the notation simple, in this chapter we consider the problem as stated in (3.1). However, the methods discussed here can be easily generalised to solve the original Hermite problem.

As for Lagrange interpolation, we are interested in the analysis of

$$e_m(x) = f(x) - g_m(x)$$

as the number of nodes increases. So we consider a family of interpolation nodes (2.4) and we analyse the behavior of $e_m(x)$ as $n \to \infty$. Also in this case the Hermite interpolant of order m depends on n and f, that is $g_m = g_{m,n} = g_{m,n}[f]$, but we shall omit the dependence on n and f, whenever no confusion is likely.

In the previous chapter we have seen that, when it comes to solving the Lagrange interpolation problem, the Floater–Hormann interpolant represents a valuable alternative to several other interpolation methods such as splines, classical rational interpolants and polynomials. On the one hand it is assured to be infinitely smooth while, on the other, it does not suffer from divergence problems, occurrence of poles and unattainable points. It is therefore natural to investigate whether it is possible to generalise this family of interpolants to the Hermite setting, so as to inherit these favorable properties.

The main result of this chapter is the introduction of a general, iterative approach that allows us to generalise any Lagrange interpolant of the form

$$g(x) = \sum_{i=0}^{n} b_i(x) f_i^{(0)}$$

to the Hermite setting, under assumptions on the continuity of the basis functions b_i.

In the following sections, we first present the classical polynomial approach, highlighting its advantages and critical issues. Then, we generalise the barycentric form (2.21) and some related result to the Hermite setting and we present some state-of-the-art methods for solving the Hermite problem with barycentric rational interpolants. In Section 3.3 we present the iterative method for the Hermite problem and we apply it to the Floater–Hormann basis functions (2.31). An analysis of the convergence and several numerical examples conclude this chapter.

3.1 Polynomial Hermite interpolation

Let $m \in \mathbb{N}$ be fixed. Given a set of $n+1$ nodes as in (2.1), Szabados [1993] proves that there exists a unique set of $(m+1)(n+1)$ polynomials in $\mathscr{P}_{(m+1)(n+1)-1}$

$$\ell_{i,j}(x) = \frac{\ell_i(x)^{m+1}}{j!} \sum_{k=0}^{m-j} \frac{l_{i,m}^{(k)}(x_i)}{k!} (x - x_i)^{k+j} \tag{3.2}$$

with

$$l_{i,m}(x) = \frac{1}{\ell_i(x)^{m+1}}, \qquad i = 0, \dots, n, \tag{3.3}$$

that satisfies the *Hermite property*

$$\ell_{i,j}^{(p)}(x_k) = \delta_{j,p}\delta_{i,k}, \qquad i,k = 0,\dots,n, \quad j,p = 0,\dots,m. \tag{3.4}$$

The polynomials $\ell_{i,j}$ are the generalisation of the Lagrange basis functions, and, in analogy to ℓ_i, $i = 0, \dots, n$, we refer to them as the *Hermite basis functions of order* m, see Figure 3.1. This name is justified by the fact that $\ell_{i,j}$ are a basis for $\mathscr{P}_{(m+1)(n+1)-1}$, a fact that we shall show in a moment. Given a function $f \in C^m[a,b]$, let

$$p_m(x) = \sum_{j=0}^{m} \sum_{i=0}^{n} \ell_{i,j}(x) f_i^{(j)}. \tag{3.5}$$

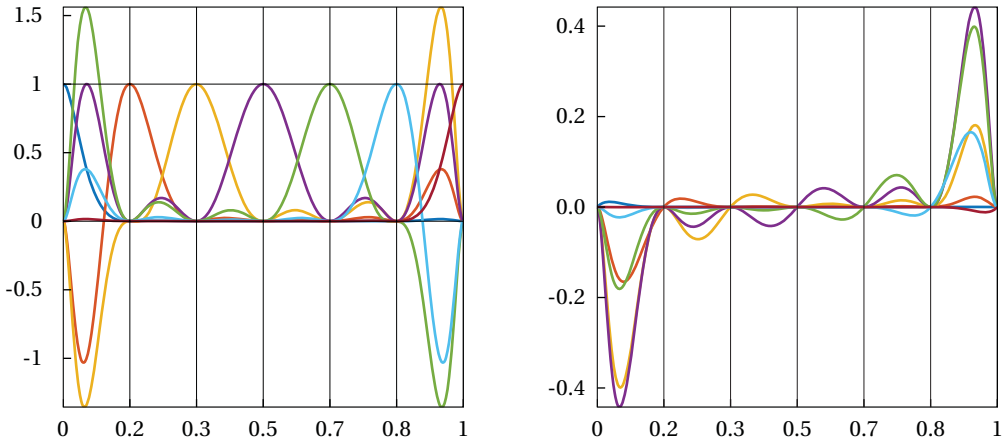

Figure 3.1. Left: the Hermite basis functions $\ell_{i,0}(x)$ at 7 equispaced nodes for $m = 1$. Right: the corresponding basis functions $\ell_{i,1}(x)$.

By the Hermite property and the uniqueness of the Hermite basis functions, p_m is the unique polynomial solution of minimal degree for the Hermite interpolation problem (3.1), see Figure 3.2.

For any choice of n, the polynomial p_m satisfies the following, see Stoer and Bulirsch [1993].

Theorem 3.1. Let $f \in C^{(m+1)(n+1)}[a, b]$. Then the polynomial interpolant (3.5) satisfies

$$e_m(x) = \ell(x)^{m+1} \frac{f^{(m+1)(n+1)}(\xi)}{((m+1)(n+1))!},$$

where ξ is inside the convex hull of $x, x_0, x_1, \ldots, x_n$ and depends on f, and ℓ is the nodal polynomial in (2.8).

Letting $A_{m,n}(x) = \ell(x)^{m+1} \|f^{(m+1)(n+1)}\|$, the previous result gives a condition for the convergence of the polynomial Hermite interpolants to the function f, that is

$$\lim_{n\to\infty} \frac{\|A_{m,n}\|}{((m+1)(n+1))!} = 0. \tag{3.6}$$

In this case the sequence of polynomial interpolants converges to f as $O(h^{(m+1)(n+1)})$, with h as in (2.10).

It follows from Theorem 3.1 that the Hermite functions are a basis for the vector space $\mathscr{P}_{(m+1)(n+1)-1}$, since it shows that, if $f \in \mathscr{P}_{(m+1)(n+1)-1}$, it can be written as a linear combination of the $\ell_{i,j}$'s, with coefficients given by the samples of f and its derivatives at the nodes.

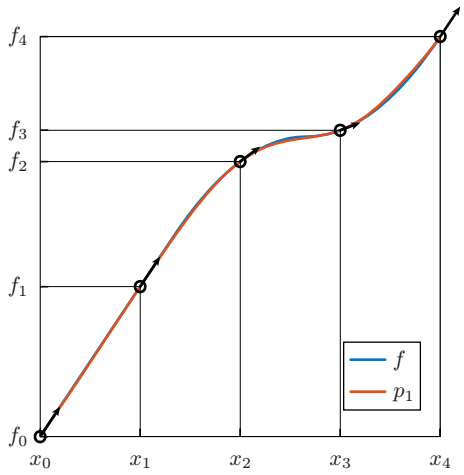

Figure 3.2. The Hermite polynomial p_1 (in red) for $m = 1$ of the function f (in blue) at 5 equispaced points. Compare Figure 2.1.

The evaluation of the interpolant p_m in (3.5) is computationally expensive. Besides the obvious cost of summing up the $(n+1)(m+1)$ terms in (3.5), the computation of $\ell_i(x)^{m+1}$ and $l_{i,m}^{(k)}(x_i)$ in (3.2) adds extra operations. Even assuming that these last constants are precomputed, each evaluation of the interpolant still requires $O(m^2 n(m+n))$ operations.

In order to decrease this number, also in this case it is possible to resort to more convenient forms. Such expressions are the generalisation of the first and second barycentric form (2.13) and (2.14). To get the former, we recall 3.2 and 3.5 and the first barycentric form of the Lagrange basis functions (2.11) to write

$$\begin{aligned}
p_m(x) &= \sum_{j=0}^{m}\sum_{i=0}^{n} \frac{\ell_i(x)^{m+1}}{j!} \sum_{k=0}^{m-j} \frac{l_{i,m}^{(k)}(x_i)}{k!}(x-x_i)^{k+j} f_i^{(j)} \\
&= \ell(x)^{m+1} \sum_{i=0}^{n}\sum_{j=0}^{m} \frac{\omega_i^{m+1}}{j!(x-x_i)^{m+1}} \sum_{k=0}^{m-j} \frac{l_{i,m}^{(k)}(x_i)}{k!}(x-x_i)^{k+j} f_i^{(j)} \\
&= \ell(x)^{m+1} \sum_{i=0}^{n}\sum_{k=0}^{m} \frac{\omega_i^{m+1}}{(x-x_i)^{m+1-k}} \frac{l_{i,m}^{(k)}(x_i)}{k!} \sum_{j=0}^{m-k} \frac{f_i^{(j)}}{j!}(x-x_i)^{j} \\
&= \ell(x)^{m+1} \sum_{i=0}^{n}\sum_{j=0}^{m} \frac{\omega_{i,j}^{[m]}}{(x-x_i)^{j+1}} \sum_{k=0}^{j} \frac{f_i^{(k)}}{k!}(x-x_i)^{k},
\end{aligned}$$

where

$$\omega_{i,j}^{[m]} = \frac{l_{i,m}^{(m-j)}(x_i)}{(m-j)!}\omega_i^{m+1}$$

and ω_i as in (2.12). We will refer to this form as the *first Hermite barycentric form*, in analogy to the Lagrange counterpart.

As pointed out by Floater and Schulz [2009], considering again (2.11) and (3.3), the barycentric weights $\omega_{i,j}^{[m]}$ can be simplified to

$$\omega_{i,j}^{[m]} = \frac{l_{i,m}^{(m-j)}(x_i)}{(m-j)!}. \tag{3.7}$$

A straightforward approach might still require a considerable number of operations for the computation of the barycentric weights but Schneider and Werner [1991] propose an algorithm to compute them in $O(m^2n^2)$ operations. Once this is done, the evaluation of the polynomial itself requires additional $O(m^2n)$ operations. Clearly, also for the first Hermite barycentric form it is possible to precompute the barycentric weights $\omega_{i,j}^{[m]}$ in higher precision and to store them for specific sets of nodes. We remark that, in most practical scenarios, $m \ll n$ and, in the analysis of the convergence of p_m, it can be considered constant. Hence, the quadratic behavior on m should not be a source of worries.

Similar to what we have observed in the Lagrange case, the first barycentric form can be further improved. Theorem 3.1 leads us to the partition of unity property of the Hermite basis functions

$$\ell(x)^{m+1} \sum_{i=0}^{n} \sum_{j=0}^{m} \frac{\omega_{i,j}^{[m]}}{(x-x_i)^{j+1}} = 1. \tag{3.8}$$

Thus, dividing the first barycentric form by 1 and simplifying the common factor $\ell(x)^{m+1}$, we get the *second Hermite barycentric form*,

$$p_m(x) = \frac{\displaystyle\sum_{i=0}^{n} \sum_{j=0}^{m} \frac{\omega_{i,j}^{[m]}}{(x-x_i)^{j+1}} \sum_{k=0}^{j} \frac{f_i^{(k)}}{k!}(x-x_i)^k}{\displaystyle\sum_{i=0}^{n} \sum_{j=0}^{m} \frac{\omega_{i,j}^{[m]}}{(x-x_i)^{j+1}}}. \tag{3.9}$$

This form of the polynomial interpolant can also be evaluated in $O(m^2n)$ operations, but, as the Lagrange counterpart, it is less susceptible to rounding errors in the computation of the weights, as we show in the next section, where we review additional properties of this Hermite barycentric form for general weights.

Relation (3.6) shows that the convergence of the sequence of polynomial interpolants is strongly influenced by the system of interpolation nodes and by the continuity of the derivatives of f. For this reason, most of the literature

about Hermite interpolation studies the convergence of p_m for fixed m and some special sets of nodes. For example, Grünwald [1942] provides several theorems on the convergence of the sequence of polynomials to the function f in the case $m = 1$. In this case the Hermite basis functions in (3.2) simplify to

$$\begin{aligned} \ell_{i,0}(x) &= u_i(x)\ell_i^2(x) \\ \ell_{i,1}(x) &= (x - x_i)\ell_i^2(x), \end{aligned} \tag{3.10}$$

with

$$u_i(x) = 1 - 2(x - x_i)\ell_i'(x_i), \qquad i = 0, \ldots, n.$$

Grünwald focuses on the so-called *normal* and ρ-*normal* nodes.

Definition 3.1. A system of interpolation nodes $X = (X_n)_{n\in\mathbb{N}}$ is said to be normal if there exists a $\rho \in \mathbb{R}$ such that

$$u_i(x) \geq \rho \geq 0, \qquad i = 0, \ldots, n, \quad x \in [a, b]$$

holds for any set X_n. If $\rho > 0$, X is said to be ρ-normal.

He points out that examples of normal families are the roots of certain Jacobi polynomials $P_{n+1}^{(\alpha,\beta)}$ in $[-1, 1]$. For $0 \leq \alpha, \beta \leq 1/2$, the corresponding family is normal with $\rho = \min\{1 - 2\alpha, 1 - 2\beta\}$. In Figure 3.3 we show such sets of nodes for $(\alpha, \beta) = (1/10, 1/10)$ (left) and $(\alpha, \beta) = (1/2, 1/2)$ (right) and we notice that, similarly to Chebyshev nodes of the first and second kind, the roots of the Jacobi polynomials tend to cluster near the endpoints of the interpolation interval.

If the function f has a continuous derivative, uniform convergence is guaranteed as long as we sample f at ρ-normal nodes.

Theorem 3.2 (Grünwald [1942])**.** Let $f \in C^1[a, b]$ and X be a ρ-normal system of interpolation nodes. Then the sequence of polynomial Hermite interpolants converges uniformly to f in $[a, b]$, that is

$$\lim_{n\to\infty} \|e_m(x)\| = 0. \tag{3.11}$$

If the function is only continuous, the derivatives of f must be uniformly bounded or X must be ρ-normal.

Theorem 3.3 (Grünwald [1942])**.** Let $f \in C^0[a, b]$ and suppose that f' exists at each point of $[a, b]$. Then (3.11) holds if one of the following conditions does

- X is a (ρ-)normal family and $\|f'\| \leq A$, $A \in \mathbb{R}$,

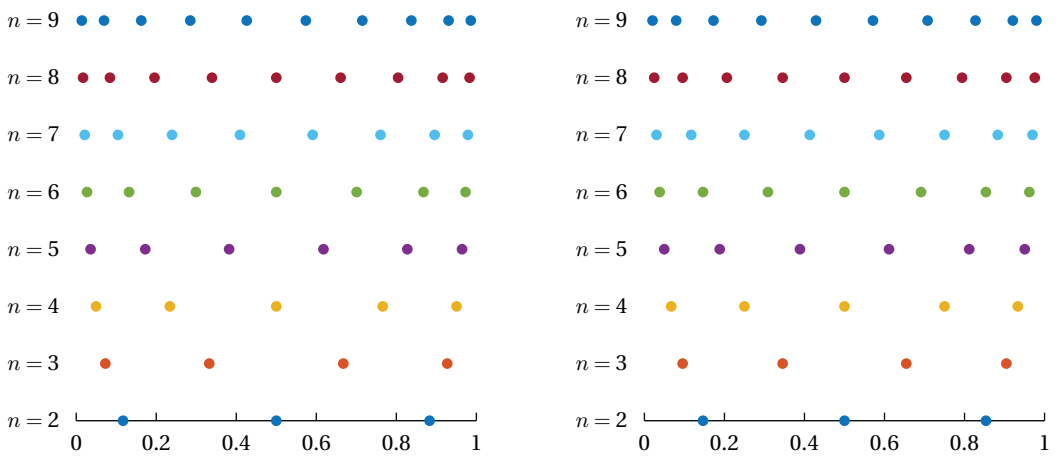

Figure 3.3. Two normal family of interpolation points, corresponding to the roots of Jacobi polynomials for $n = 2, \dots, 9$. Left: the family corresponding to $(\alpha, \beta) = (1/10, 1/10)$. Right: the one corresponding to $(\alpha, \beta) = (1/2, 1/2)$.

- X is a ρ-normal family and $\|f'\| \leq n^{\rho-\varepsilon}$, for some $\varepsilon > 0$.

More recently, Shi gives a more general result about arbitrary sets of nodes.

Theorem 3.4 (Shi [2000])**.** Let $m \geq 1$ be odd and $f \in C^{m+1}[a, b]$. Then (3.11) holds if

$$\max_{x \in [a,b]} \sum_{i=0}^{n} |\ell_{i,0}(x)| \leq C,$$

for some constant C independent of n.

We emphasize that, even though there is no explicit requirement on the distribution of the points, the function $\sum_{i=0}^{n} |\ell_{i,0}(x)|$ is strongly influenced by the location of the interpolation nodes. We give further details on the behavior of this important quantity in the next chapter, where the conditioning of the polynomial interpolant is analysed.

In Figure 3.4 we display the polynomial interpolants of the $C^0[-1, 1]$ function

$$f(x) = \frac{1}{2}|3x + 1| - \frac{9}{16}x^2 - \frac{3}{4}x$$

sampled at the root of the Jacobi polynomials $P_{n+1}^{(1/4,1/4)}$, for $n = 10, 20, 40, 80$. For more results about the convergence of polynomial Hermite interpolants, see Szabados [1993], Shi [2000] and references therein.

It should be by now clear to the reader that the polynomial Hermite interpolation converges remarkably well under assumptions on the distribution of the

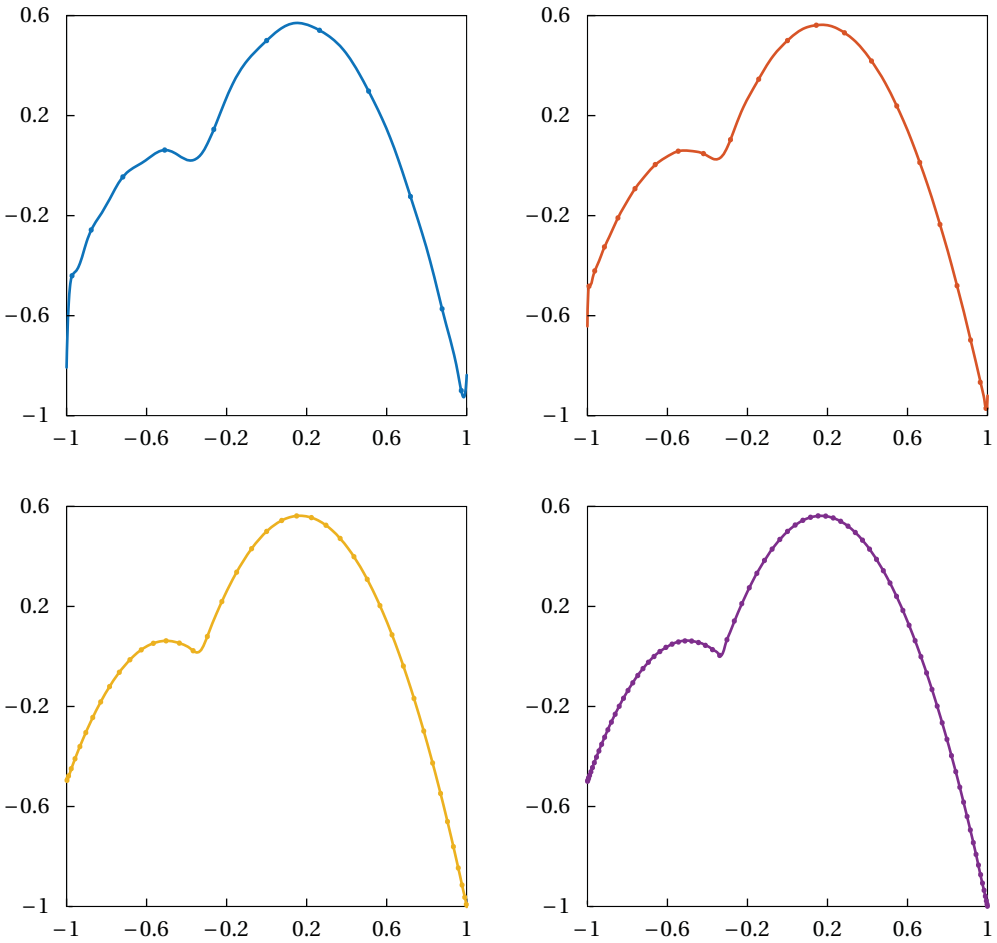

Figure 3.4. From top left to bottom right: the Hermite interpolation polynomials for $n = 10, 20, 40, 80$ at the roots of the Jacobi polynomial $P_{n+1}^{(1/4,1/4)}$.

nodes. However, the similarity between Theorem 3.1 and Theorem 2.1 might convince us that polynomial Hermite interpolation can behave catastrophically in the equispaced setting, and this is actually the case, see Figure 3.5. The result of the Hermite interpolation of the Runge function (2.16) shows the same behavior highlighted in the previous chapter, with exponential convergence in the middle of the interpolation interval and exponential divergence as we approach the tails of $[-1, 1]$. When comparing with Figure 2.2, we notice that the width of the oscillation is roughly the same already for lower values of n. The reason for this is the factor $\ell(x)^{m+1}$ in the expression of the error for Hermite interpolation in Theorem 3.1. As m increases, this factor becomes predominant in (3.6) and the Runge phenomenon becomes stronger. Therefore, no matter

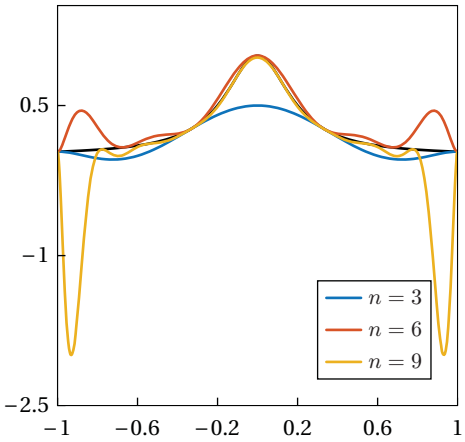

Figure 3.5. The Hermite polynomials interpolating the Runge function in (2.16) (in black), for $n = 3, 6, 9$ and $m = 1$ at equispaced nodes.

how many derivatives of f we know and how many samples we can get from them, the sequence of polynomial interpolants is not going to converge to the function. This problem easily disappears as long as we can modify the distribution of the nodes, see Figure 3.6, but, as noticed in the previous chapter, this is not always possible.

It is therefore necessary to look for some different means of solving the Hermite interpolation problem at equispaced points. In the next section we present the generalisation of the barycentric form (2.21) to the Hermite setting and statements equivalent to Propositions 2.2, 2.3 and 2.4. Moreover, we show how to retrieve the barycentric weights from the denominator of a rational Hermite interpolant, similarly as in Theorem 2.6. Finally, we review a particular choice of barycentric weights.

3.2 Barycentric Hermite rational interpolation

A rational Hermite interpolant r_m is said to be in barycentric form if

$$r_m(x) = \frac{\displaystyle\sum_{i=0}^{n}\sum_{j=0}^{m} \frac{\beta_{i,j}^{[m]}}{(x-x_i)^{j+1}} \sum_{k=0}^{j} \frac{f_i^{(k)}}{k!}(x-x_i)^k}{\displaystyle\sum_{i=0}^{n}\sum_{j=0}^{m} \frac{\beta_{i,j}^{[m]}}{(x-x_i)^{j+1}}}, \tag{3.12}$$

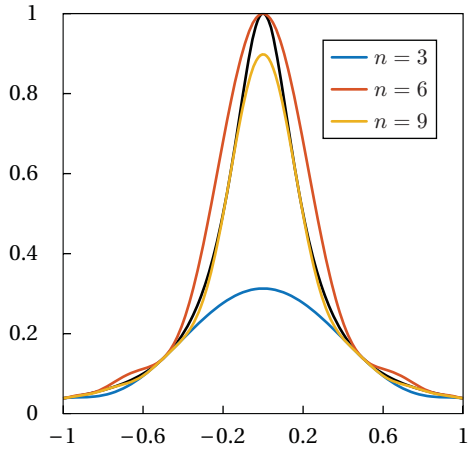

Figure 3.6. The Hermite polynomials interpolating the Runge function in (2.16) (in black), at Chebyshev nodes for $n = 3, 6, 9$ and $m = 1$.

for some barycentric weights

$$\boldsymbol{\beta}^{[m]} = \begin{pmatrix} \beta_{0,0}^{[m]} & \beta_{0,1}^{[m]} & \cdots & \beta_{0,n}^{[m]} \\ \beta_{1,0}^{[m]} & \beta_{1,1}^{[m]} & \cdots & \beta_{1,n}^{[m]} \\ \vdots & & \ddots & \vdots \\ \beta_{m,0}^{[m]} & \beta_{m,1}^{[m]} & \cdots & \beta_{m,n}^{[m]} \end{pmatrix}.$$

Schneider and Werner [1991] prove several important properties of the barycentric weights $\beta_{i,j}^{[m]}$ and how they affect the behavior of r_m. In particular, they give a sufficient condition for a barycentric Hermite interpolant in reduced form to be a solution of (3.1) and a necessary condition for the absence of poles in the interpolation interval.

Proposition 3.1 (Schneider and Werner [1991])**.** Let r_m be as in (3.12). If $\beta_{i,m-k+1}^{[m]} = \cdots = \beta_{i,m}^{[m]} = 0$ and $\beta_{i,m-k}^{[m]} \neq 0$ for some $0 \leq k \leq m$, then

$$r_m^{(j)}(x_i) = f_i^{(j)}, \qquad j = 0, \ldots, m-k.$$

Moreover, if r_m has no pole in $[a, b]$, then

$$\operatorname{sign}\beta_{i,m}^{[m]} = (-1)^{m+1}\operatorname{sign}\beta_{i+1,m}^{[m]}, \qquad i = 0, \ldots, n.$$

The previous result states two important properties for the Hermite barycentric form. On the one hand, r_m is a solution of the Hermite interpolation problem as long as $\beta_{i,m}^{[m]} \neq 0$, $i = 0, \ldots, n$, while no restriction is needed for all

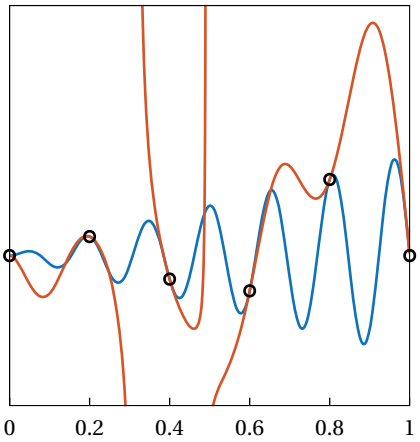

(a) $\boldsymbol{\beta}^{[1]} = \begin{pmatrix} 41 & -25 & -10 & 10 & -25 & 41 \\ 3 & 12 & -12 & 12 & 12 & 3 \end{pmatrix}$

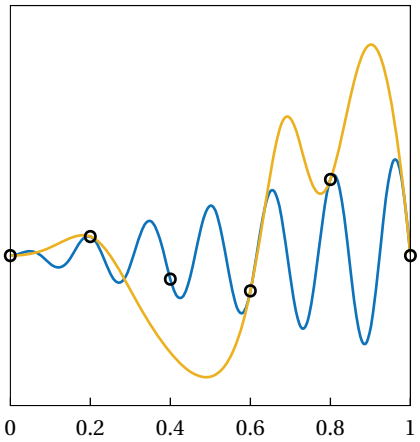

(b) $\boldsymbol{\beta}^{[1]} = \begin{pmatrix} 47 & -25 & 0 & -20 & 25 & -47 \\ 6 & 6 & 0 & 6 & 6 & 6 \end{pmatrix}$

Figure 3.7. An example illustrating Proposition 3.1 for two different interpolants of the same function (in blue) at 6 equispaced points: (a) an interpolant (in red) with two poles in (x_1, x_2) and (x_2, x_3); (b) an interpolant (in yellow) with an unattainable point.

other barycentric weights. On the other hand, we can easily identify the first unattainable support point $(x_i, f_i^{(m-k+1)})$ by finding the integer k such that $\beta_{i,m-k+1}^{[m]} = \cdots = \beta_{i,m}^{[m]} = 0$ but $\beta_{i,m-k}^{[m]} \neq 0$, see Figure 3.7, left. From these properties and the uniqueness of the Hermite basis functions, we deduce that $\omega_{i,j}^{[m]}$ in (3.7) are the only non-zero weights for which the function (3.12) is a polynomial. Moreover, denoting with

$$q(x) = \ell(x)^{m+1} \sum_{i=0}^{n} \sum_{j=0}^{m} \frac{\beta_{i,j}^{[m]}}{(x - x_i)^{j+1}}$$

the polynomial denominator of r_m, it has been proved the following closed form for the error of r_m.

Proposition 3.2 (Schneider and Werner [1991])**.** Let r_m be as in (3.12) and $x \in \mathbb{R}$ be such that $q(x) \neq 0$. Then

$$e_m(x) = \frac{\ell(x)^{m+1}}{q(x)} \sum_{i=0}^{n} \sum_{j=0}^{m} \beta_{i,j}^{[m]} f[(x_i)^{k+1}, x]. \tag{3.13}$$

Schneider and Werner [1991] also provide formulas for the computation of the derivatives of r_m, both at the nodes and at the intermediate points.

Proposition 3.3 (Schneider and Werner [1991])**.** Let r_m be as in (3.12). Then the following holds.

- If $x \in \mathbb{R} \setminus X_n$ and $q(x) \neq 0$,

$$\frac{r_m^{(p)}(x)}{p!} = \frac{\displaystyle\sum_{i=0}^{n}\sum_{j=0}^{m} \frac{\beta_{i,j}^{[m]}}{(x-x_i)^{j+1}} \sum_{k=0}^{j} r[(x_i)^{k+1}, (x)^p]}{\displaystyle\sum_{i=0}^{n}\sum_{j=0}^{m} \frac{\beta_{i,j}^{[m]}}{(x-x_i)^{j+1}}}.$$

- If $\beta_{i,m-p}^{[m]} \neq 0$ for some $0 \leq p \leq m$ but $\beta_{i,m-q}^{[m]} = 0$ for $1 \leq q \leq p$, then for any $s \in \mathbb{N}$ such that $s - p + m \geq 0$

$$\frac{r_m^{(s-p+m)}(x_j)}{(s-p+m)!} = \\ -\frac{1}{\beta_{j,m-p}^{[m]}} \left(\sum_{i=0, i\neq j}^{n} \sum_{k=0}^{m} \beta_{i,k}^{[m]} r[(x_i)^{k+1}, (x_j)^s] + \sum_{k=0}^{m-1-p} \beta_{j,k}^{[m]} \frac{r_m^{(k+s)}(x_j)}{(k+s)!} \right).$$

This proposition will be useful in next section, where we provide an upper bound for the error of our interpolant for $m = 2$. Finally, the same authors find a relation between the denominator q and the barycentric weights.

Lemma 3.1 (Schneider and Werner [1991])**.** The barycentric weights of the Hermite interpolant r_m satisfy

$$\beta_{i,m-k} = \frac{1}{k!} \left(\Omega_i^{[m]}\right)^{(k)}(x_i),$$

with

$$\Omega_i^{[m]}(x) = l_{i,m}(x) q(x),$$

and $l_{i,m}$ in (3.3).

Lemma 3.1 will be useful in Section 3.3, to obtain a closed form for the barycentric weights of our family of interpolants. Note that if r_m is the Hermite polynomial interpolant, by the partition of unity property (3.8), the barycentric weights formula simplifies to (3.7).

Since the interpolant (3.12) is defined by the barycentric weights $\beta_{i,j}^{[m]}$ and the support points $(x_i, f_i^{(k)})$, Lemma 3.1 shows that, also in this setting, the interpolant r_m is completely determined by its denominator. Therefore, Schneider and Werner [1991] propose to prescribe q and define the interpolant r_m accordingly. Their strategy consists in choosing a positive denominator in $[a, b]$

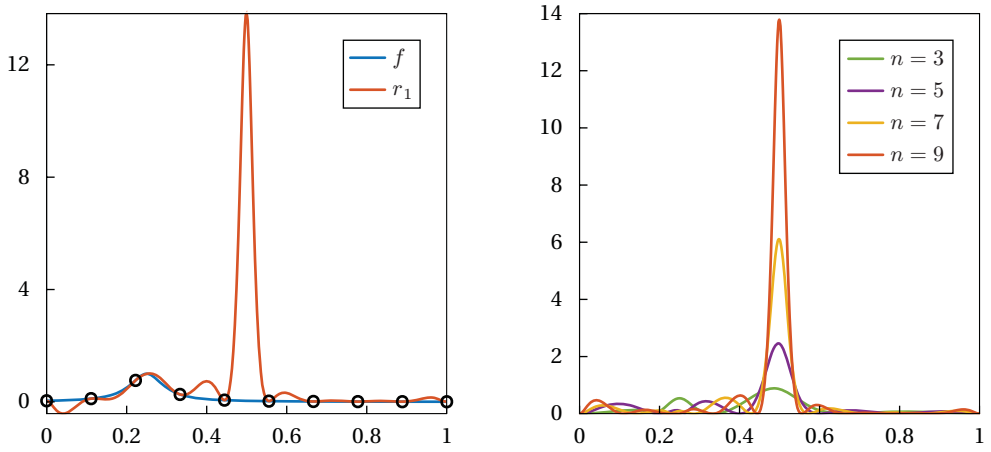

Figure 3.8. Left: Schneider–Werner interpolant r_1 (in red) of the function f (in blue) in (3.15) at 10 equispaced nodes. Right: error produced by r_1 for the same function and $n = 3, 5, 7, 9$, at equidistant nodes.

such that it minimises the term $|\ell(x)^{m+1}/q(x)|$ in (3.13) and they focus on the choice

$$q(x) = \frac{1}{2}\left(\prod_{j=0}^{a_n}(x - x_j)^2 + \prod_{j=b_n}^{n}(x - x_j)^2\right) \tag{3.14}$$

where

$$a_n = \begin{cases} n/2 - 1 & \text{if } n \text{ is even,} \\ (n-1)/2 & \text{if } n \text{ is odd,} \end{cases} \qquad \text{and} \qquad b_n = \begin{cases} n/2 + 1 & \text{if } n \text{ is even,} \\ (n+1)/2 & \text{if } n \text{ is odd.} \end{cases}$$

Unfortunately the corresponding interpolant r_m can give huge approximation errors near the center of $[a, b]$ for odd n, see Figure 3.8, left. Already for $n = 9$ we observe a huge oscillation of the interpolant r_1 of the function

$$f(x) = \frac{1}{400x^2 - 200x + 26}, \qquad x \in [0, 1], \tag{3.15}$$

near the center of $[0, 1]$. This effect is due to the fact that (3.14) has been chosen in order to uniformly bound the term $|\ell(x)^{m+1}/q(x)|$ only near the end points of the interpolation interval, in order to prevent the appearance of the Runge phenomenon due to the factor $\ell(x)^{m+1}$ in (3.13). The corresponding error for $n = 3, 5, 7, 9$ is displayed in Figure 3.8, right.

Zhao et al. [2010] propose a different approach based on the optimisation of the weights $\beta_{i,j}^{[m]}$. Their method minimises the square of the approximation error subject to certain constraints, including the positivity of q. Anyway this

requires to solve a nonlinear optimization problem and the resulting weights are not independent of f.

In order to get barycentric rational Hermite interpolants with no poles in $\mathbb{R}$ and good approximation rates, the Floater–Hormann interpolant has been generalised in two ways.

Floater and Schulz [2009] derive a Hermite version of the Floater–Hormann interpolant by considering a set of interpolation nodes with multiplicity $m+1$, that is

$$\underbrace{y_0, \dots, y_m}_{=x_0}, \underbrace{y_{m+1}, \dots, y_{2m+1}}_{=x_1}, \dots, \underbrace{y_{n(m+1)}, \dots, y_{n(m+1)+m}}_{=x_n}.$$

Their idea arises from the fact that the polynomial interpolant in *Newton form*

$$p(x) = \sum_{i=0}^{n(m+1)+m} \prod_{j=0}^{i-1} (x - y_j) f[y_0, \dots, y_i] \tag{3.16}$$

coincides with the Hermite interpolant p_m in (3.5) (Gautschi [1997]). The Floater–Hormann interpolant (2.24) defined on such a set of nodes results then to be a blend of local Hermite polynomial interpolants of different orders. If we denote this interpolant with r_m^{FS}, it can be shown that it satisfies the following result.

Proposition 3.4 (Floater and Schulz [2009])**.** If $d \geq m$, the rational function r_m^{FS} has no poles in $\mathbb{R}$ and is a solution of the Hermite interpolation problem (3.1). If $d < m$, the support points $(x_i, f_i^{(m)})$, $i = 0, \dots, n$, are unattainable.

The interpolant r_m^{FS} does not suffer from the same problem shown for the approach proposed by Schneider and Werner [1991], see Figure 3.9. Indeed, since it is defined as the classical Floater–Hormann interpolant on a particular set of nodes, the interpolant r_m^{FS} satisfies Theorem 2.7 and so converges uniformly as $O(h^{d+1})$, as $h \to 0$. Floater and Schulz [2009] also provide a closed form for the barycentric weights $\beta_{i,j}^{[m]}$ and propose to compute them efficiently with the algorithm by Schneider and Werner [1991].

The second generalisation of Floater–Hormann interpolants is the one proposed by Jing et al. [2015] who focus on the special case $m = 1$ and propose to define the rational function

$$r_1^{\mathsf{JKZ}}(x) = \sum_{i=0}^{n} \lambda_i(x)^2 q_i(x) \Big/ \sum_{i=0}^{n} \lambda_i(x)^2,$$

where q_i denotes the unique Hermite polynomial of degree at most d that interpolates $f_j^{(0)}$ and $f_j^{(1)}$ at x_j, $j = i, \dots, i+(d-1)/2$ and λ_i defined as in (2.23).

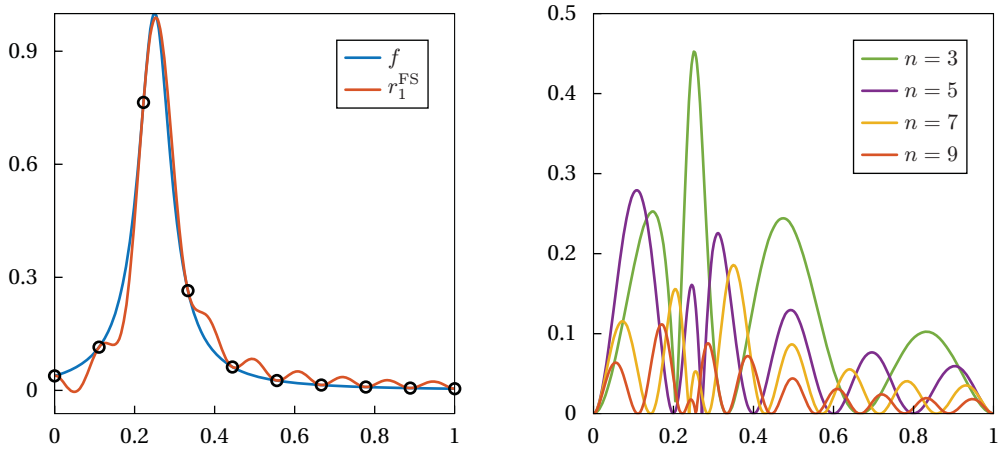

Figure 3.9. Left: the Hermite interpolant r_1^{FS} (in red) of the function f (in blue) in (3.15) at 10 equispaced nodes. Right: error produced by r_1^{FS} for the same function and $n = 3, 5, 7, 9$, at equidistant nodes. Compare with Figure 3.8.

Since $m = 1$, the local polynomial interpolant must have odd degree, so the q_i's are well-defined. For any d, $0 < d \leq n$, such a construction guarantees that r_1^{JKZ} is a solution for the Hermite problem (3.1).

The approaches of Jing et al. [2015] and Floater and Schulz [2009] are similar but the latter is a blend of a larger number of local polynomial interpolants, see Figure 3.10. In the example, we show the local polynomials of degree at most 1 that are used to construct r_1^{JKZ} and r_1^{FS}. While the former blends only local Hermite polynomials of maximal order at every point, the approach by Floater and Schulz [2009] additionally blends the Lagrange polynomials of degree 1 connecting the support points $(x_j, f_j^{(0)})$, $j = 0, \ldots, n$.

The lower number of local interpolants clearly must have an effect on the approximation order of the method. Indeed, if we denote with e_1^{JKZ} the error produced by r_1^{JKZ}, it is possible to show the following.

Theorem 3.5 (Jing et al. [2015])**.** Suppose $d = 2k+1$, $k \geq 0$, and $f \in C^{d+1}[a, b]$. If the system of nodes is quasi-equispaced, then

$$\|e_1^{\mathrm{JKZ}}\| \leq Ch^d,$$

where C is a constant depending on d, the constant c in (2.5), the interpolation interval $[a, b]$ and derivatives of f.

Jing et al. [2015] derive also bounds for the approximation rate of the first derivative of r_1^{JKZ}.

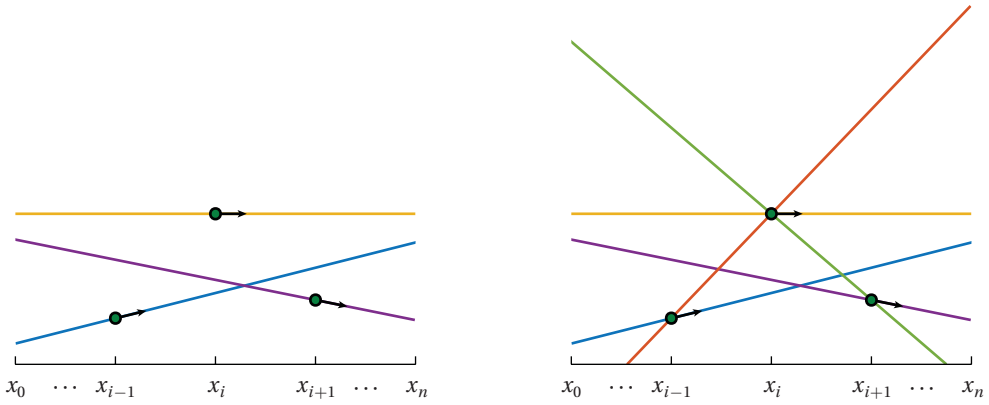

Figure 3.10. Left: the linear local polynomial interpolants used to construct r_1^{JKZ}. Right: the linear polynomials used to construct r_1^{FS}.

Theorem 3.6 (Jing et al. [2015])**.** Suppose $d = 2k+1$, $k \geq 2$, and $f \in C^{d+2}[a, b]$. In the system of nodes is quasi-equispaced, then

$$\|e_1^{\text{JKZ}'}\| \leq Ch^{d-2},$$

where C is a constant depending on the constant c in (2.5), the interpolation interval $[a, b]$ and derivatives of f.

Jing et al. improve this last result for $d = 3$, but at the cost of requiring that (2.33) is bounded. Finally, they also provide a closed form for the barycentric weights $\beta_{i,j}^{[m]}$ that can be computed in $O(d^2 n)$ operations.

In the next section we propose an iterative approach which is general enough to extend the Floater–Hormann interpolant to the Hermite setting, providing an alternative barycentric rational solution to (3.1). The main idea behind our approach is that it is possible to define a Hermite interpolant starting from the simpler Lagrange solution, by iteratively correcting its higher order derivatives at the nodes. After the description of the method and an example, we analyse the convergence rate of the proposed interpolant and we compare it with the methods reviewed in this section. We show that our approach produces an interpolant r_m that has the same convergence rate as the interpolant by Floater and Schulz [2009], but with a smaller maximum approximation error in all our numerical tests (Section 3.4.3).

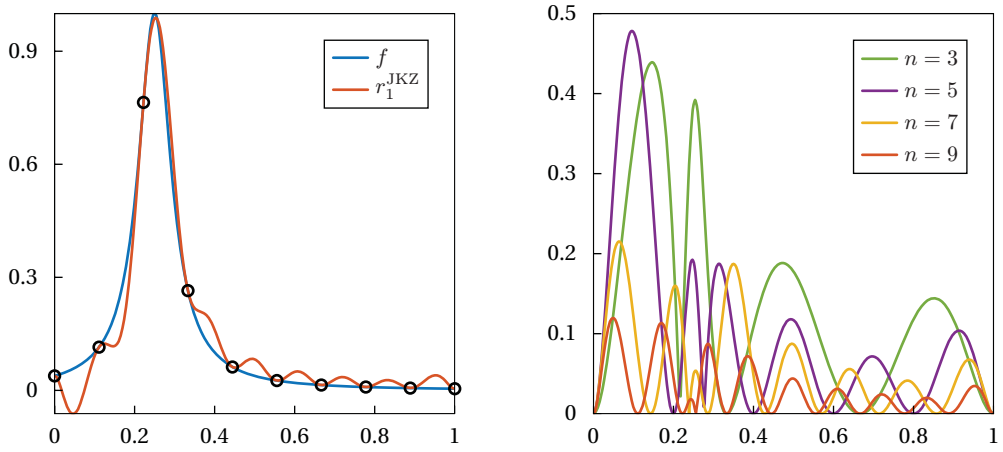

Figure 3.11. Left: the Hermite interpolant r_1^{JKZ} (in red) of the function f (in blue) in (3.15) at 10 equispaced nodes. Right: error produced by r_1^{JKZ} for the same function and $n = 3, 5, 7, 9$, at equidistant nodes. Compare Figures 3.8 and 3.9.

3.3 An iterative approach to barycentric rational Hermite interpolation

In the last section we have seen that the polynomial Hermite interpolant can either be expressed as (3.5) or in Newton form (3.16), but it can also be obtained *iteratively* in the following way.

Starting from the Lagrange polynomial

$$p_0(x) = \sum_{i=0}^{n} \ell_i(x) f_i^{(0)},$$

the polynomial $p_1 \in \mathscr{P}_{2n+1}$ that additionally interpolates the first derivatives $f_0^{(1)}, \ldots, f_n^{(1)}$ at $x_0, \ldots, x_n$, can be obtained by adding the correction term

$$q_1(x) = \sum_{i=0}^{n} \ell_{i,1}(x)\Big(f_i^{(1)} - p_0'(x_i)\Big),$$

with $\ell_{i,1}$ as in (3.10). Indeed, since $\ell_{i,1}$ satisfies the Hermite property (3.4), it is clear that

$$p_1(x) = p_0(x) + q_1(x) = \sum_{i=0}^{n}\Big(\ell_i(x) f_i^{(0)} + \ell_{i,1}(x)\Big(f_i^{(1)} - p_0'(x_i)\Big)\Big),$$

satisfies the conditions in (3.1) for $m = 1$, and by the uniqueness of the polynomial Hermite interpolant, p_1 coincides with the interpolant (3.5). A similar

approach can be used to construct the polynomial $r_m \in \mathscr{P}_{(m+1)(n+1)-1}$ that fits the data up to the m-th derivatives by iteratively adding appropriate correction terms.

Our key observation is that this construction works for any sufficiently smooth initial set of basis functions that satisfy the Lagrange property, and the main purpose of this section is to discuss the combination of this approach with the rational basis functions of the Floater–Hormann interpolation scheme. The resulting Hermite interpolant has no poles in $\mathbb{R}$ and has numerator and denominator of degree at most $(m+1)(n+1)-1$ and $(m+1)(n-d)$, where d is the degree of the local polynomial interpolants in (2.24). After the discussion of the iterative approach, and some clarifying example, we proceed with the derivation of the barycentric form of the new interpolant.

3.3.1 Iterative Hermite interpolation

Let $m \in \mathbb{N}$ and $b_0, \dots, b_n$ be some basis functions that satisfy the Lagrange property (2.6) and are m times differentiable at x_l for $l = 0, \dots, n$. We then define the functions

$$b_{i,j}(x) = \frac{(x - x_i)^j}{j!} b_i(x)^{j+1}, \qquad i = 0, \dots, n, \quad j = 0, \dots, m. \tag{3.17}$$

Lemma 3.2. The functions $b_{i,j}$ in (3.17) satisfy the Hermite property (3.4).

Proof. For $j = 0$, the statement follows directly from the Lagrange property of the functions b_i. For $j > 0$, we prove it by induction over j. To this end, let

$$c_i(x) = (x - x_i) b_i(x),$$

so that we can write $b_{i,j}$ as

$$b_{i,j}(x) = \frac{1}{j} c_i(x) b_{i,j-1}(x).$$

By the Leibniz rule,

$$b_{i,j}^{(k)}(x) = \frac{1}{j} \sum_{p=0}^{k} \binom{k}{p} c_i^{(k-p)}(x) b_{i,j-1}^{(p)}(x),$$

and since $c_i(x_l) = 0$ and $b_{i,j-1}^{(p)}(x_l) = 0$ for $p < j-1$ by the induction hypothesis, we get

$$b_{i,j}^{(k)}(x_l) = \frac{1}{j} \sum_{p=j-1}^{k-1} \binom{k}{p} c_i^{(k-p)}(x_l) b_{i,j-1}^{(p)}(x_l).$$

The statement then follows by noticing that the sum is empty if $k < j$, and that if $k = j$, then

$$b_{i,j}^{(k)}(x_l) = \frac{1}{j}\binom{j}{j-1} c_i'(x_l) b_{i,j-1}^{(j-1)}(x_l) = \delta_{i,l},$$

again by the induction hypothesis and the fact that $c_i'(x_i) = 1$. □

Starting from the Lagrange interpolant

$$g_0(x) = \sum_{i=0}^{n} b_{i,0}(x) f_i^{(0)},$$

we can now use the functions $b_{i,j}$ to construct

$$g_j(x) = g_{j-1}(x) + q_j(x), \qquad j = 1, \ldots, m, \tag{3.18}$$

by iteratively adding the correction terms

$$q_j(x) = \sum_{i=0}^{n} b_{i,j}(x)\Big(f_i^{(j)} - g_{j-1}^{(j)}(x_i)\Big), \qquad j = 1, \ldots, m,$$

to get the Hermite interpolant g_m.

Theorem 3.7. The function g_m in (3.18) satisfies the Hermite interpolation conditions (3.1).

Proof. By Lemma 3.2 we have

$$q_j^{(k)}(x_l) = \sum_{i=0}^{n} b_{i,j}^{(k)}(x_l)\Big(f_i^{(j)} - g_{j-1}^{(j)}(x_i)\Big) = \begin{cases} 0, & \text{if } k < j, \\ f_l^{(k)} - g_{j-1}^{(k)}(x_l), & \text{if } k = j, \end{cases}$$

hence

$$g_j^{(k)}(x_l) = \begin{cases} g_{j-1}^{(k)}(x_l), & \text{if } k < j, \\ f_l^{(k)}, & \text{if } k = j, \end{cases}$$

and the statement then follows by induction over j. □

By construction, it is clear that the Hermite interpolant g_m depends linearly on the given data. In the special case of polynomial interpolation, where the b_i are the Lagrange basis functions (2.5), we notice that $b_{i,j} \in \mathscr{P}_{(j+1)(n+1)-1}$ for $i = 0, \ldots, n$ and $j = 0, \ldots, m$, hence $g_m \in \mathscr{P}_{(m+1)(n+1)-1}$. Therefore, by the uniqueness of the polynomial Hermite interpolant, the iteratively defined and the classical Hermite interpolant must be the same.

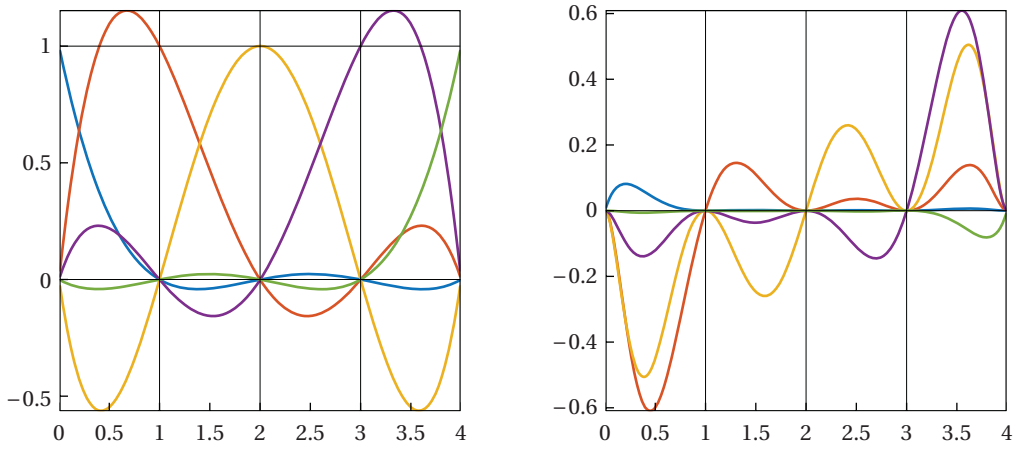

Figure 3.12. The Hermite basis functions for $m = 1$ and the interpolation nodes $x_i = i$, $i = 0, \ldots, 4$. Left: the polynomials $b_i = b_{i,0} = \ell_i$. Right: the polynomials $b_{i,1} = \ell_{i,1}$.

Example 3.1. For $n = 4$, let us consider the interpolation nodes

$$x_0 = 0, \qquad x_1 = 1, \qquad x_2 = 2, \qquad x_3 = 3, \qquad x_4 = 4,$$

the function values

$$f_0^{(0)} = 5, \qquad f_1^{(0)} = 3, \qquad f_2^{(0)} = -5, \qquad f_3^{(0)} = -7, \qquad f_4^{(0)} = 9,$$

and the derivative data

$$f_0^{(1)} = 17, \qquad f_1^{(1)} = -7, \qquad f_2^{(1)} = -2, \qquad f_3^{(1)} = 0, \qquad f_4^{(1)} = 33.$$

Taking the Lagrange basis functions, see Figure 3.12, left, as b_i in (3.17) gives the polynomial Lagrange interpolant

$$p_0(x) = 2x^3 - 9x^2 + 5x + 5,$$

see Figure 3.13. Its first order derivatives

$$p_0'(0) = 5, \qquad p_0'(1) = -7, \qquad p_0'(2) = -7, \qquad p_0'(3) = 5, \qquad p_0'(4) = 29$$

do not match the given derivative data, except at $x_1 = 1$. This can be fixed by adding the correction term

$$q_1(x) = 12b_{0,1}(x) + 5b_{2,1}(x) - 5b_{3,1}(x) + 4b_{4,1}(x),$$

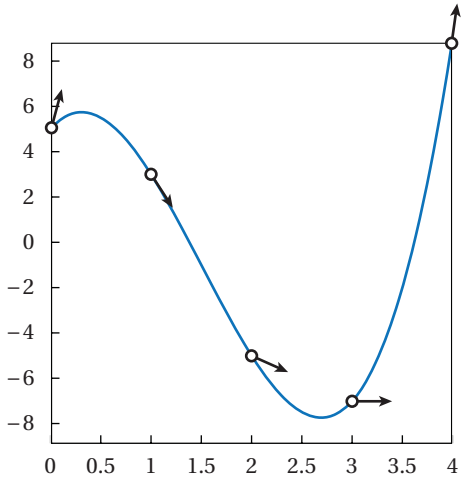

Figure 3.13. Lagrange interpolant p_0 for the data in Example 3.1 and the basis functions in Figure 3.12.

see Figure 3.14, left, because the basis functions

$$b_{i,1}(x) = (x - x_i)b_i(x)^2 = (x - x_i)\ell_i(x)^2,$$

see Figure 3.12, right, of this correction term modify only the first derivatives at the interpolation nodes, but not the function values, to yield the polynomial Hermite interpolant

$$\begin{aligned} p_1(x) &= p_0(x) + q_1(x) \\ &= \tfrac{29}{144}x^9 - \tfrac{91}{24}x^8 + \tfrac{237}{8}x^7 - 124x^6 + \tfrac{14371}{48}x^5 + \\ &\quad - \tfrac{3343}{8}x^4 + \tfrac{2887}{9}x^3 - \tfrac{370}{3}x^2 + 17x + 5, \end{aligned}$$

see Figure 3.14, right.

3.3.2 Iterative rational Hermite interpolation

In order to combine the iterative construction in Subsection 3.3.1 with the Floater–Hormann interpolation scheme, we recall that it can be rewritten in barycentric form as

$$r_0(x) = \sum_{i=0}^{n} b_i(x) f_i^{(0)}, \tag{3.19}$$

with the basis functions b_i in (2.31) that satisfy the Lagrange property and the barycentric weights in (2.26).

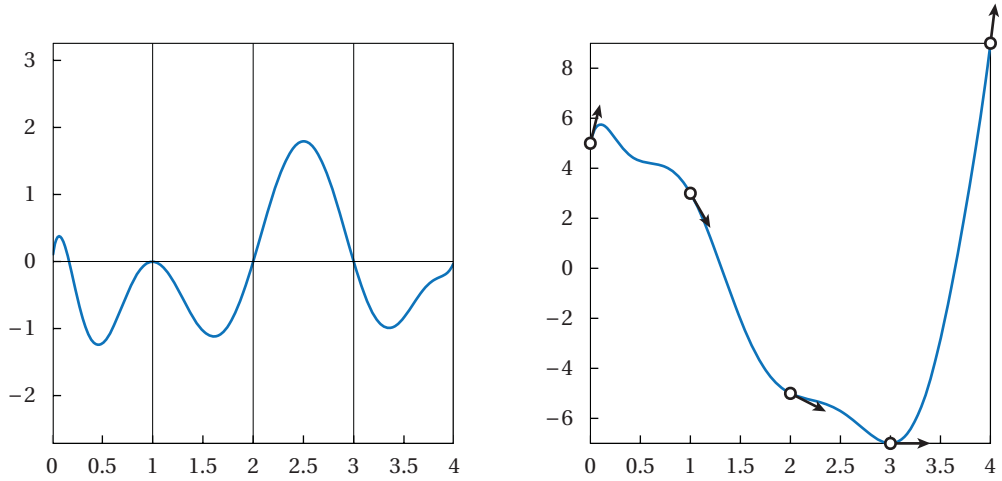

Figure 3.14. Left: correction term q_1 for the data in Example 3.1 and the basis functions in Figure 3.12. Right: the corresponding Hermite interpolant p_1.

Following the construction in (3.18), we now define the *iterative rational Hermite interpolant* as

$$r_m(x) = \sum_{i=0}^{n} \sum_{j=0}^{m} (x - x_i)^j b_i(x)^{j+1} g_{i,j}, \tag{3.20}$$

where

$$g_{i,0} = f_i^{(0)}, \qquad g_{i,j} = \left(f_i^{(j)} - r_{j-1}^{(j)}(x_i)\right)/j! \tag{3.21}$$

for $j = 1, \ldots, m$.

It follows from Theorem 3.7 that r_m satisfies (3.1), and since Floater–Hormann interpolants and in particular the basis functions in (2.31) do not have any poles in $\mathbb{R}$, it is clear by construction that the same holds for r_m. Let us now investigate the degree of r_m.

Proposition 3.5. The numerator and denominator of the iterative rational Hermite interpolant r_m in (3.20) have degree at most $(m+1)(n+1) - 1$ and $(m+1)(n-d)$, respectively.

Proof. We first recall from Theorem 2.8 that the degrees of the numerator and the denominator of the Floater–Hormann interpolant r are at most n and $n - d$, respectively. Therefore, the basis functions b_i in (2.31) can be written in rational form as

$$b_i(x) = \frac{P_i(x)}{Q(x)}, \qquad i = 0, \ldots, n,$$

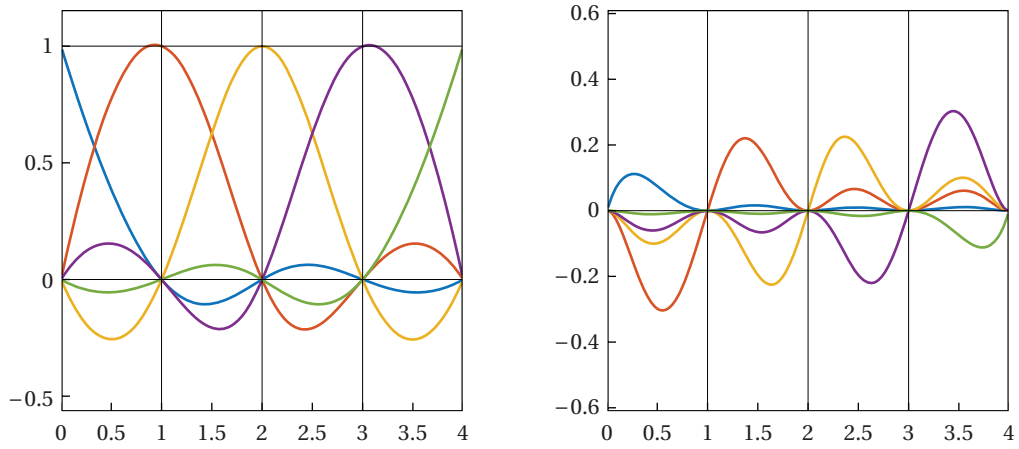

Figure 3.15. The rational Floater–Hormann basis functions for $m = 1$, $d = 1$ and the interpolation nodes $x_i = i$, $i = 0, \ldots, 4$. Left: the rational functions $b_i = b_{i,0}$. Right: the rational functions $b_{i,1}$.

with certain numerators $P_i \in \mathscr{P}_n$ and a common denominator $Q \in \mathscr{P}_{n-d}$, so that

$$\begin{aligned} r_m(x) &= \sum_{i=0}^{n} \sum_{j=0}^{m} (x - x_i)^j \left(\frac{P_i(x)}{Q(x)} \right)^{j+1} g_{i,j} \\ &= \frac{\sum_{i=0}^{n} \sum_{j=0}^{m} (x - x_i)^j P_i(x)^{j+1} Q(x)^{m-j} g_{i,j}}{Q(x)^{m+1}}. \end{aligned} \tag{3.22}$$

Independently of i, the degrees of the terms in the numerator of r_m in (3.22) are

$$j + (j+1)n + (m-j)(n-d) \le (m+1)(n+1) - 1, \qquad j = 0, \ldots, m,$$

and the degree of the denominator of r_m is at most $(m+1)(n-d)$. □

Example 3.2. For the interpolation nodes, functions values, and derivative data from Example 3.1, the Floater–Hormann basis functions b_i in (2.31) for $d = 1$, see Figure 3.15, left, give rise to the rational Lagrange interpolant

$$r_0(x) = \frac{3x^4 - 17x^3 + 31x^2 - 38x + 30}{x^2 - 4x + 6},$$

see Figure 3.16, whose first order derivatives

$$r_0'(0) = -3, \qquad r_0'(1) = -3, \qquad r_0'(2) = -11, \qquad r_0'(3) = 9, \qquad r_0'(4) = 21$$

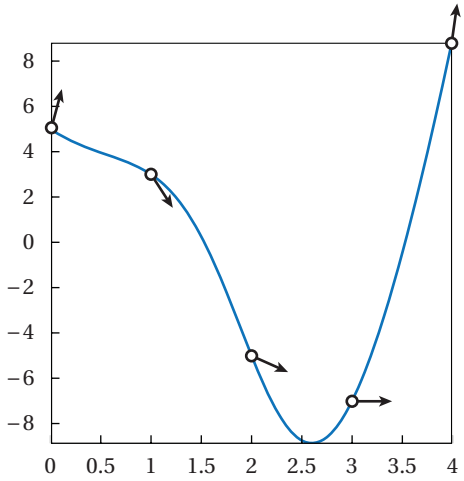

Figure 3.16. Lagrange interpolant r_0 for the data in Example 3.1 and the basis functions in Figure 3.15.

do not match the given derivative data. This can be fixed by adding the correction term

$$q_1(x) = 20b_{0,1}(x) - 4b_{1,1} + 9b_{2,1}(x) - 9b_{3,1}(x) + 12b_{4,1}(x),$$

see Figure 3.17, left, resulting in the rational Hermite interpolant

$$r_1(x) = \frac{4x^9-81x^8+699x^7-3321x^6+9445x^5-16446x^4+17120x^3-9520x^2+1488x+720}{4(x^2-4x+6)^2},$$

see Figure 3.17, right.

3.3.3 The barycentric form

Neither of the formulas in (3.20) and (3.22) are suitable for an efficient construction and evaluation of the rational Hermite interpolant r_m, because the data values $g_{i,j}$ in (3.21) are defined recursively in terms of the derivatives of the interpolants r_j, $j = 0, \ldots, m-1$ and depend on the data $f_i^{(k)}$. A better choice is to write r_m in barycentric form (3.12). We can use Lemma 3.1 to find a closed form expression for our barycentric weights $w_{i,j}^{[m]}$.

Theorem 3.8. The iterative rational Hermite interpolant r_m in (3.20) can be written in barycentric form (3.12) with barycentric weights

$$w_{i,j}^{[m]} = (-1)^{j+1} \sum_{|\gamma|=m-j} \prod_{k=1}^{m+1} \vartheta_{i,\gamma_k}, \qquad i = 0, \ldots, n, \quad j = 0, \ldots, m, \tag{3.23}$$

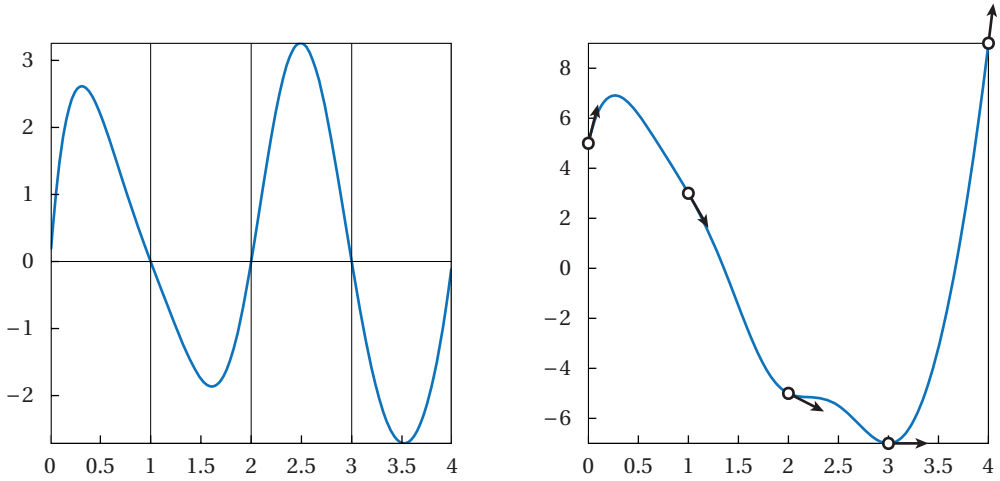

Figure 3.17. Left: correction term q_1 for the data in Example 3.2 and the basis functions in Figure 3.15. Right: the corresponding Hermite interpolant r_1.

where the sum ranges over all $(m+1)$-dimensional multi-indices $\boldsymbol{\gamma} = (\gamma_1, \ldots, \gamma_{m+1})$ whose non-negative integer components sum up to $m - j$ and

$$\vartheta_{i,0} = -w_i, \qquad \vartheta_{i,j} = \sum_{k=0,k\neq i}^{n} \frac{w_k}{(x_i - x_k)^j}, \qquad j = 1, \ldots, m, \tag{3.24}$$

with w_i in (2.26).

Proof. We first notice that $l_{i,m}$ in (3.3) can be written as

$$l_{i,m} = \left(\frac{x - x_i}{\ell(x)}\right)^{m+1},$$

and therefore, $\Omega_i^{[j]}$ in Lemma 3.1 reads

$$\Omega_i^{[j]}(x) = \eta_i(x)^{j+1}, \qquad j \geq 0, \tag{3.25}$$

where

$$\eta_i(x) = w_i + (x - x_i) \sum_{k=0,k\neq i}^{n} \frac{w_k}{x - x_k}.$$

By the general Leibniz rule for higher order derivatives of a product of several functions,

$$\left(\Omega_i^{[m]}\right)^{(j)}(x) = \sum_{|\boldsymbol{\gamma}|=j} \binom{j}{\gamma_1, \ldots, \gamma_{m+1}} \prod_{k=1}^{m+1} \eta_i^{(\gamma_k)}(x),$$

	$w_{i,0}^{[m]}$	$w_{i,1}^{[m]}$	$w_{i,2}^{[m]}$	$w_{i,3}^{[m]}$
$m=0$	w_i			
$m=1$	$2w_i\vartheta_{i,1}$	w_i^2		
$m=2$	$-3w_i^2\vartheta_{i,2}+3w_i\vartheta_{i,1}^2$	$3w_i^2\vartheta_{i,1}$	w_i^3	
$m=3$	$4w_i^3\vartheta_{i,3}-12w_i^2\vartheta_{i,2}\vartheta_{i,1}+4w_i\vartheta_{i,1}^3$	$-4w_i^3\vartheta_{i,2}+6w_i^2\vartheta_{i,1}^2$	$4w_i^3\vartheta_{i,1}$	w_i^4

Table 3.1. Barycentric weights of the iterative rational Hermite interpolant r_m for $m \leq 3$.

where the sum ranges over all $(m+1)$-dimensional multi-indices $\boldsymbol{\gamma} = (\gamma_1, \ldots, \gamma_{m+1})$ whose non-negative integer components sum up to j. Since

$$\eta_i^{(j)}(x_i) = (-1)^{j+1} j! \vartheta_{i,j}, \tag{3.26}$$

with $\vartheta_{i,j}$ as defined in (3.24), by Lemma 3.1 we have

$$w_{i,m-j}^{[m]} = (-1)^{m-j+1} \sum_{|\boldsymbol{\gamma}|=j} \prod_{k=1}^{m+1} \vartheta_{i,\gamma_k},$$

and the statement follows after substituting $m-j$ with j. □

Table 3.1 lists the weights in (3.23) for $m \leq 3$.

Remark 3.1. In the special case of equidistant interpolation nodes, the weights w_i of the Floater–Hormann interpolant are known to be very simple, see Equations (2.28) and (2.29), and the same is true for the weights $w_{i,m}^{[m]} = w_i^{m+1}$. For $j < m$, however, the weights $w_{i,j}^{[m]}$ do not seem to have a simple form, and, unlike the weights of the interpolants by Floater and Schulz [2009] and Jing et al. [2015], they depend on n.

Remark 3.2. Although we did not notice any numerical problems in our experiments, it remains future work to study the stability of computing the weights $w_{i,j}^{[m]}$ as in (3.23). Indeed, if two nodes x_i and x_{i+1} are very close and m is large, then the evaluation of $\vartheta_{i,j}$ in (3.24) may suffer from cancellation. However, by Proposition 3.1, the barycentric form (3.12) comes with the advantage of maintaining the interpolation property even if rounding errors occur during the computation of the weights, as long as $w_{i,m}^{[m]} \neq 0$. And since the weights are determined in a preprocessing step, it is also possible to carry out these computations in high precision arithmetic, despite the additional cost.

3.4 Approximation error

Let us now analyse the approximation power of the iterative rational Hermite interpolant defined in Section 3.3. We show that the interpolant r_m in (3.20) converges to the function f as $O(h^{(m+1)(d+1)})$. In the following two sections we prove this approximation rate separately for the cases $m = 1, 2$ and for $m > 3$. The two proofs use completely different techniques as, for the cases $m = 1, 2$, it is sufficient to exploit the closed-form expression of the barycentric weights $w_{i,j}^{[m]}$ in Theorem 3.8, while for the general case we need a new form of the interpolant r_m.

3.4.1 The cases $m = 1$ and $m = 2$

We start with the case $m = 1$. Denoting the denominator of (2.31) by

$$W(x) = \sum_{j=0}^{n} \frac{w_j}{x - x_j}, \tag{3.27}$$

it follows from (3.20) that

$$\begin{aligned} f(x) - r_1(x) &= f(x) - \frac{1}{W(x)} \sum_{i=0}^{n} \frac{w_i}{x - x_i} g_{i,0} - \frac{1}{W(x)^2} \sum_{i=0}^{n} \frac{w_i^2}{x - x_i} g_{i,1} \\ &= \frac{1}{W(x)^2} \sum_{i=0}^{n} \frac{w_i}{x - x_i} \left(\sum_{j=0}^{n} \frac{w_j}{x - x_j} (f(x) - f(x_j)) - w_i g_{i,1} \right) \\ &= \frac{A(x)}{W(x)^2}, \end{aligned} \tag{3.28}$$

with

$$A(x) = \sum_{i=0}^{n} \frac{w_i}{x - x_i} \left(\sum_{j=0}^{n} w_j f[x, x_j] - w_i g_{i,1} \right).$$

Recalling from Proposition 2.4 that

$$-w_i r_0'(x_i) = \sum_{j=0, j \neq i}^{n} w_j f[x_i, x_j],$$

hence

$$w_i g_{i,1} = w_i f[x_i, x_i] - w_i r_0'(x_i) = \sum_{j=0}^{n} w_j f[x_i, x_j], \tag{3.29}$$

we observe that $A(x)$ simplifies to

$$A(x) = \sum_{i=0}^{n} w_i \sum_{j=0}^{n} w_j f[x, x_i, x_j]. \tag{3.30}$$

But before we proceed to bound the error, we need an auxiliary result.

Lemma 3.3. The barycentric weights in (2.26) satisfy

$$\sum_{i=0}^{n} w_i f[x, x_i] = \sum_{i=0}^{n-d} (-1)^i f[x, x_i, \ldots, x_{i+d}]$$

for any $x \in \mathbb{R}$.

Proof. Following Hormann and Schaefer [2016], we let

$$V_i^d = 1, \qquad i = 0, \ldots, n-d$$

and

$$V_i^{j-1} = \frac{V_{i-1}^j}{x_{i+j-1} - x_{i-1}} + \frac{V_i^j}{x_{i+j} - x_i}, \qquad i = 0, \ldots, n-j+1,$$

for $j = d, d-1, \ldots, 1$, tacitly assuming that $V_i^j = 0$ for $i < 0$ and $i > n-j$ to keep the notation simple. Then,

$$\begin{aligned}
&\sum_{i=0}^{n-d} (-1)^i f[x, x_i, \ldots, x_{i+d}] \\
&\quad = \sum_{i=0}^{n-d} (-1)^i V_i^d \frac{f[x, x_{i+1}, \ldots, x_{i+d}] - f[x, x_i, \ldots, x_{i+d-1}]}{x_{i+d} - x_i} \\
&\quad = \sum_{i=1}^{n-d+1} (-1)^{i-1} \frac{V_{i-1}^d}{x_{i+d-1} - x_{i-1}} f[x, x_i, \ldots, x_{i+d-1}] \\
&\qquad - \sum_{i=0}^{n-d} (-1)^i \frac{V_i^d}{x_{i+d} - x_i} f[x, x_i, \ldots, x_{i+d-1}] \\
&\quad = \sum_{i=0}^{n-d+1} (-1)^{i-1} V_i^{d-1} f[x, x_i, \ldots, x_{i+d-1}] = \cdots = \sum_{i=0}^{n} (-1)^{i-d} V_i^0 f[x, x_i],
\end{aligned}$$

and the statement follows by recalling from Section 3 by Hormann and Schaefer [2016] that $V_i^0 = (-1)^{i+d} w_i$. □

Note that Lemma 3.3 is also true if x is replaced by two or more variables. Now we are ready to get an error bound in the maximum norm.

Theorem 3.9. Suppose $d \geq 0$ and $f \in C^{2(d+2)}[a, b]$, and let h be as in (2.10). Then the error of the iterative interpolant r_1 satisfies

$$\|e_1\| \leq C h^{2(d+1)},$$

where the constant C depends only on d, the derivatives of f, the interval length $b - a$, and, only in the case $d = 0$, on the local mesh ratio β in (2.25)

Proof. Since r_1 interpolates f at the interpolation nodes, it suffices to consider $x \in [a,b] \setminus \{x_0, \ldots, x_n\}$. Our main idea is to derive an upper and a lower bound on the numerator and the denominator of the quotient in (3.28), respectively, and we proceed as in the proof of Theorem 2 by [Floater and Hormann, 2007].

For the numerator, we first apply Lemma 3.3 twice to (3.30) and thus get

$$A(x) = \sum_{i=0}^{n-d} (-1)^i \sum_{j=0}^{n-d} (-1)^j f[x, x_i, \ldots, x_{i+d}, x_j, \ldots, x_{j+d}].$$

Let us now assume that $n-d$ is odd, so that the number of terms in both sums is even. Combining the first and second terms of the second sum, the third and forth, and so on, we then have

$$A(x) = -\sum_{i=0}^{n-d} (-1)^i \sum_{j=0,\ j \text{ even}}^{n-d} (x_{j+d+1} - x_j) f[x, x_i, \ldots, x_{i+d}, x_j, \ldots, x_{j+d+1}],$$

and after applying the same strategy with respect to the first sum, we arrive at

$$\begin{aligned} A(x) = &\sum_{i=0,\ i \text{ even}}^{n-d} (x_{i+d+1} - x_i) \\ &\sum_{j=0,\ j \text{ even}}^{n-d} (x_{j+d+1} - x_j) f[x, x_i, \ldots, x_{i+d+1}, x_j, \ldots, x_{j+d+1}]. \end{aligned} \tag{3.31}$$

Since

$$\sum_{i=0}^{n-d-1} (x_{i+d+1} - x_i) \le (d+1)(b-a), \tag{3.32}$$

as shown in the proof of Theorem 2 by Floater and Hormann [2007], it follows that

$$|A(x)| \le (d+1)^2 (b-a)^2 \frac{\|f^{(2d+4)}\|}{(2d+4)!}. \tag{3.33}$$

If $n-d$ is even, then a similar reasoning reveals that

$$|A(x)| \le (d+1)^2 (b-a)^2 \frac{\|f^{(2d+4)}\|}{(2d+4)!} + 2(d+1)(b-a) \frac{\|f^{(2d+3)}\|}{(2d+3)!} + \frac{\|f^{(2d+2)}\|}{(2d+2)!}. \tag{3.34}$$

For the denominator, we remember from Section 4 by Floater and Hormann [2007] that

$$W(x) = \sum_{i=0}^{n-d} \lambda_i(x), \tag{3.35}$$

with λ_i as defined in (2.23), and from the proofs of Theorem 2 and Theorem 3 by Floater and Hormann [2007] that

$$|W(x)| \geq \frac{1}{d!\, h^{d+1}} \tag{3.36}$$

if $d \geq 1$ and

$$|W(x)| \geq \frac{1}{(1+\beta)h} \tag{3.37}$$

if $d = 0$. The statement then follows by combining these bounds. □

Equations (3.33) and (3.34) allow us to deduce the degree of polynomial reproduction of r_1.

Corollary 3.1. The iterative rational Hermite interpolant r_1 reproduces polynomials of degree $2d+1$ and even of degree $2d+3$, if $n-d$ is odd.

Let us now turn to the case $m = 2$. By (3.20) and (3.28), we have

$$f(x) - r_2(x) = f(x) - r_1(x) - \frac{1}{W(x)^3} \sum_{i=0}^{n} \frac{w_i^3}{x - x_i} g_{i,2} = \frac{B(x)}{W(x)^3}, \tag{3.38}$$

with

$$B(x) = \sum_{i=0}^{n} \frac{w_i}{x - x_i} \Big(A(x) - w_i^2 g_{i,2} \Big).$$

To simplify $B(x)$, we first note that

$$\begin{aligned}
\sum_{j=0}^{n} w_{j,0}^{[1]} f[x_i, x_j] &= 2 \sum_{j=0}^{n} w_j \sum_{k=0, k\neq j}^{n} \frac{w_k}{x_j - x_k} f[x_i, x_j] \\
&= \sum_{j=0}^{n} w_j \sum_{k=0, k\neq j}^{n} w_k \frac{f[x_i, x_j]}{x_j - x_k} - \sum_{j=0}^{n} w_j \sum_{k=0, k\neq j}^{n} w_k \frac{f[x_i, x_k]}{x_j - x_k} \\
&= \sum_{j=0}^{n} w_j \sum_{k=0, k\neq j}^{n} w_k f[x_i, x_j, x_k].
\end{aligned}$$

We then recall from Proposition 3.3 that

$$\begin{aligned}
-\frac{1}{2} w_{i,1}^{[1]} r_1''(x_i) &= \sum_{j=0}^{n} w_{j,0}^{[1]} f[x_i, x_j] + \sum_{j=0, j\neq i}^{n} w_{j,1}^{[1]} f[x_i, x_j, x_j] \\
&= \sum_{j=0}^{n} w_j \sum_{k=0, k\neq j}^{n} w_k f[x_i, x_j, x_k] + \sum_{j=0, j\neq i}^{n} w_j^2 f[x_i, x_j, x_j],
\end{aligned}$$

hence

$$\begin{aligned} w_i^2 g_{i,2} &= w_i^2 f[x_i, x_i, x_i] - \frac{1}{2} w_{i,1}^{[1]} r_1''(x_i) \\ &= \sum_{j=0}^{n} w_j \sum_{k=0, k\neq j}^{n} w_k f[x_i, x_j, x_k] + \sum_{j=0}^{n} w_j^2 f[x_i, x_j, x_j] \\ &= \sum_{j=0}^{n} w_j \sum_{k=0}^{n} w_k f[x_i, x_j, x_k]. \end{aligned} \tag{3.39}$$

Using (3.30), we then get

$$B(x) = \sum_{i=0}^{n} w_i \sum_{j=0}^{n} w_j \sum_{k=0}^{n} w_k f[x, x_i, x_j, x_k].$$

The approximation order and degree of polynomial reproduction of r_2 can then be proven along the same lines as for r_1 above.

Theorem 3.10. Suppose $d \geq 0$ and $f \in C^{3(d+2)}[a, b]$, and let h be as in (2.10). Then the error of the iterative interpolant r_2 satisfies

$$\|e_2\| \leq C h^{3(d+1)},$$

where the constant C depends only on d, the derivatives of f, the interval length $b - a$, and, only in the case $d = 0$, on the local mesh ratio (2.25).

Corollary 3.2. The iterative rational Hermite interpolant r_2 reproduces polynomials of degree $3d + 2$ and even of degree $3d + 5$, if $n - d$ is odd.

For $m > 2$, the closed-form of the barycentric weights becomes more difficult to handle and the approach we have just seen for the cases $m = 1, 2$ becomes too complex. The challenging task consists in proving that (3.29) and (3.40) generalise to

$$w_i^m g_{i,m} = \sum_{j_1=0}^{n} w_{j_1} \cdots \sum_{j_m=0}^{n} w_{j_m} f[x_i, x_{j_1}, \ldots, x_{j_m}]. \tag{3.40}$$

If we could prove the previous relation, the following generalisation of (3.28) would follow immediately.

Conjecture 3.1. Suppose $d \geq 0$ and $f \in C^{(m+1)(d+2)}[a, b]$. Then

$$e_m(x) = f(x) - r_m(x) = \frac{A_m(x)}{W(x)^{m+1}},$$

where

$$A_m(x) = \sum_{i_0=0}^{n} w_{i_0} \cdots \sum_{i_m=0}^{n} w_{i_m} f[x, x_{i_0}, \ldots, x_{i_m}], \tag{3.41}$$

and W as in (3.27).

Instead of proving (3.40), in the following section, we use a different strategy and prove Conjecture 3.1 directly. From this we shall easily deduce the following results.

Conjecture 3.2. Suppose $d \geq 0$ and $f \in C^{(m+1)(d+2)}[a, b]$, and let h be as in (2.10). Then,

$$\|e_m\| \leq C h^{(m+1)(d+1)},$$

where the constant C depends only on d, the derivatives of f, the interval length $b - a$, and, only in the case $d = 0$, on the local mesh ratio (2.25).

Conjecture 3.3. The iterative rational Hermite interpolant r_m reproduces polynomials of degree $(m + 1)(d + 1) - 1$ and even of degree $(m + 1)(d + 2) - 1$, if $n - d$ is odd.

3.4.2 The general case

The main task of this subsection is to prove Conjectures 3.2 and 3.3 and, to this end, we define the function

$$q_m(x) = f(x) - \frac{A_m(x)}{W(x)^{m+1}} \tag{3.42}$$

that clearly satisfies Conjecture 3.1, and prove that q_m and r_m coincide. From this the main results will follow easily.

In order to do that we need to prove that q_m satisfies (3.1) but first we need an auxiliary result regarding the functions $\Omega_i^{[j]}$ in (3.25).

Lemma 3.4. For any $k \geq 0$,

$$\left|\left(\Omega_i^{[j]}\right)^{(k)}(x_i)\right| \leq \frac{(k+j)!}{j!} \max_{l=0,\ldots,k} |\vartheta_{i,l}|^{j+1},$$

with $\vartheta_{i,j}$ as in (3.24).

Proof. First, let us fix the index i. Then, following the same arguments as in the proof of Theorem 3.8, the k-th derivative of $\Omega_i^{[j]}$ can be written as

$$\left(\Omega_i^{[j]}\right)^{(k)}(x) = \sum_{|\boldsymbol{\gamma}|=k} \binom{k}{\gamma_1, \ldots, \gamma_{j+1}} \prod_{l=1}^{j+1} \eta_i^{(\gamma_l)}(x),$$

where the sum ranges over all multi-indices $\boldsymbol{\gamma} = (\gamma_1, \ldots, \gamma_{j+1})$ whose non-negative integer components sum up to k. We now recall (3.26) and observe that there are exactly $\binom{k+j}{j}$ possible $\boldsymbol{\gamma}$'s whose components sum up to k, and therefore we conclude that

$$\begin{aligned}\left|\left(\Omega_i^{[j]}\right)^{(k)}(x_i)\right| &= k!\left|\sum_{|\boldsymbol{\gamma}|=k}\prod_{l=1}^{j+1}\vartheta_{i,\gamma_l}\right| \\ &\leq k!\binom{k+j}{j}\max_{l=0,\ldots,k}|\vartheta_{i,l}|^{j+1}.\end{aligned}$$

□

By considering (3.41) and Newton's error formula (Gautschi [1997]) for the polynomial interpolant of the values $f_{i_0}^{(0)}, \ldots, f_{i_m}^{(0)}$ at the nodes $x_{i_0}, \ldots, x_{i_m}$,

$$f(x) - \sum_{k=0}^{m} f[x_{i_0}, \ldots, x_{i_k}] \prod_{j=0}^{k-1}(x - x_{i_j}) = f[x, x_{i_0}, \ldots, x_{i_m}] \prod_{k=0}^{m}(x - x_{i_k}),$$

we rewrite q_m as

$$\begin{aligned}q_m(x) &= f(x) - \frac{A_m(x)}{W(x)^{m+1}} \\ &= \frac{1}{W(x)^{m+1}}\left(\sum_{i_0=0}^{n} w_{i_0} \cdots \sum_{i_m=0}^{n} w_{i_m}\left(\frac{f(x)}{\prod_{j=0}^{m}(x - x_{i_j})} - f[x, x_{i_0}, \ldots, x_{i_0}]\right)\right) \\ &= \frac{1}{W(x)^{m+1}}\sum_{i_0=0}^{n} w_{i_0} \cdots \sum_{i_m=0}^{n} w_{i_m}\sum_{k=0}^{m}\frac{f[x_{i_0}, \ldots, x_{i_k}]}{\prod_{j=k}^{m}(x - x_{i_j})}. \end{aligned} \tag{3.43}$$

We now prove that q_m is a Hermite interpolant of order m.

Proposition 3.6. Let $f \in C^{2m+1}[a, b]$. Then q_m satisfies

$$e_m^{(k)}(x_i) = 0, \qquad i = 0, \ldots, n,$$

for any $k = 0, \ldots, m$.

Proof. In order to prove this result, we follow the same arguments as in the proof of Lemma 2.3. Let us start by fixing the index i and by rewriting e_m as

$$e_m(x) = \phi_m(x)\hat{e}_m(x),$$

with

$$\phi_m(x) = (x - x_i)^{m+1}, \qquad \hat{e}_m(x) = A_m(x)B_m(x), \qquad B_m(x) = \frac{1}{\phi_m(x)W(x)^{m+1}}.$$

Then, for any $k = 0, \dots, m$, the Leibniz rule gives

$$e_m^{(k)}(x_i) = \sum_{j=0}^{k} \binom{k}{j} \phi_m^{(k-j)}(x_i) \hat{e}_m^{(j)}(x_i) \tag{3.44}$$

and we only need to prove that $|\hat{e}_m^{(j)}(x_i)|$ is bounded for any $j = 0, \dots, m$. We apply again the Leibniz rule to obtain

$$\hat{e}_m^{(j)}(x_i) = \sum_{l=0}^{j} \binom{j}{l} A_m^{(j-l)}(x_i) B_m^{(l)}(x_i),$$

and we proceed by considering separately the terms $A_m^{(j-l)}$ and $B_m^{(l)}$. By the derivative formula for divided differences (Atkinson [1989]; Isaacson and Keller [1966]) we get

$$\begin{aligned} \left| A_m^{(j-l)}(x_i) \right| &= (j-l)! \left| \sum_{i_0=0}^{n} w_{i_0} \cdots \sum_{i_m=0}^{n} w_{i_m} f[(x_i)^{j-l+1}, x_{i_0}, \dots, x_{i_m}] \right| \\ &\leq C \| f^{(m+j-l+1)} \|, \end{aligned}$$

where C is a constant depending on m, n, the indices j and l, and the barycentric weights w_i.

As for the term $B_m^{(l)}(x_i)$, we notice that

$$B_m(x) = \frac{1}{\Omega_i^{[m]}(x)},$$

with $\Omega_i^{[m]}(x)$ as in (3.25), and then, resorting to Hoppe's formula, we get

$$\begin{aligned} B_m^{(l)}(x_i) &= \sum_{p=0}^{l} \frac{(-1)^p}{\Omega_i^{[m]}(x_i)^{p+1}} \sum_{q=0}^{p} \binom{p}{q} (-1)^{p-q} \Omega_i^{[m]}(x_i)^{p-q} \left((\Omega_i^{[m]})^q \right)^{(l)}(x_i) \\ &= \sum_{p=0}^{l} \left(\frac{\delta_{l,0}}{\Omega_i^{[m]}(x_i)} + \sum_{q=1}^{p} \binom{p}{q} (-1)^q \frac{\left(\Omega_i^{[q(m+1)-1]} \right)^{(l)}(x_i)}{\Omega_i^{[(q+1)(m+1)-1]}(x_i)} \right), \end{aligned} \tag{3.45}$$

where we use the relation

$$\Omega_i^{[m]}(x)^k = \begin{cases} 1, & \text{if } k = 0, \\ \Omega_i^{[k(m+1)-1]}(x), & \text{if } k > 0. \end{cases}$$

By recalling (3.25), and noting that $\eta_i(x_i) = w_i$, we conclude that

$$\Omega_i^{[m]}(x_i) = {w_i}^{m+1}, \tag{3.46}$$

and hence all denominators in (3.45) are non-zero. Therefore, we deduce by Lemma 3.4 that $\left|B_m^{(l)}(x_i)\right|$ is bounded, and so is $|\hat{e}_m^{(j)}(x_i)|$, $j = 0, \ldots, m$. The statement then follows directly from (3.44) by noting that

$$\phi_m^{(k)}(x_i) = 0, \qquad k = 0, \ldots, m.$$

□

Before proving Conjecture 3.1, we need to rewrite the interpolant r_m in rational form. To this end we recall (2.31), (3.35) and (3.20) to write

$$\begin{aligned} r_m(x) &= \sum_{i=0}^{n} \sum_{j=0}^{m} (x - x_i)^j b_i(x)^{j+1} g_{i,j} \\ &= \frac{1}{W(x)^{m+1}} \sum_{i=0}^{n} \sum_{j=0}^{m} \frac{{w_i}^{j+1}}{x - x_i} W(x)^{m-j} g_{i,j}. \end{aligned} \tag{3.47}$$

Then we multiply numerator and denominator in (3.47) by $\ell(x)^{m+1}$ to obtain

$$r_m(x) = \frac{1}{Q(x)^{m+1}} \sum_{i=0}^{n} \sum_{j=0}^{m} \frac{{w_i}^{j+1}}{x - x_i} Q(x)^{m-j} \ell(x)^{j+1} g_{i,j},$$

where

$$Q(x) = \ell(x) W(x)$$

is a polynomial of degree at most $n - d$.

Theorem 3.11. Suppose $d \geq 0$ and $f \in C^{(m+1)(d+2)}[a, b]$. Then the iterative interpolant r_m satisfies

$$e_m(x) = \frac{A_m(x)}{W(x)^{m+1}}, \tag{3.48}$$

with A_m in (3.41) and W in (3.27).

Proof. It is sufficient to prove that q_m in (3.42) coincides with r_m. Using the same idea outlined above we multiply numerator and denominator of q_m in (3.43) by $\ell(x)^{m+1}$, obtaining

$$q_m(x) = \frac{1}{Q(x)^{m+1}} \sum_{i_0=0}^{n} w_{i_0} \cdots \sum_{i_m=0}^{n} w_{i_m} \sum_{k=0}^{m} f[x_{i_0}, \cdots, x_{i_k}] p_{k,m}(x),$$

where

$$p_{k,m}(x) = \frac{\ell(x)^{m+1}}{\prod_{j=k}^{m} (x - x_{i_j})}$$

is a polynomial of degree at most

$$(m+1)(n+1) - (m-k+1) \leq (m+1)(n+1) - 1.$$

Thus r_m and q_m share the same denominator and, by Proposition 3.5, have two numerators of the same degree. Therefore the coefficients that define both numerators are completely determined by the $(m+1)(n+1)$ conditions required to solve the Hermite interpolation problem and therefore must coincide. □

With the error e_m written as in (3.48), we now prove Conjecture 3.2.

Theorem 3.12. Suppose $d \geq 0$ and $f \in C^{(m+1)(d+2)}[a,b]$, and let h be as in (2.10). Then,

$$\|e_m\| \leq Ch^{(m+1)(d+1)},$$

where the constant C depends only on d, the derivatives of f, the interval length $b-a$, and, only in the case $d=0$, on the local mesh ratio (2.25).

Proof. We point out that this theorem can be proved following similar arguments as those used in the proof of Theorem 3.9. We assume the reader to be familiar with those arguments and keep the exposition short.

Since r_m interpolates f at the nodes, it is sufficient to bound this quantity for any $x \in [a,b] \setminus \{x_0, \ldots, x_n\}$. By Theorem 3.11 we proceed by deriving an upper bound for the numerator and a lower bound for the denominator of (3.48), again as in the proof of Theorem 2 in Floater and Hormann [2007].

As for the former, we apply Lemma 3.3 $(m+1)$ times to A_m to obtain

$$A_m(x) = \sum_{i_0=0}^{n-d} (-1)^{i_0} \cdots \sum_{i_m=0}^{n-d} (-1)^{i_m} f[x, x_{i_0}, \ldots, x_{i_0+d}, \ldots, x_{i_m}, \ldots, x_{i_m+d}].$$

Applying to the $m+1$ sums of A_m the same strategy as that used in the proof of Theorem 3.9 and recalling (3.32), we conclude that

$$|A_m(x)| \leq (d+1)^{m+1}(b-a)^{m+1} \frac{\|f^{((m+1)(d+2))}\|}{((m+1)(d+2))!}, \tag{3.49}$$

if $n-d$ is odd, and

$$|A_m(x)| \leq \sum_{k=0}^{m+1} \binom{m+1}{k} (d+1)^k (b-a)^k \frac{\|f^{((m+1)(d+2)-k)}\|}{((m+1)(d+2)-k)!}, \tag{3.50}$$

if $n-d$ is even. The statement then follows from recalling (3.36) and (3.37) and combining these bounds. □

Equations (3.49) and (3.50) also allow us to deduce the following result.

Corollary 3.3. The rational Hermite interpolant r_m reproduces polynomials of degree $(m+1)(d+1)-1$ and even of degree $(m+1)(d+2)-1$, if $n-d$ is odd.

We are now able to show Equation (3.40).

Corollary 3.4. If $m \geq 0$ and $f \in C^{2m+1}[a,b]$, then

$$w_i{}^{m+1} g_{i,m+1} = \sum_{i_0=0}^{n} w_{i_0} \cdots \sum_{i_m=0}^{n} w_{i_m} f[x_i, x_{i_0}, \ldots, x_{i_m}],$$

for every $i = 0, \ldots, n$.

Proof. Let the index i be fixed. By Theorem 3.11, we notice that

$$\begin{aligned} g_{i,m+1} &= \frac{1}{(m+1)!} e_m^{(m+1)}(x_i) \\ &= \frac{1}{(m+1)!} \big(A_m C_m\big)^{(m+1)}(x_i), \qquad i = 0, \ldots, n, \end{aligned}$$

where

$$C_m(x) = \phi_m(x) B_m(x), \qquad B_m(x) = \frac{1}{\phi_m(x) W(x)^{m+1}}, \qquad \phi_m(x) = (x - x_i)^{m+1}.$$

Then, by applying the Leibniz rule and the derivative formula for divided differences we obtain

$$\begin{aligned} w_i{}^{m+1} g_{i,m+1} &= \frac{w_i{}^{m+1}}{(m+1)!} \sum_{k=0}^{m+1} \binom{m+1}{k} A_m^{(m+1-k)}(x_i) C_m^{(k)}(x_i) \\ &= w_i{}^{m+1} \sum_{k=0}^{m+1} \frac{1}{k!} \sum_{i_0=0}^{n} w_{i_0} \cdots \sum_{i_m=0}^{n} w_{i_m} f[(x_i)^{m+2-k}, x_{i_0}, \ldots, x_{i_m}] C_m^{(k)}(x_i), \end{aligned}$$

and therefore it remains to prove that

$$C_m^{(k)}(x_i) = \begin{cases} 0 & \text{if } k \leq m, \\ (m+1)!/w_i{}^{m+1}, & \text{if } k = m+1. \end{cases}$$

To this end, let us apply again the Leibniz rule to C_m to get

$$C_m^{(k)}(x_i) = \sum_{j=0}^{k} \binom{k}{j} \phi_m^{(j)}(x_i) B_m^{(k-j)}(x_i). \tag{3.51}$$

rational Hermite interpolant	numerator degree	denominator degree	approximation order
r_m in (3.47)	$(m+1)(n+1)-1$	$(m+1)(n-d)$	$(m+1)(d+1)$
Floater and Schulz [2009]	$(m+1)(n+1)-1$	$(m+1)(n-d)$	$(m+1)(d+1)$
Jing et al. [2015] ($m=1$)	$2n+1$	$2(n-d)$	$2d+1$

Table 3.2. Properties of the rational Hermite interpolants that we compare in our numerical experiments.

By recalling (3.25) and noting that

$$B_m(x_i) = \frac{1}{\Omega_i^{[m]}(x_i)},$$

a similar argument as the one used in the proof of Proposition 3.6 can be used to conclude that $\left|B_m^{(j)}(x_i)\right|$ is bounded for every $j = 0, \dots, m+1$. Moreover, since,

$$\phi_m^{(j)}(x_i) = 0, \qquad 0 \le j \le m, \tag{3.52}$$

we deduce that $C_m^{(k)}(x_i) = 0$ for any $k = 0, \dots, m$.

For $k = m+1$, (3.51) reads

$$\begin{aligned} C_m^{(m+1)}(x_i) &= \phi_m^{(m+1)}(x_i) B_m(x_i) + \sum_{j=0}^{m} \binom{m+1}{j} \phi_m^{(j)}(x_i) B_m^{(m+1-j)}(x_i) \\ &= \frac{\phi_m^{(m+1)}(x_i)}{\Omega_i^{[m]}(x_i)} + \sum_{j=0}^{m} \binom{m+1}{j} \phi_m^{(j)}(x_i) B_m^{(m+1-j)}(x_i) \end{aligned}$$

and the statement follows from (3.46), (3.52) and the boundedness of $\left|B_m^{(j)}(x_i)\right|$ for $j = 1, \dots, m+1$. □

3.4.3 Numerical experiments

We have tested our rational Hermite interpolant r_m and compared it with the rational Hermite interpolants proposed by Floater and Schulz [2009], r_m^{FS}, and by Jing et al. [2015], r_m^{JKZ}. Table 3.2 lists the degrees of numerator and denominator, as well as the approximation orders of these three interpolants.

We recall that the interpolant of Jing, Kang and Zhu is defined only for the case $m = 1$ and so we can compare with their interpolant only in this case. Moreover we use $2d+1$ and $(m+1)(d+1)-1$ as degrees of the local

Experiment	m	d	f	Figure	Table
1	1	0	$1/(1+25(2x-1)^2)$	3.18	3.4
2	2	1	$(1+\tanh(-9x+1))/2$	3.19	3.5
3	4	1	$e^{-(x-1/2)^2/2}$	3.20	3.6
4	1	1	$101e^x/((100x-101)(100x+1))+1$	3.21	3.7
5	2	4	$\lvert 3x-1\rvert+(3x-1)/2-(3x-1)^2$	3.22	3.8
6	1	3	$e^x/cos(x)$	3.23	–
7	2	2	$\sin(10\pi x)x$	3.24	–

Table 3.3. Parameters m and d, functions f, and interpolation nodes x_i used in our numerical experiments.

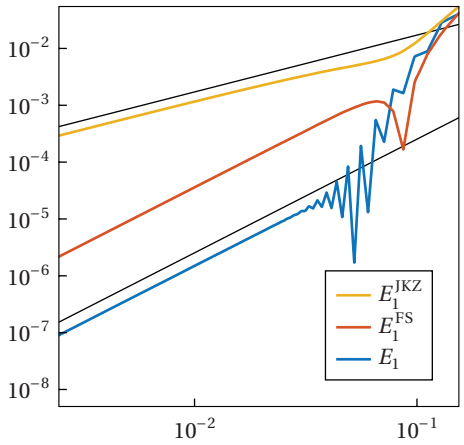

Figure 3.18. Log-log plot of the error with respect to h for Experiment 1. The straight reference lines (in black) represent the expected behaviors.

polynomial interpolants in the construction of Jing, Kang and Zhu and Floater and Schulz, respectively, so that both their interpolants have the same degree as ours. In our numerical experiments, we chose various values for the order m and the degree d of the local polynomials used in the construction of the rational interpolants, and we tested several test functions f, with equidistant, Chebyshev, and other nodes, but the interpolation interval was always $[a,b] = [0,1]$.

Table 3.3 summarises the settings. Note that, except for Experiment 1, we decided to mainly focus on equidistant nodes, since polynomial Hermite interpolation behaves badly in this case. In Experiment 1 we utilize Chebyshev nodes of the second kind in the interval $[0,1]$. We observed similar results for

n	E_1	order	E_1^{FS}	order	E_1^{JKZ}	order
10	4.07e−02		4.19e−02		5.49e−02	
20	1.89e−03	4.51	7.92e−04	5.83	7.43e−03	2.94
40	2.92e−05	6.05	5.40e−04	0.56	4.00e−03	0.90
80	5.72e−06	2.35	1.38e−04	1.97	2.20e−03	0.87
160	1.44e−06	1.99	3.47e−05	1.99	1.14e−03	0.95
320	3.61e−07	2.00	8.67e−06	2.00	5.80e−04	0.98
640	9.03e−08	2.00	2.17e−06	2.00	2.92e−04	0.99

Table 3.4. Errors and approximation orders for Experiment 1.

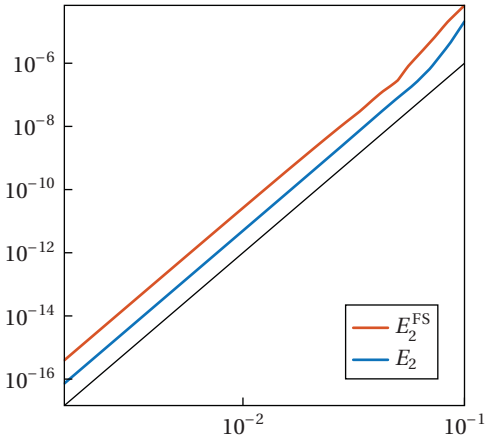

Figure 3.19. Log-log plot of the error with respect to h for Experiment 2. The straight reference line (in black) represents the expected $O(h^{3(d+1)})$ behavior.

other nodes.

For each experiment we report the maximum error

$$E_m = \|e_m\|$$

and the approximation order, where E_m is computed by evaluating the pointwise error at 100 equidistant points in each of the n subintervals $[x_i, x_{i+1}]$, $i = 0, \ldots, n-1$. Also for E_m we use the superscripts '**FS**', '**JKZ**', and '**FH**' to refer to the Hermite interpolants proposed by Floater and Schulz [2009] and by Jing et al. [2015], and to the barycentric Lagrange rational interpolant by Floater and Hormann [2007], respectively.

The first three experiments support Theorems 3.9, 3.10, and 3.12, and more generally confirm the approximation orders listed in Table 3.2. In order to verify the approximation orders even for small h, all computations were

n	E_2	order	E_2^{FS}	order
10	2.09e−05		6.79e−05	
20	8.11e−08	8.01	2.86e−07	7.89
40	1.23e−09	6.04	5.68e−09	5.65
80	1.90e−11	6.01	9.87e−11	5.85
160	2.98e−13	6.00	1.59e−12	5.95
320	4.66e−15	6.00	2.52e−14	5.98
640	7.28e−17	6.00	3.96e−16	5.99

Table 3.5. Error and approximation order for Experiment 2.

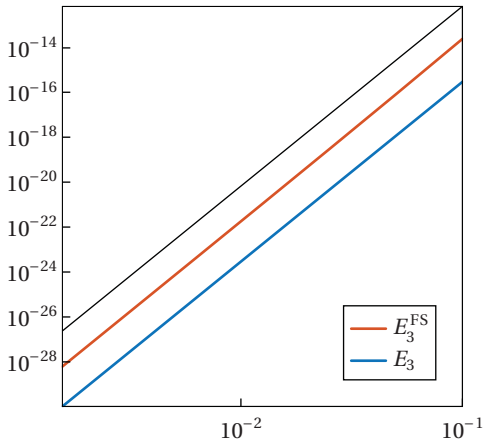

Figure 3.20. Log-log plot of the error with respect to h for Experiment 3. The straight reference line (in black) represents the expected $O(h^{5(d+1)})$ behavior.

performed in *C++* using the multiple-precision *MPFR* (Fousse et al. [2007]). Note that the plots in Figures 3.18–3.20 show the error only for the even values of n, from 10 to 640, because the errors for the odd values follow the same trend but with a lower constant and would thus have resulted in more confusing graphs. The thin straight reference lines represent and support the expected convergence rates, that is, $O(h^{(m+1)(d+1)})$ for E_m and E_m^{FS} and $O(h^{2d+1})$ for E_1^{JKZ}.

Overall, these experiments show that for $m = 1$, our interpolant is better, in terms of approximation error and order, than the one proposed by Jing et al. [2015]. For general m, it matches the interpolant proposed by Floater and Schulz [2009], but we observed that it typically gives an approximation error which is smaller by a factor of 2 to 5.

n	E_3	order	E_3^{FS}	order
10	2.91e−16		2.38e−14	
20	1.14e−18	8.00	8.02e−17	8.21
40	4.44e−21	8.00	2.89e−19	8.12
80	1.73e−23	8.00	1.08e−21	8.06
160	6.77e−26	8.00	4.12e−24	8.03
320	2.64e−28	8.00	1.59e−26	8.02
640	1.03e−30	8.00	6.18e−29	8.01

Table 3.6. Error and approximation order for Experiment 3.

n	E_1	order	E_1^{FS}	order	E_1^{JKZ}	order	E_0^{FH}	order
10	1.78		2.01		2.51		7.82e−01	
20	5.64e−01	1.66	6.58e−01	1.61	8.71e−01	1.53	4.44e−01	0.82
40	1.35e−01	2.07	1.66e−01	1.99	2.44e−01	1.84	2.03e−01	1.13
80	2.23e−02	2.60	2.99e−02	2.47	5.31e−02	2.20	7.36e−02	1.46
160	2.51e−03	3.15	3.81e−03	2.97	9.14e−03	2.54	2.24e−02	1.72
320	2.10e−04	3.58	3.63e−04	3.39	1.34e−03	2.77	6.11e−03	1.87
640	1.48e−05	3.83	2.86e−05	3.67	1.82e−04	2.89	1.59e−03	1.94

Table 3.7. Error and approximation order for Experiment 4.

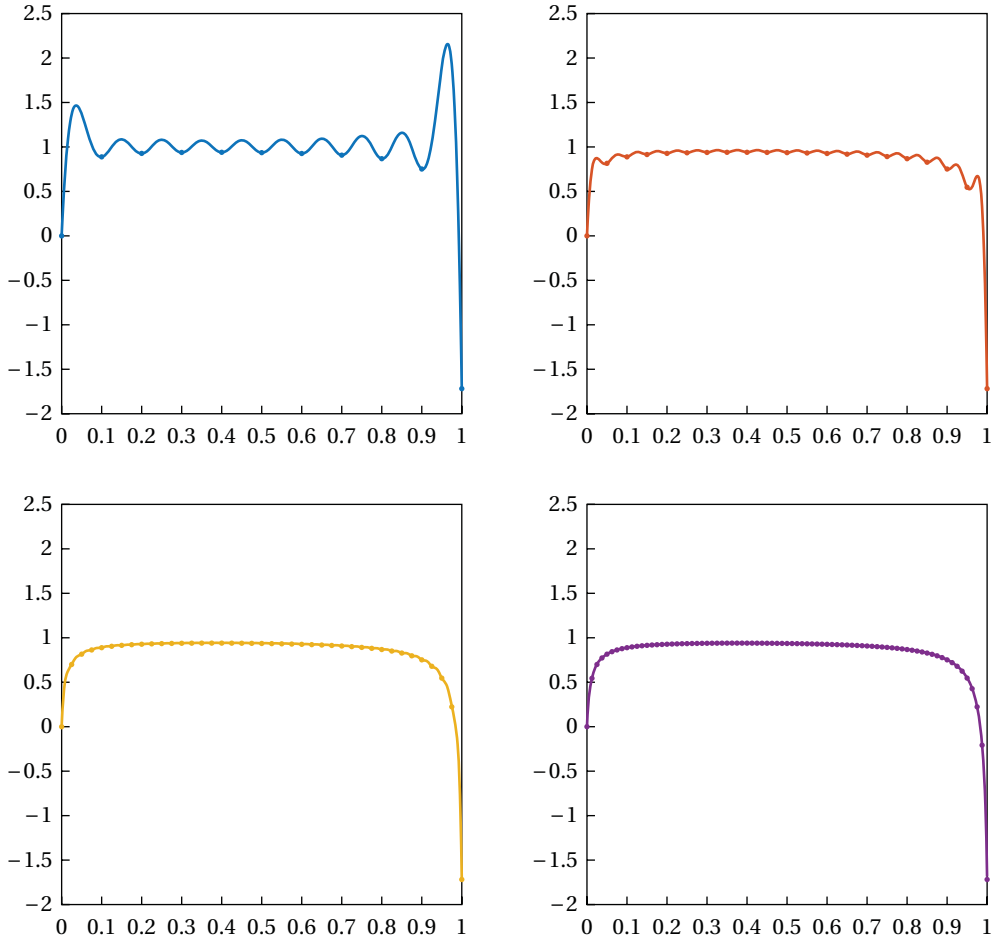

Figure 3.21. From top left to bottom right: the iterative rational Hermite interpolant for $n = 10, 20, 40, 80$ for Experiment 4.

Experiments 4 and 5 show the interpolation quality of the proposed iterative rational Hermite interpolant at equidistant nodes for a C^∞ function with poles outside but near the endpoints of the interpolation interval in Figure 3.21 and for a C^0 function in Figure 3.22. Tables 3.7 and 3.8 report the corresponding numerical results for all rational Hermite interpolants and for the classical Floater–Hormann interpolant at $(m+1)(n+1)$ equidistant nodes, that is, for the same number of overall data values.

All computations were carried out in *MATLAB* with standard precision. For the smooth function in Experiment 4, our interpolant has the smallest approximation error among the three Hermite interpolants. The Lagrange Floater–Hormann interpolant is more accurate for small $n \leq 20$, but it is out-

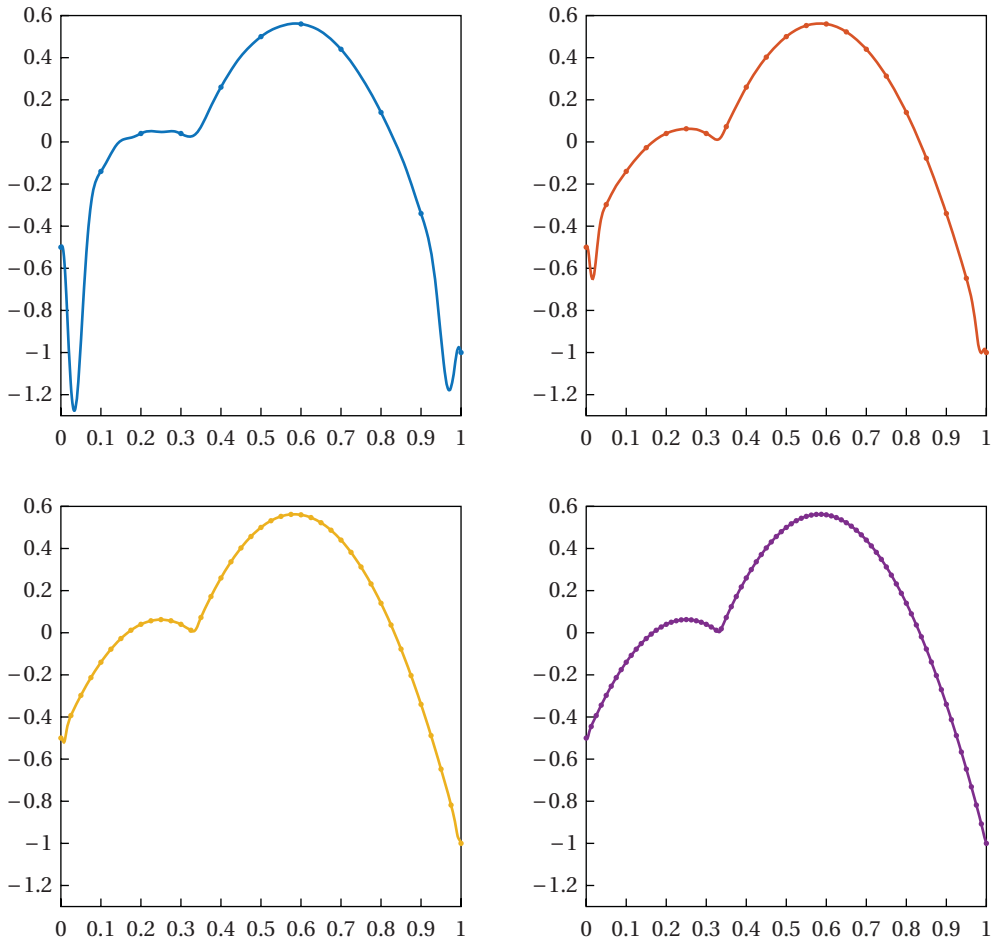

Figure 3.22. From top left to bottom right: the iterative rational Hermite interpolant for $n = 10, 20, 40, 80$ for Experiment 5.

performed by the Hermite interpolants for larger n, because the latter have a higher approximation order. Experiment 5 shows that the smoothness condition on f in Theorems 3.9, 3.10 and 3.12 is essential for the approximation order of our rational Hermite interpolant, which drops to $O(h)$, if f is only continuous. The same is true for the other interpolants, and we observe that the best approximation error is obtained by the Floater–Hormann interpolant in this experiment.

In Experiments 6 and 7, we compare the numerical stability of the rational Hermite interpolants in the case of equidistant interpolation nodes. All computations were performed in *C++* with 15 decimal digits of precision. Figures 3.23 and 3.24 show that all interpolants reach the level of rounding errors

n	E_2	order	E_2^{FS}	order	E_0^{FH}	order
10	9.19e−01		2.35e−01		1.90e−02	
20	2.23e−01	2.05	5.30e−02	2.15	9.50e−03	1.00
40	5.58e−02	2.00	1.33e−02	2.00	4.75e−03	1.00
80	1.36e−02	2.04	3.74e−03	1.83	2.38e−03	1.00
160	3.40e−03	2.00	1.87e−03	1.00	1.19e−03	1.00
320	9.36e−04	1.86	9.36e−04	1.00	5.94e−04	1.00
640	4.68e−04	1.00	4.68e−04	1.00	2.97e−04	1.00

Table 3.8. Error and approximation order for Experiment 5.

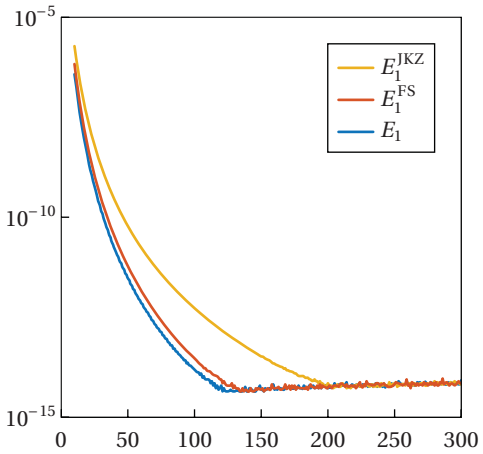

Figure 3.23. Semi-log plot of the error with respect to n for Experiment 6.

for sufficiently large n and that our interpolant is the fastest to converge. However, we noticed that further increasing n may lead to a slight increase of the error for some test functions, as shown in Figure 3.23. Since this occurs for all three interpolants, it is probably not related to the computation of the barycentric weights, but it may indicate a numerical instability of the barycentric form (3.12). It remains future work to further investigate this phenomenon.

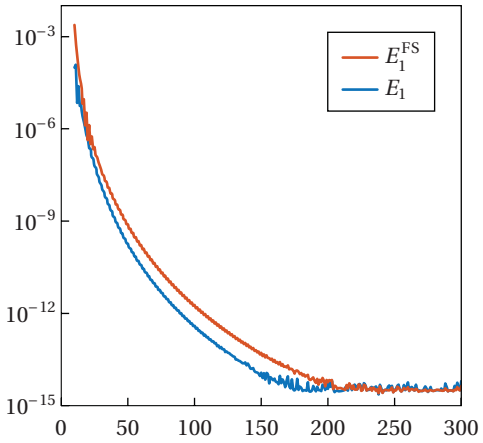

Figure 3.24. Semi-log plot of the error with respect to n for Experiment 7.

Chapter 4

The Lebesgue constant

In the first chapter we have seen that the $n+1$ Lagrange basis functions constitute a basis of the polynomial space $\mathscr{P}_n$ and therefore the Lagrange polynomial interpolant of a function f sampled at $n+1$ arbitrary nodes can be interpreted as its projection on $\mathscr{P}_n$. In order to formalise this concept, we define the *Lagrange interpolation operator*

$$L_n \colon C^0[a,b] \longrightarrow \mathscr{P}_n$$

that associates to each function $f \in C^0[a,b]$ the corresponding interpolant p of degree at most n, that is

$$L_n f = p \in \mathscr{P}_n.$$

L_n is a continuous and linear operator between the two function spaces and, since L_n reproduces polynomials up to degree n, it is a *projection* on this space of polynomials, that is

$$L_n L_n f = L_n p = p.$$

This formalisation of an interpolation scheme as a projection on some function space is not a purely theoretical exercise, since, as we shall see in this chapter, the study of the norm of L_n

$$\|L_n\| = \sup_{\|f\| \leq 1} \|L_n f\|.$$

gives important information on the quality of the interpolant.

In this chapter we present some well-known results about the unfavorable behavior of $\|L_n\|$ for equispaced nodes as $n \to \infty$, and we emphasise how this influences the quality of the overall polynomial interpolation scheme. We then present some literature regarding the behavior of the interpolation operator for

the Berrut and Floater–Hormann schemes in the Lagrange setting, and show how they compare to L_n.

Then, we focus on the Hermite interpolation operator and we compare its behavior with that of the operator associated to the barycentric rational Hermite interpolation scheme presented in the previous chapter.

4.1 The Lagrange polynomial interpolation operator

In this section we focus on the Lagrange polynomial interpolation operator L_n. The first step to undertake is to retrieve a closed form for the norm of the Lagrange polynomial interpolation operator, see Cheney and Light [2000].

Lemma 4.1. The operator norm $\|L_n\|$ satisfies

$$\|L_n\| = \max_{x\in[a,b]} \sum_{i=0}^{n} |\ell_i(x)|,$$

where ℓ_i, $i = 0, \ldots, n$, are the Lagrange basis functions (2.5).

This is a classical result in approximation theory and can be obtained as follows. For any f with $\|f\| \leq 1$

$$\|L_n f\| = \max_{x\in[a,b]} \left| \sum_{i=0}^{n} \ell_i(x) f_i \right| \leq \max_{x\in[a,b]} \sum_{i=0}^{n} |\ell_i(x) f_i| \leq \max_{x\in[a,b]} \sum_{i=0}^{n} |\ell_i(x)|$$

and therefore $\|L_n\| \leq \max \sum_{i=0}^{n} |\ell_i(x)|$. In order to prove the inequality in the other direction, it is sufficient to pick $\xi \in [a, b]$ such that

$$\max_{x\in[a,b]} \sum_{i=0}^{n} |\ell_i(x)| = \sum_{i=0}^{n} |\ell_i(\xi)|$$

and a function f such that $f_i = \operatorname{sign} \ell_i(\xi)$. Then we get

$$\|L_n\| \geq \|L_n f\| \geq \left| \sum_{i=0}^{n} \ell_i(\xi) f_i \right| = \sum_{i=0}^{n} |\ell_i(\xi)| = \max_{x\in[a,b]} \sum_{i=0}^{n} |\ell_i(x)|.$$

The function

$$\lambda_n(x) = \sum_{i=0}^{n} |\ell_i(x)|$$

and the constant

$$\Lambda_n = \Lambda(X_n) = \max_{x\in[a,b]} \Lambda_n(x) \tag{4.1}$$

are respectively called the *Lebesgue function* and the *Lebesgue constant* for Lagrange interpolation (Gautschi [1997]) and are fundamental quantities to estimate the quality of the polynomial interpolant. For example, if the Lebesgue constant is small, the forward stability of the second barycentric form of Lagrange polynomial interpolant is guaranteed by Theorem 2.4, but, even ignoring the issues related to floating point arithmetic, Λ_n gives also important information on the theoretical behavior of the polynomial p. Indeed, since

$$\|p\| = \|L_n f\| \leq \Lambda_n \|f\|, \tag{4.2}$$

the Lebesgue constant gives information about the potential oscillations of the interpolant p, independently of f. Moreover, it provides a first estimate for the interpolation error (Gautschi [1997]). If $\hat{p}$ is the *polynomial of best approximation* of the function f, that is

$$\hat{p} = \arg\min_{p \in \mathscr{P}_n} \|f - p\|,$$

then the Lebesgue constant is useful to estimate how far the Lagrange polynomial interpolant is from $\hat{p}$. Indeed we have

$$\|f - p\| \leq \|f - \hat{p}\| + \|L_n(f - \hat{p})\| \leq (1 + \Lambda_n)\|f - \hat{p}\|, \tag{4.3}$$

and therefore, the smaller the Lebesgue constant, the more we approach the best possible among the polynomial solutions of the Lagrange interpolation problem (2.2).

The use of floating-point arithmetic in modern computers makes the function values $f_0, \ldots, f_n$ only an approximation of the real values we want to interpolate. In many practical applications, these values are further manipulated, increasing the difference between the real values and the ones that we actually use. This most certainly has an effect on the quality of the interpolation of the original data and the Lebesgue constant provides a good measure for this. Let $f_0, \ldots, f_n$ be the real values we want to interpolate and $\tilde{f}_0, \ldots, \tilde{f}_n$ be the values subject to round-off and possible measurement errors and suppose that

$$\max_{i=0,\ldots,n} |f_i - \tilde{f}_i| = \varepsilon.$$

The approximated values can be seen as samples of a different function $\tilde{f}$ such that $\|f - \tilde{f}\| = \varepsilon$. The constant Λ_n is then a good measure of the sensitivity of the polynomial interpolant to perturbation of the data since, by (4.2), we get

$$\|p - \tilde{p}\| = \|L_n(f - \tilde{f})\| \leq \Lambda_n \varepsilon, \tag{4.4}$$

where $\tilde{p} = L_n\tilde{f}$ is the interpolant of the perturbed function $\tilde{f}$. It is then clear that the difference between the 'desired' interpolant and the interpolant of $\tilde{f}$ is strongly influenced by the Lebesgue constant, and, if $\Lambda_n \gg \varepsilon$, this can easily lead to undesired results. In this sense we say that the Lebesgue constant measures the *conditioning* of polynomial interpolation with respect to perturbations of the values f_i.

The role of the Lebesgue constant in polynomial interpolation should now be clear to the reader and it should not be a surprise that its behavior as $n \to \infty$ has been extensively studied. It is clear from its definition that the behavior of the Lebesgue constant is strongly influenced by the distribution of the nodes and Brutman [1997] recalls that there exists an optimal set of nodes X_n^* such that

$$\Lambda_n^* = \Lambda(X_n^*) = \min_{X_n} \Lambda(X_n).$$

The problem of finding the optimal set of nodes X_n^* for any $n \in \mathbb{N}$ is still unresolved, but it has been shown by Bernstein [1931] that the corresponding Lebesgue constant grows at least logarithmically, that is

$$\Lambda_n^* > \left(\frac{2}{\pi} + o(1)\right) \ln(n+1), \qquad n \to \infty.$$

Erdős [1961] makes this statement more precise, by proving the following.

Theorem 4.1 (Erdős [1961])**.** Let X_n be any system of interpolation nodes in $[-1, 1]$. Then there exist two constants $C_1 > 0$ and $C_2 > 0$ such that

$$\frac{2}{\pi} \ln(n+1) - C_1 \leq \Lambda(X_n) \leq \frac{2}{\pi} \ln(n+1) + C_2.$$

Since the closed form for the nodes X_n^* is unknown, these results might seem discouraging. How well can the Lebesgue constant behave for some prescribed distribution of nodes? Rivlin [1974] provides a first answer to this question by proving the following result regarding the Chebyshev nodes of the first kind.

Theorem 4.2 (Rivlin [1974])**.** Let T_n be the set of $n+1$ Chebyshev nodes of the first kind. Then the sequence $(t_n)_{n\in\mathbb{N}}$ defined by

$$t_n = \Lambda(T_n) - \frac{2}{\pi} \ln(n+1), \qquad n \in \mathbb{N}$$

is strictly monotonically decreasing with maximum value $t_1 = 1$.

This remarkable result has been generalised to the Chebyshev nodes of the second kind.

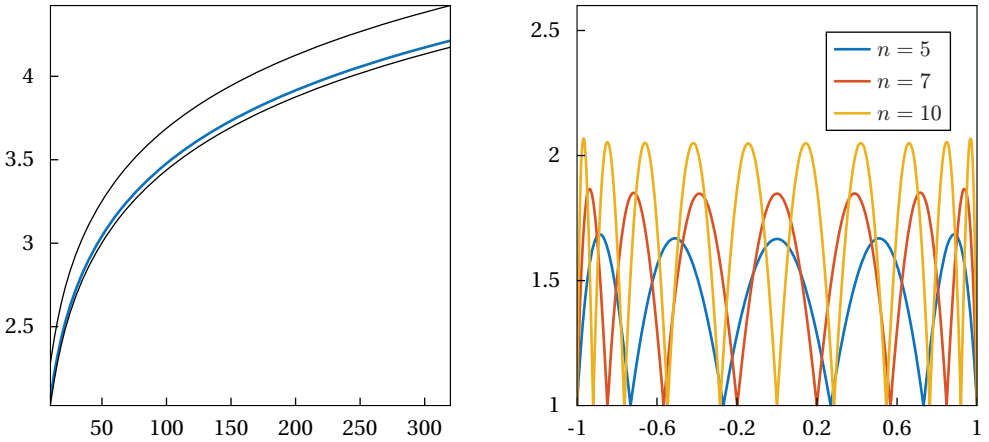

Figure 4.1. Left: the Lebesgue constant for $n = 10, 11, \ldots, 320$ of polynomial interpolation at extended Chebyshev nodes (in blue) with the lower and upper bounds in (4.5) (in black). Right: the Lebesgue function for $n = 5, 7, 10$ extended Chebyshev nodes. Compare Figure 4.4.

Theorem 4.3 (Brutman [1984])**.** Let U_n be the set of $n+1$ Chebyshev nodes of the second kind. Then

$$\Lambda(U_n) = \begin{cases} \Lambda(T_{n-1}), & \text{if } n \text{ is odd,} \\ \Lambda(T_{n-1}) - \alpha_n, & \text{if } n \text{ is even,} \end{cases}$$

where

$$\frac{\pi/8}{4n^2} \leq \alpha_n \leq \frac{2(\sqrt{2}-1)}{4n^2}.$$

Finally, Brutman [1978] shows that a similar result holds also for extended Chebyshev nodes $\hat{T}_n$. In particular he proves that

$$\frac{1}{2} + \frac{2}{\pi}\ln(n+1) < \lambda(\hat{T}_n) < \Lambda(X_n^*) < \Lambda(\hat{T}_n) < \frac{3}{4} + \frac{2}{\pi}\ln(n+1), \tag{4.5}$$

where $\lambda(X_n)$ denotes the least local maximum of the Lebesgue function for the set of nodes X_n, see Figure 4.1.

By Theorem 4.1, the Chebyshev nodes are nearly optimal for polynomial interpolation and this results in a good conditioning of polynomial interpolation for Chebyshev-spaced values.

Example 4.1. For $n = 10$, let us consider the Chebyshev nodes of the second kind, and the function

$$f = \Big(|\sin(2\pi x)|\sin(2\pi x)\Big)^3 \in C^3[0,1]. \tag{4.6}$$

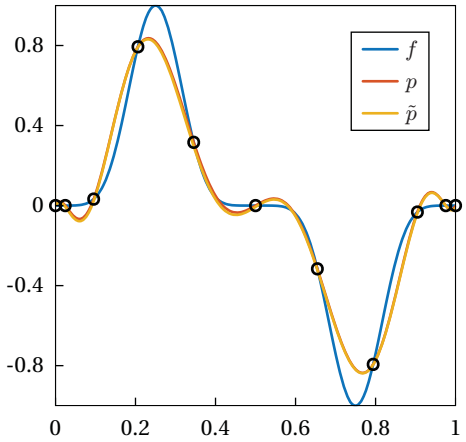

Figure 4.2. Effect of the perturbation of the data, with $\varepsilon = 1.9908 \cdot 10^{-2}$, on the polynomial interpolant at 11 Chebyshev nodes of the second kind.

Let

$$\tilde{f}_i = f(x_i) + \varepsilon_i$$

and $\tilde{f}$ be the corresponding 'perturbed' function. Figure 4.2, displays the result of the perturbation corresponding to

$$\varepsilon = \max_{i=0,\dots,n} \varepsilon_i \approx 1.9908 \cdot 10^{-2}.$$

The original polynomial, p, and the perturbed one, $\tilde{p}$, differ by at most

$$\|p - \tilde{p}\| \approx 2.00 \cdot 10^{-2},$$

while the ratio

$$\frac{\|p - \tilde{p}\|}{\varepsilon} \approx 1.0047 \tag{4.7}$$

shows that the perturbation of the interpolant is roughly as large as ε.

The situation can change quite dramatically if we modify the setting, and again the use of equispaced nodes reveals the issues of polynomial interpolation. Let us show with another example the effect of a perturbation of the data in the equispaced setting.

Example 4.2. For $n = 10$, let us consider the function f in Example 4.1 sampled at equispaced nodes. By considering the same width for the perturbation as in Example 4.1, the original and perturbed polynomials differ as much as

$$\|p - \tilde{p}\| \approx 1.2181 \cdot 10^{-1},$$

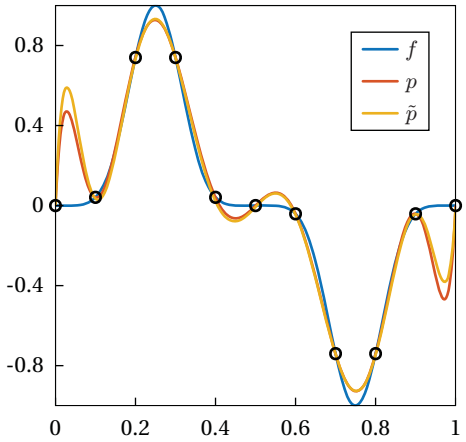

Figure 4.3. Effect of the perturbation of the data, with $\varepsilon = 1.9908 \cdot 10^{-2}$ for the polynomial interpolant at 11 equispaced nodes. Compare Figure 4.2.

while the ratio

$$\frac{\|p - \tilde{p}\|}{\varepsilon} \approx 6.1185$$

shows that, in this setting, the same perturbation as in Example 4.1 produces a difference in the interpolating polynomials which is roughly 6 times larger than ε, see Figure 4.3.

Considering the importance of equispaced nodes in many practical scenarios, the behavior of the Lebesgue constant in this setting has been extensively analysed. The first result about the growth of Λ_n goes back to Tietze [1917], who proves a result regarding the local maxima of the Lebesgue function at equispaced nodes and observes that these values decrease monotonically as we get closer to the center of the interpolation interval, see Figure 4.4, left. Schönhage [1961] proves the following result related to the asymptotic expression of Λ_n at equispaced nodes,

Theorem 4.4 (Schönhage [1961])**.** Let $E = (E_n)_{n\in\mathbb{N}}$ be the system of equispaced nodes. Then

$$\Lambda(E_n) \sim \frac{2^{n+1}}{en(\ln n + \gamma)}, \qquad n \to \infty$$

where γ is the *Euler–Mascheroni constant*

$$\gamma = \lim_{n\to\infty} \left(\sum_{k=1}^{n} \frac{1}{k} - \ln n \right) \approx 0.5772. \tag{4.8}$$

Trefethen and Weideman [1991] instead prove the following theorem that holds for any $n \geq 1$, see Figure 4.4, right.

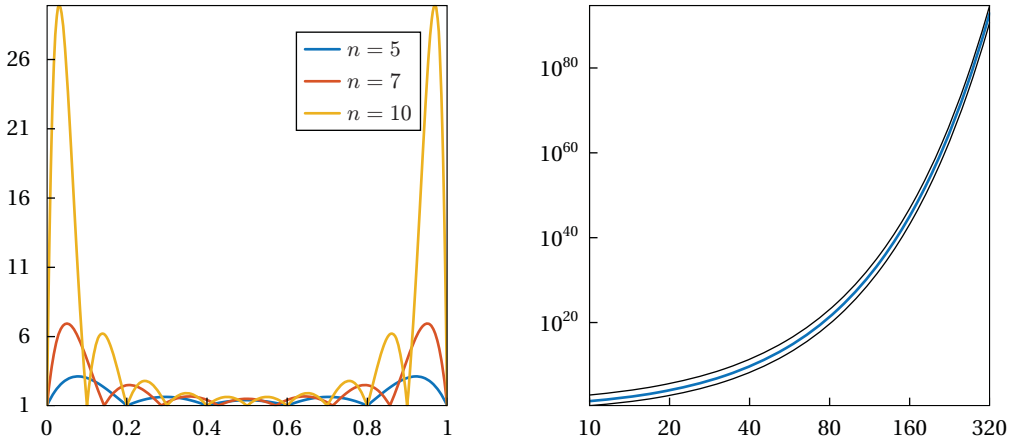

Figure 4.4. Left: the Lebesgue function at equispaced nodes for $n = 5, 7, 10$. Compare Figure 4.1. Right: the Lebesgue constant for $n = 10, \ldots, 320$ of polynomial interpolation at equispaced nodes (in blue) with lower and upper bounds in (4.9) (in black).

Theorem 4.5 (Trefethen and Weideman [1991])**.** For each integer $n \geq 1$,

$$\frac{2^{n-2}}{n^2} < \Lambda(E_n) < \frac{2^{n+3}}{n}. \tag{4.9}$$

Theorem 4.5 shows how the effects of a perturbation such as the one depicted in Example 4.2 can get worse very quickly as n increases and that even smaller perturbations, like those obtained by using floating-point arithmetic, can give unpredictable results.

We remark that these results are independent of the function f and of the location of its poles and, unlike the Runge phenomenon, they regard all functions, even the ones that are analytic in the whole complex plane. This makes polynomial interpolation at equispaced nodes practically useless as soon as $n > 70$. It is therefore necessary to look again at some other tool for solving the interpolation problem in this setting and, as we have seen in the previous chapters, Floater–Hormann interpolants are a natural candidate for this role.

4.2 The Berrut and Floater–Hormann interpolation operators

The Floater–Hormann interpolation scheme can also be understood as the result of a projection of f on the space $\mathscr{R}_{\boldsymbol{w}_d}$ in (2.32). To illustrate this we define

the operators

$$I_n^d \colon C^0[a,b] \longrightarrow \mathscr{R}_{\boldsymbol{w}_d}, \qquad d = 0, \dots, n$$

that at each function in $C^0[a,b]$ associates the corresponding Floater–Hormann interpolant of degree d, that is

$$I_n^d f = r \in \mathscr{R}_{\boldsymbol{w}_d},$$

with r as in (2.24). In the case $d = 0$, we refer to the corresponding operator I_n^0 as the *Berrut interpolation operator* and we denote it as I_n, omitting the dependance on d. We call the general I_n^d the *Floater–Hormann interpolation operator*.

For any d, $0 \leq d \leq n$, I_n^d is a continuous linear projection on the space $\mathscr{R}_{\boldsymbol{w}_d}$ and similar relations to (4.2), (4.3) and (4.4) are valid also for the Floater–Hormann interpolation scheme. It is therefore natural to extend the analysis we have seen for L_n to this case.

The same techniques used to prove Lemma 4.1 can be used to prove that the norm of I_n^d can be expressed in closed form as

$$\|I_n^d\| = \max_{x\in[a,b]} \sum_{i=0}^{n} \frac{|w_i|}{|x - x_i|} \Bigg/ \left| \sum_{i=0}^{n} \frac{w_i}{x - x_i} \right|,$$

where the w_i's are the barycentric weights in (2.26). Therefore, in analogy with the polynomial case, we define the function

$$\Lambda_n^d(x) = \sum_{i=0}^{n} \frac{|w_i|}{|x - x_i|} \Bigg/ \left| \sum_{i=0}^{n} \frac{w_i}{x - x_i} \right|$$

and the quantity

$$\Lambda_n^d = \Lambda^d(X_n) = \max_{x\in[a,b]} \Lambda_n^d(x),$$

as the Lebesgue function and the Lebesgue constant of the Floater–Hormann interpolant of degree d.

One of the main issues in the analysis of the Lebesgue constant in this setting consists in bounding adequately the barycentric weights w_i and this is the reason for which most of the literature focuses on special family of nodes or on the case $d = 0$ (Berrut's interpolant), for which the expression of the weights is particularly simple.

The first result in this direction is the work of Bos et al. [2011] who focus on the study of the Lebesgue constant Λ_n^0 at equispaced nodes and prove the following.

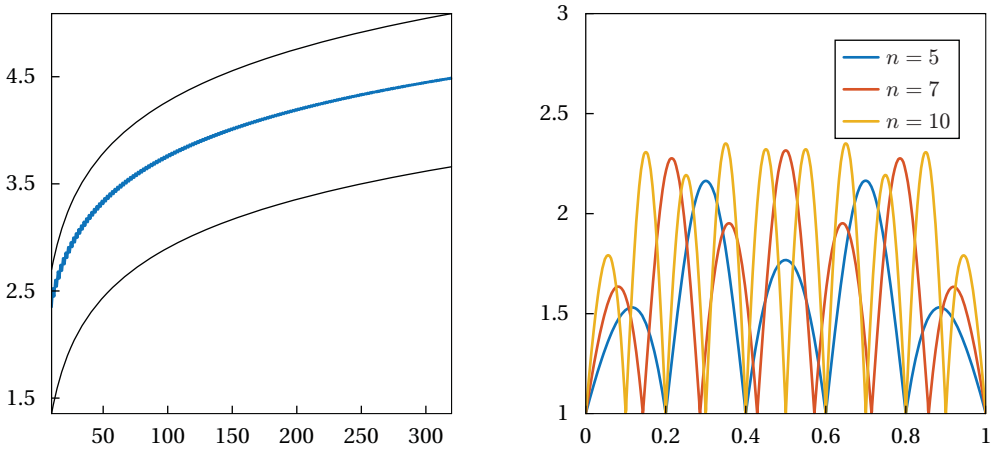

Figure 4.5. Left: the Lebesgue constant of Berrut's interpolant at equispaced nodes for $n = 10, \dots, 320$ (in blue) with the lower bound in Theorem 4.6 and the upper bound in Theorem 4.7 (in black). Right: the Lebesgue function at equispaced nodes for $n = 5, 7, 10$.

Theorem 4.6 (Bos et al. [2011])**.** For the set E_n of equispaced nodes

$$\frac{2n}{4 + n\pi} \ln(n+1) \leq \Lambda^0(E_n) \leq 2 + \ln(n).$$

Since the Lebesgue constant at the nodes is always equal to 1, the main idea behind their proof is to consider separately numerator and denominator for $x \in (x_k, x_{k+1})$ and to multiply these quantities by $(x - x_k)(x_{k+1} - x)$, in order to avoid terms that grow indefinitely.

More recently, a sharper upper bound for equispaced nodes has been provided.

Theorem 4.7 (Zhang [2014])**.** For a set of equispaced nodes

$$\Lambda^0(E_n) \leq \frac{24}{24 + \pi^2} \ln(n+1) + 1, \qquad n \geq 174.$$

Figure 4.5, left, shows that the upper and lower bounds provided by Theorems 4.6 and 4.7 are not yet sharp and that much can still be improved. Moreover the bound provided by Zhang [2014] holds also for $n < 174$, showing that this is not a practical limitation. Moreover it is possible to notice that, unlike polynomials, the maximum of the Lebesgue function seems to be attained towards the midpoint of the interpolation interval, see Figure 4.5, right. We remark that a sharper upper bound for Λ_n^0 for equispaced nodes has been provided by Deng et al. [2016].

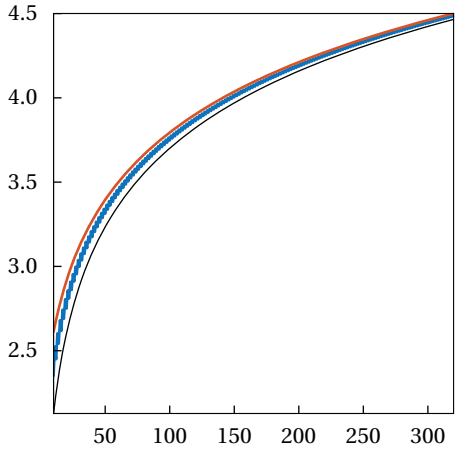

Figure 4.6. The Lebesgue constant for $n = 10, \ldots, 320$ of Berrut's interpolant at equispaced nodes (in blue) with the lower bound (in black) and the estimate (in red) in (4.10).

Finally, we would like to mention the article by Ibrahimoglu and Cuyt [2016] that, after extensive numerical studies on the behavior of the Lebesgue function, concludes that

$$\frac{2}{\pi + \frac{4}{n+3}}(\ln(n+1)+\ln 2+\gamma) \leq \Lambda_n^0 \simeq \frac{2}{\pi - \frac{4}{n+2}}\left(\ln(n+1)+\ln 2+\gamma+\frac{1}{24n}\right) \quad (4.10)$$

with γ as in (4.8), see Figure 4.6. This result seems to give sharper upper and lower bounds but is based on the assumption that the maximum of the Lebesgue function is attained near the midpoint of a subinterval (x_i, x_{i+1}). This is justified by their numerical observations but cannot be considered as a formal proof for the bounds of the Lebesgue constant.

The consequences of these results are remarkable. As Zhang [2014] notices, the results in Theorems 4.6 and 4.7 overall suggest that the asymptotic behavior of Λ_n^0 could be

$$\Lambda_n^0 \sim C_n \ln(n+1), \qquad n \to \infty$$

with

$$\frac{2n}{4+n\pi} \leq C_n \leq \frac{24}{24+\pi^2}.$$

Since

$$\lim_{n\to\infty} \frac{2n}{4+n\pi} = \frac{2}{\pi} \approx 0.6366,$$

Zhang suggests that there might be an optimal factor $C \in [\frac{2}{\pi}, \frac{24}{24+\pi^2}]$ such that

$$\Lambda_n^0 \sim C \ln(n+1).$$

Moving from this idea and inspired by the observations of Bos et al. [2011], Zhang [2017] proves that the exact constant is $2/\pi$ and concludes that the Lebesgue constant of Berrut's interpolant at equispaced nodes grows asymptotically as the polynomial one for Chebyshev nodes. This result is further confirmed by Ibrahimoglu and Cuyt [2016].

The situation seems to be slightly different at extended Chebyshev nodes, as the following result shows.

Theorem 4.8 (Bos et al. [2013])**.** If $X = (X_n)_{n\in\mathbb{N}}$ is a family of well-spaced nodes, then there exists a constant $C > 0$ such that

$$\Lambda^0(X_n) \leq C \ln(n).$$

In particular, for $\hat{T} = (\hat{T}_n)_{n\in\mathbb{N}}$,

$$\Lambda^0(\hat{T}_n) \leq 3 + 3\pi^2 \ln(n).$$

The upper bound in Theorem 4.8 is larger than the one obtained in Theorem 4.3 for the operator L_n. In the following example we demonstrate the effect of the perturbation on Berrut's interpolant at Chebyshev and equispaced nodes.

Example 4.3. We consider the same setting as in Example 4.1 and we interpolate the original function f in (4.6) and the perturbed one with Berrut's interpolant, see Figure 4.8, left. The perturbation in the data produces a difference

$$\|r - \tilde{r}\| \approx 1.9910 \cdot 10^{-2}$$

and the ratio

$$\frac{\|r - \tilde{r}\|}{\varepsilon} \approx 1.0001$$

shows that the perturbation of the interpolant is roughly as big as ε. Comparing this value with the one obtained in (4.7) we see that the polynomial interpolant seems to be more susceptible to the perturbation of the data in this particular example, despite the lower upper bound in Theorem 4.3 for polynomials. Figure 4.7 shows that the upper bound of Theorem 4.8 is indeed far from being tight.

We remark that, despite the favorable behavior of Berrut's interpolant in this particular example, polynomials should be everyone's choice for interpolation at Chebyshev-spaced data, because of the favorable result of Theorem 4.3 and the faster convergence rate warranted by polynomials at these nodes (Trefethen [2013]). Anyway, Theorem 4.8 shows that the growth of Λ_n^0, also in this

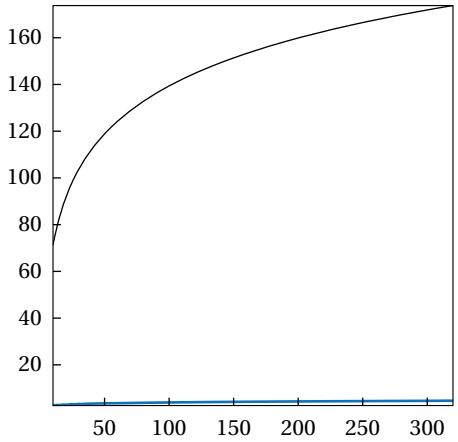

Figure 4.7. The Lebesgue constant for $n = 10, \dots, 320$ of Berrut's interpolant at extended Chebyshev nodes (in blue) with the upper bound in Theorem 4.8 (in black).

case, is far from being exponential and Berrut's interpolant represents still a valid alternative to polynomials.

If we choose equispaced nodes instead, the situation is completely different, see Figure 4.8, right. The perturbation produces a difference

$$\|r - \tilde{r}\| \approx 1.9925 \cdot 10^{-2}$$

in Berrut's interpolant and the ratio

$$\frac{\|r - \tilde{r}\|}{\varepsilon} \approx 1.0009$$

shows that the perturbation of the interpolant is still roughly comparable with ε up to the third digit.

The bound of the Lebesgue constant Λ_n^d for $d \geq 1$ requires in general more efforts, as bounding the barycentric weights w_i for a general family of nodes is far from being a trivial task. For this reason, all results make strong assumptions about the distribution of the nodes. The first result in this setting is the one by Bos et al. [2012] who prove the following result for equispaced nodes.

Theorem 4.9 (Bos et al. [2012])**.** If $1 \leq d \leq \lfloor \frac{n}{2} \rfloor$, then

$$\frac{1}{2^{d+2}} \binom{2d+1}{d} \ln\left(\frac{n}{d} - 1\right) \leq \Lambda^d(E_n) \leq 2^{d-1}(2 + \ln n).$$

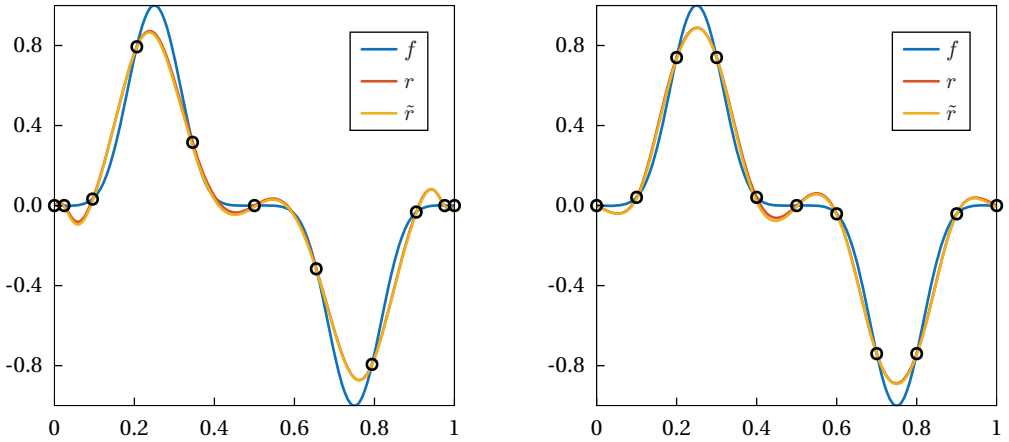

Figure 4.8. Left: effect of the perturbation of the data, with $\varepsilon = 1.9908 \cdot 10^{-2}$ for Berrut's rational interpolant at 11 Chebyshev nodes of the second kind. Right: the effect of the same perturbation at 11 equispaced nodes. Compare Figures 4.2 and 4.3.

The idea behind their proof is to exploit the particular form (2.30) that the weights assume at equispaced nodes and to bound these quantities by 2^d. Figure 4.9, left, shows that the bounds in Theorem 4.9 for $d = 4$ are not sharp. This is probably due to the fact that the barycentric weights play a role in keeping the Lebesgue constant low and that bounding each w_i by 2^d, is not the best strategy to find a tight upper bound for Λ_n^d. We moreover remark that, unlike Berrut's interpolant, for this particular choice of d, the maximum of the Lebesgue function seems to be always attained towards the extremities of the interpolation interval.

Hormann et al. [2012] generalise this result to quasi-equispaced nodes and improve the upper bound provided by Theorem 4.6 for Berrut's interpolant. Furthermore, Ibrahimoglu and Cuyt [2016] remark that (4.10) also holds for $d = 1$, while for $d > 1$,

$$\Lambda_n^d \leq \frac{2^d}{\pi - \frac{4}{n+2}} \left(\ln(n+1) + \ln 2 + \gamma + \frac{1}{24n} \right). \tag{4.11}$$

The strategy used to obtain this last result always resorts to the form (2.30) and, though sharper than the bound provided by Hormann et al. [2012], it is still quite distant from the actual values of Λ_n^d, see Figure 4.10.

Example 4.4. Under the same assumptions as in Example 4.3, we interpolate the original and the perturbed function with the Floater–Hormann interpolant

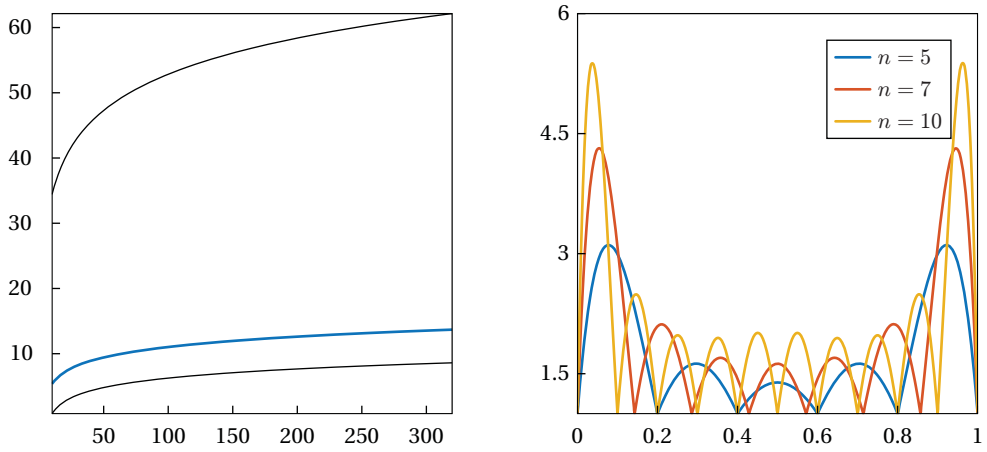

Figure 4.9. Left: the Lebesgue constant of Floater–Hormann interpolant for $d = 4$ and $n = 10, \dots, 320$ at equispaced nodes (in blue) with the upper and lower bounds in Theorem 4.9 (in black). Right: the Lebesgue function at equispaced nodes for $n = 5, 7, 10$.

with $d = 5$. With the Chebyshev nodes of the second kind, the perturbation produces a difference in the original interpolant

$$\|r - \tilde{r}\| \approx 2.0225 \cdot 10^{-2}$$

and the ratio

$$\frac{\|r - \tilde{r}\|}{\varepsilon} \approx 1.0159,$$

see Figure 4.11, left. The same experiment with equispaced nodes produces instead

$$\|r - \tilde{r}\| \approx 2.2731 \cdot 10^{-2}$$

and the ratio

$$\frac{\|r - \tilde{r}\|}{\varepsilon} \approx 1.1418,$$

see Figure 4.11, right.

Comparing the values obtained in this last example with the ones in Example 4.3, it is possible to notice a stronger sensitivity of the Floater–Hormann interpolant to the perturbation of the data. Plotting the Lebesgue constant Λ_n^d for fixed n, it is possible indeed to notice an exponential growth with respect to d, see Figure 4.12. We remark that the case $d = 1$ seems to even have a better Lebesgue constant than the case $d = 0$. Overall we can conclude that, even

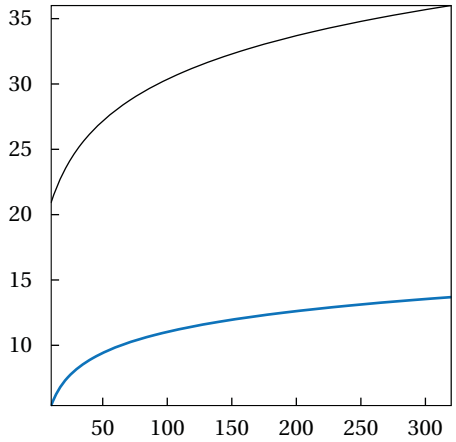

Figure 4.10. The Lebesgue constant of Floater–Hormann interpolant at equispaced nodes (in blue) for $n = 10, \dots, 320$ and $d = 4$ with the upper bound in (4.11) (in black).

though the bound 2^d for the weights does not seem to be tight, the Lebesgue constant increases exponentially with d.

In the next sections we extend this kind of analysis to the Hermite setting for $m = 1$. We first introduce the Hermite interpolation operator and show that the polynomial interpolant is again extremely well conditioned at Chebyshev nodes. After presenting a result regarding the Lebesgue constant at equispaced nodes, we study the Lebesgue constant of the operator associated with the iterative Hermite interpolant introduced in Section 3.3 for equispaced nodes.

4.3 The Hermite interpolation operator

Also the Hermite polynomial can be seen as the result of a projection operator from the space of m times differentiable functions to the space of polynomials of degree at most $(m+1)(n+1)-1$. In this section we focus on the case $m = 1$ and on the interpolant

$$p_1(x) = \sum_{i=0}^{n} \ell_{i,0}(x) f_i + \sum_{i=0}^{n} \ell_{i,1}(x) f_i', \tag{4.12}$$

with $\ell_{i,0}$ and $\ell_{i,1}$ as in (3.10). Most of the previous results are indeed related to this setting, even if some of them can be extended to the interpolation of higher order derivatives.

Let us define the *Hermite interpolation operator*

$$H_n \colon C^1[a,b] \longrightarrow \mathscr{P}_{2n+1},$$

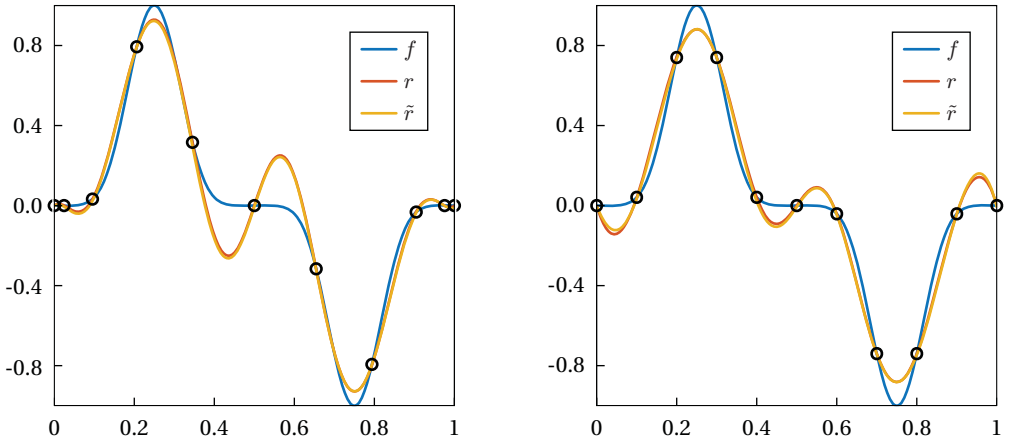

Figure 4.11. Left: effect of the perturbation of the data, with $\varepsilon = 1.9908 \cdot 10^{-2}$, for Floater–Hormann interpolant for $d = 5$ at 11 Chebyshev nodes of the second kind. Right: the effect of the same perturbation at 11 equispaced nodes. Compare with Figures 4.2, 4.3 and 4.8.

that to each function $f \in C^1[a, b]$ associates the corresponding Hermite interpolant r_1 in (4.12), that is

$$H_n f = p_1 \in \mathscr{P}_{2n+1}.$$

As its Lagrange counterpart, H_n is a continuous linear projection on the polynomial space $\mathscr{P}_{2n+1}$ and, extending the concept from Lagrange interpolation, we call

$$\Lambda_n = \sup_{\|f\|_1 \leq 1} \|H_n f\|,$$

the Lebesgue constant of the Hermite interpolant (4.12), where

$$\|f\|_1 = \|f\| + \|f'\|.$$

It is easy to verify that, substituting $\|f\|$ with $\|f\|_1$, the relations (4.2) and (4.4) generalise to the Hermite setting but, unfortunately, in this case it is not possible to express Λ_n in a simple closed form equivalent to the one in Lemma 4.1. Anyway, as Manni [1993] notices,

$$\Omega_{1,n} \leq \Lambda_n \leq \max\{\Omega_{0,n}, \Omega_{1,n}\}, \tag{4.13}$$

where

$$\Omega_{0,n} = \max_{a \leq x \leq b} \Omega_{0,n}(x), \qquad \Omega_{1,n} = \max_{a \leq x \leq b} \Omega_{1,n}(x), \tag{4.14}$$

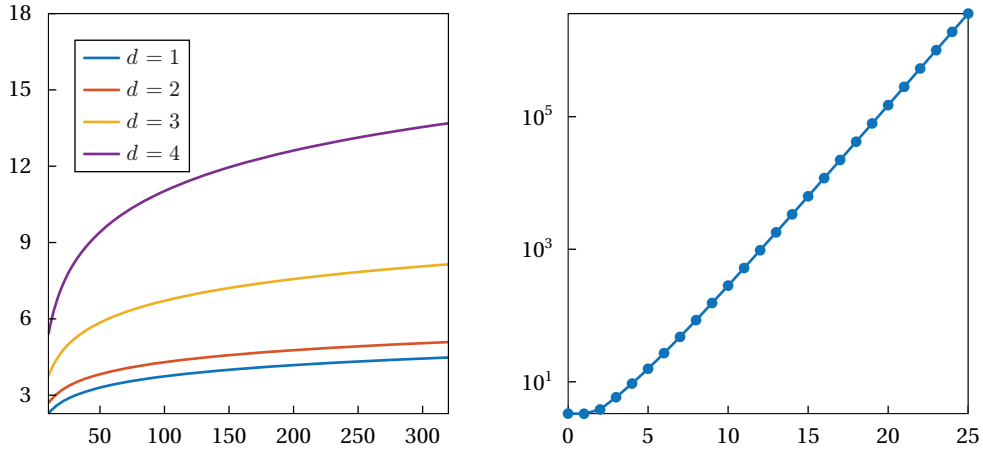

Figure 4.12. Left: the Lebesgue constant Λ_n^d for $n = 10, \ldots, 320$ and $d = 1, \ldots, 4$. Right: semi-log plot of Λ_{50}^d for $d = 0, \ldots, 25$.

and

$$\Omega_{0,n}(x) = \sum_{i=0}^{n} |\ell_{i,0}(x)|, \qquad \Omega_{1,n}(x) = \sum_{i=0}^{n} |\ell_{i,1}(x)|. \tag{4.15}$$

Both $\Omega_{0,n}$ and $\Omega_{1,n}$ play a crucial role in measuring the approximation quality of p_1, as Natanson [1965] mentions

$$\|f - p_1\| \leq \Big((b-a)(1+\Omega_{0,n}) + \Omega_{1,n}\Big)\|f' - \hat{p}\|,$$

where $\hat{p}$ is the polynomial of degree at most $2n$ that best approximates f' on $[a, b]$.

The constants $\Omega_{0,n}$ and $\Omega_{1,n}$ have been extensively studied for many distribution of nodes and, for example, Natanson [1965] recalls that, for ρ-normal sets of nodes,

$$\Omega_{0,n} = 1, \qquad \Omega_{1,n} \leq \frac{b-a}{\rho}, \tag{4.16}$$

which in turn implies convergence of the Hermite interpolation process, by Theorem 3.4. For Chebyshev nodes, the upper bound in (4.16) can be significantly improved.

Theorem 4.10 (Szabados [1993])**.** For the Chebyshev nodes of the first kind there exists a constant C independent of n such that

$$\Omega_{1,n} \leq C\frac{\ln n}{n}.$$

In the same work Szabados proves a more general result regarding any system of nodes.

Theorem 4.11 (Szabados [1993])**.** For an arbitrary system of nodes, there exists a constant C independent of n such that

$$\Omega_{1,n} \geq C\frac{\ln n}{n}.$$

Therefore the Lebesgue constant for polynomial interpolants at ρ-normal sets of nodes is bounded from above and below by two constants, while for Chebyshev nodes of the first kind it satisfies

$$C\frac{\ln n}{n} \leq \Lambda_n \leq 1,$$

see Figures 4.13 and 4.14. This clearly has a favourable effect on the conditioning of the Hermite polynomial interpolant at Chebyshev nodes of the first kind, which is very insensitive to the perturbation of the data.

Example 4.5. For $n = 10$, let us consider the Chebyshev nodes of the first kind, and the function in (4.6). Let

$$\tilde{f}_i = f(x_i) + \varepsilon_i$$
$$\tilde{f}'_i = f'(x_i) + \varepsilon'_i$$

and $\tilde{f}$ be the corresponding 'perturbed' function. Figure 4.15 shows the result of the perturbation corresponding to

$$\varepsilon = \max_{i=0,\dots,n}(|\varepsilon_i| + |\varepsilon'_i|) \approx 2.9670 \cdot 10^{-2}.$$

The original polynomial (in red) and the perturbed one (in yellow) differ by at most

$$\|p_1 - \tilde{p}_1\| \approx 1.9908 \cdot 10^{-2},$$

while the ratio

$$\frac{\|p_1 - \tilde{p}_1\|}{\|f - \tilde{f}\|} \approx 1.0000$$

confirms that the Hermite polynomial interpolant is extremely well conditioned.

However, this favorable behavior does not hold in other interpolation settings, and the equidistant case shows again all the limitations of polynomial interpolation. It can be proved that for equispaced nodes the following asymptotic behaviors for $\Omega_{0,n}$ and $\Omega_{1,n}$ hold.

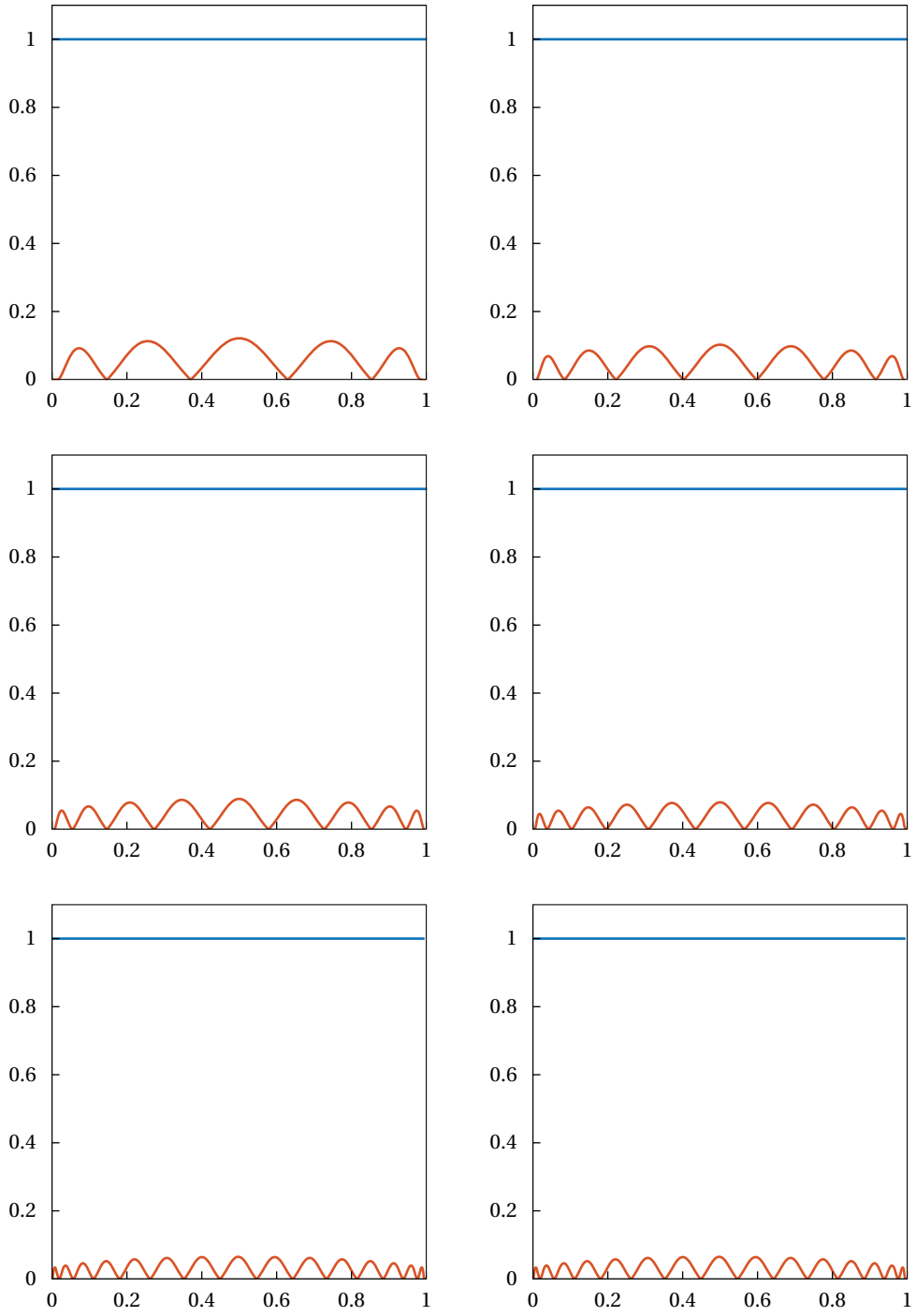

Figure 4.13. From top left to bottom right: $\Omega_{0,n}(x)$ (in blue) and $\Omega_{1,n}(x)$ (in red) for $n = 5, 7, 9, 11, 13, 15$ and Chebyshev nodes of the first kind in $[0, 1]$.

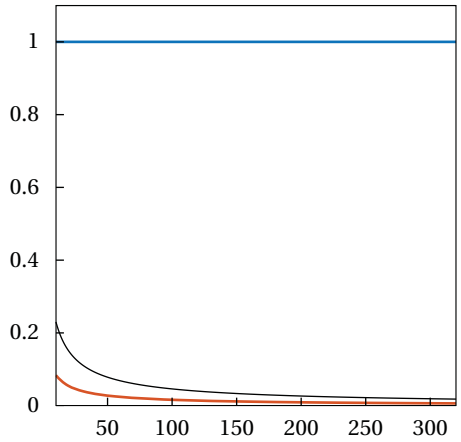

Figure 4.14. $\Omega_{0,n}$ (in blue) and $\Omega_{1,n}$ (in red) for $n = 10, \dots, 320$ at Chebyshev nodes of the first kind with the upper bound for $\Omega_{1,n}$ in Theorem 4.10 (in black).

Theorem 4.12 (Manni [1993])**.** For a set of $n+1$ equispaced nodes

$$\Omega_{0,n} \sim \frac{4}{e^2\pi}\frac{2^{2n+1}}{\gamma_n^2 n^2}, \qquad \Omega_{1,n} \sim \frac{b-a}{e^2\sqrt{\pi}}\frac{2^{2n+1}}{\gamma_n^2 n^2\sqrt{n}},$$

where $\gamma_n = \sum_{j=1}^{n} 1/j$, as $n \to \infty$.

We can therefore expect wild effects on polynomial Hermite interpolant if the original data are perturbed, as the following example confirms.

Example 4.6. For $n = 10$, we sample the function f in (4.6) at equispaced nodes and we perturb the corresponding values f_i and $\tilde{f}_i$ with the same perturbation as in Example 4.5. The interpolants after the perturbation differ by at most

$$\|p_1 - \tilde{p}_1\| \approx 1.4078,$$

while the ratio

$$\frac{\|p_1 - \tilde{p}_1\|}{\|f - \tilde{f}\|} \approx 70.7200$$

shows that the interpolants differ 70 times more than the initial perturbation, see Figure 4.16.

In the Lagrange case, we have seen that Floater–Hormann interpolants have a much better conditioning than polynomial interpolants at equidistant nodes, since the related Lebesgue constants grow only logarithmically with n. In the following section we show that a similar result holds also for the iterative

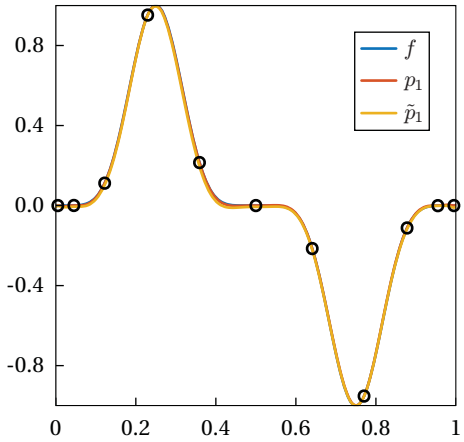

Figure 4.15. Effect of the perturbation of the data, with $\varepsilon = 2.9670 \cdot 10^{-2}$ for the Hermite polynomial interpolant at 11 Chebyshev nodes of the first kind.

interpolants presented in Chapter 3, by proving that their Lebesgue constants are bounded from above by a constant independent of n. Before doing that we shall identify the function space in which we are projecting the function f and the corresponding basis functions. We then proceed by bounding the norm of the associated operator utilising the equivalent of inequality (4.13).

4.4 The barycentric rational Hermite operator

In this section we analyse the generalisation of the operator I_n^d introduced in Section 4.2. In order to better visualize such operator we first need to rewrite the iterative interpolant defined in Chapter 3 for $m = 1$

$$r_1(x) = \sum_{i=0}^{n} b_i(x) f_i + \sum_{i=0}^{n} (x - x_i) b_i(x)^2 (f_i' - r'(x_i)), \tag{4.17}$$

in a way that is linear in the data f_i and f_i', $i = 0, \ldots, n$, so as to identify two sets of basis functions and the function space that they span.

To this end, we recall from Proposition 2.4 that

$$b_i'(x_i) = \sum_{\substack{j=0 \\ j \neq i}}^{n} \frac{w_j}{w_i(x_j - x_i)}, \qquad b_i'(x_j) = \frac{w_i}{w_j(x_j - x_i)}, \qquad j \neq i \tag{4.18}$$

and we rewrite the barycentric rational Hermite interpolant r_1 as

$$r_1(x) = \sum_{i=0}^{n} b_{i,0}(x) f_i + \sum_{i=0}^{n} b_{i,1}(x) f_i'. \tag{4.19}$$

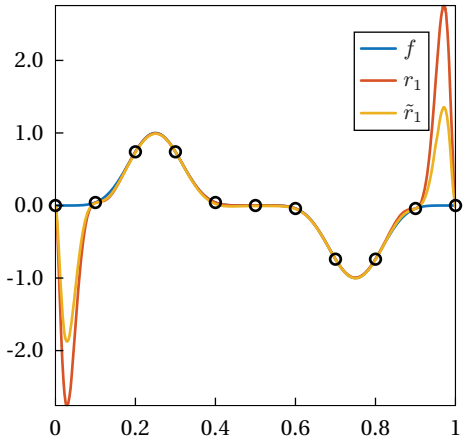

Figure 4.16. Effect of the perturbation of the data, with $\varepsilon = 2.9670 \cdot 10^{-2}$ for the Hermite polynomial interpolant at 11 equispaced nodes.

The functions $b_{i,0}$ and $b_{i,1}$ are defined as in (3.10), but with ℓ_i replaced by b_i, as the following proposition shows.

Proposition 4.1. The barycentric rational Hermite interpolant r_1 in (4.17) can be written as (4.19) with

$$b_{i,0}(x) = \Big(1 - 2(x - x_i)b_i'(x_i)\Big)b_i(x)^2, \qquad b_{i,1}(x) = (x - x_i)b_i(x)^2.$$

Proof. By (4.17),

$$r_1(x) = \sum_{i=0}^{n} b_i(x)f_i + \sum_{i=0}^{n}(x - x_i)b_i(x)^2 f_i' - \sum_{i=0}^{n}(x - x_i)b_i(x)^2 \sum_{j=0}^{n} b_j'(x_i)f_j,$$

hence it remains to show that

$$b_i(x) - \sum_{j=0}^{n}(x - x_j)b_j(x)^2 b_i'(x_j) = b_i(x)^2 - 2(x - x_i)b_i'(x_i)b_i(x)^2. \tag{4.20}$$

Using (2.20b) and (4.18) we have

$$\begin{aligned}
&b_i(x) - \sum_{j=0}^{n}(x - x_j)b_j(x)^2 b_i'(x_j) \\
&= b_i(x)^2 + \sum_{\substack{j=0 \\ j\neq i}}^{n} b_i(x)b_j(x) - (x - x_i)b_i(x)^2 b_i'(x_i) - \sum_{\substack{j=0 \\ j\neq i}}^{n}(x - x_j)b_j(x)^2 \frac{w_i}{w_j(x_j - x_i)} \\
&= b_i(x)^2 - (x - x_i)b_i(x)^2 b_i'(x_i) + \sum_{\substack{j=0 \\ j\neq i}}^{n}\left(b_i(x) - \frac{x - x_j}{x_j - x_i}b_j(x)\frac{w_i}{w_j}\right)b_j(x).
\end{aligned}$$

Now, since

$$b_j(x) = \frac{x - x_i}{x - x_j} b_i(x) \frac{w_j}{w_i}$$

by (2.31), we find that

$$\begin{aligned}\left(b_i(x) - \frac{x - x_j}{x_j - x_i} b_j(x) \frac{w_i}{w_j}\right) b_j(x) &= \left(1 - \frac{x - x_i}{x_j - x_i}\right) b_i(x) b_j(x) \\ &= -(x - x_i) b_i(x)^2 \frac{w_j}{w_i(x_j - x_i)},\end{aligned}$$

and (4.20) then follows by using again (4.18). □

Now we consider the space of rational functions

$$\mathscr{R}^{(1)}_{\boldsymbol{w}_d} = \operatorname{span}\{b_{0,0}, \ldots, b_{n,0}, b_{0,1}, \ldots, b_{n,1}\}$$

and the operator

$$I^d_{1,n} \colon C^1[a,b] \longrightarrow \mathscr{R}^{(1)}_{\boldsymbol{w}_d},$$

that associates the barycentric rational interpolant r_1 at each function $f \in C^1[a,b]$, that is

$$I^d_{1,n} f = r_1 \in \mathscr{R}^{(1)}_{\boldsymbol{w}_d}$$

in (4.19).

Before proceeding with the analysis of the norm of $I^d_{1,n}$, let us see how r_1 reacts to perturbations of data with an example.

Example 4.7. Let us consider the setting in Example 4.6. We interpolate the function f and the perturbed one $\tilde{f}$ with the barycentric rational interpolant r_1 of degree $d = 2$ at equispaced points. The perturbation produces a difference in the interpolants of

$$\|r_1 - \tilde{r}_1\| \approx 1.9908 \cdot 10^{-2}$$

and a ratio

$$\frac{\|r_1 - \tilde{r}_1\|}{\|f - \tilde{f}\|} \approx 1.0000,$$

see Figure 4.17.

The previous example suggests that the Hermite interpolant r_1 is extremely well conditioned with equispaced nodes and, in this section, we show that

$$\Lambda^d_{1,n} = \|I^d_{1,n}\|$$

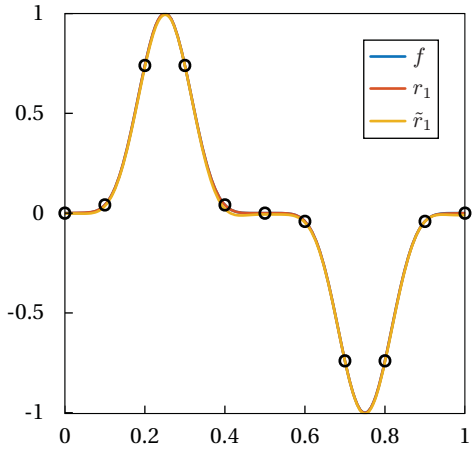

Figure 4.17. Effect of the perturbation of the data, with $\varepsilon = 2.9670 \cdot 10^{-2}$ for Floater–Hormann interpolant for $d = 2$ at 11 equispaced nodes. Compare Figure 4.16.

is bounded from above by a constant independent of n. To this end, we assume $n \geq 2d$, recall (2.30) and write

$$w_i = (-1)^i v_i, \qquad i = 0, \ldots, n,$$

with

$$v_i = \sum_{j=d}^{n} \binom{d}{j-i} \leq 2^d. \tag{4.21}$$

Now we derive an upper bound for the Lebesgue constant by bounding $\Omega_{0,n}$ and $\Omega_{1,n}$ in (4.14) for the basis functions written as in Proposition 4.1. We then resort to (4.13) to bound $\Lambda_{1,n}^d$ from above. In order to keep the notation as simple as possible we restrict ourselves to the interval $[0, 1]$, but the discussion is valid for any arbitrary interval $[a, b] \subset \mathbb{R}$.

Inspired by the proof of Theorem 1 by Bos et al. [2012], we focus on the case where $x_k < x < x_{k+1}$ for some k with $0 \leq k \leq n-1$ and rewrite $\Omega_{0,n}(x)$ and $\Omega_{1,n}(x)$ as

$$\Omega_{0,n}(x) = \frac{N_{0,k}(x)}{D_k(x)}, \qquad \Omega_{1,n}(x) = \frac{N_{1,k}(x)}{D_k(x)},$$

where

$$N_{0,k}(x) = (x - x_k)^2 (x_{k+1} - x)^2 \sum_{i=0}^{n} \left|1 - 2(x - x_i) b_i'(x_i)\right| \frac{v_i^2}{(x - x_i)^2}, \tag{4.22}$$

$$N_{1,k}(x) = (x - x_k)^2 (x_{k+1} - x)^2 \sum_{i=0}^{n} \frac{v_i^2}{|x - x_i|}, \tag{4.23}$$

and

$$D_k(x) = (x - x_k)^2 (x_{k+1} - x)^2 \left(\sum_{i=0}^{n} \frac{w_i}{x - x_i} \right)^2 .$$

As proved by Bos et al. [2012], the denominator satisfies

$$D_k(x) \geq \frac{1}{n^2}, \tag{4.24}$$

and it remains to establish appropriate upper bounds for the numerators $N_{0,k}(x)$ and $N_{1,k}(x)$.

Lemma 4.2. Let $x_k < x < x_{k+1}$ for some k with $0 \leq k \leq n-1$. Then,

$$N_{1,k}(x) \leq C \frac{4^d}{n^2},$$

for some constant C that does not depend on k, d, and n.

Proof. Since

$$\sum_{i=0}^{n} \frac{v_i^2}{|x - x_i|} = \sum_{i=0}^{k} \frac{v_i^2}{x - x_i} + \sum_{i=k+1}^{n} \frac{v_i^2}{x_i - x} \leq \sum_{i=0}^{k} \frac{v_i^2}{x - x_k} + \sum_{i=k+1}^{n} \frac{v_i^2}{x_{k+1} - x}.$$

and

$$(x - x_k)(x_{k+1} - x)^2 \leq \frac{4}{27n^3}, \qquad (x - x_k)^2 (x_{k+1} - x) \leq \frac{4}{27n^3}, \tag{4.25}$$

we have

$$N_{1,k}(x) \leq \frac{4}{27n^3} \sum_{i=0}^{n} v_i^2,$$

and the statement then follows from (4.21). □

Lemma 4.3. Let $x_k < x < x_{k+1}$ for some k with $0 \leq k \leq n-1$. Then,

$$N_{0,k}(x) \leq C \frac{4^d (d+1)}{n^2},$$

for some constant C that does not depend on k, d, and n.

Proof. Using (4.18) and (4.21), we first notice that

$$\sum_{i=0}^{n} |1 - 2(x - x_i) b_i'(x_i)| \frac{v_i^2}{(x - x_i)^2} \leq 4^d \sum_{i=0}^{n} \frac{1}{(x - x_i)^2} + 2^{d+1} \sum_{i=0}^{n} \frac{1}{|x - x_i|} \left| \sum_{\substack{j=0 \\ j \neq i}}^{n} \frac{(-1)^j v_j}{x_j - x_i} \right|,$$

and we proceed to bound the two sums over i separately. For $x_k < x < x_{k+1}$, we have

$$\begin{aligned}
\sum_{i=0}^{n} \frac{1}{(x-x_i)^2} &= \sum_{i=0}^{k-1} \frac{1}{(x-x_i)^2} + \frac{1}{(x-x_k)^2} + \frac{1}{(x_{k+1}-x)^2} + \sum_{i=k+2}^{n} \frac{1}{(x_i-x)^2} \\
&\leq \sum_{i=0}^{k-1} \frac{1}{(x_k-x_i)^2} + \frac{(x_{k+1}-x_k)^2}{(x-x_k)^2(x_{k+1}-x)^2} + \sum_{i=k+2}^{n} \frac{1}{(x_i-x_{k+1})^2} \\
&= \sum_{i=0}^{k-1} \frac{n^2}{(k-i)^2} + \frac{1}{n^2} \frac{1}{(x-x_k)^2(x_{k+1}-x)^2} + \sum_{i=k+2}^{n} \frac{n^2}{(i-k-1)^2} \\
&= n^2 \sum_{i=1}^{k} \frac{1}{i^2} + \frac{1}{n^2} \frac{1}{(x-x_k)^2(x_{k+1}-x)^2} + n^2 \sum_{i=1}^{n-k-1} \frac{1}{i^2} \\
&\leq n^2 \frac{\pi^2}{6} + \frac{1}{n^2} \frac{1}{(x-x_k)^2(x_{k+1}-x)^2} + n^2 \frac{\pi^2}{6},
\end{aligned}$$

and since

$$(x-x_k)^2(x_{k+1}-x)^2 \leq \frac{1}{16n^4}, \tag{4.26}$$

we conclude that

$$(x-x_k)^2(x_{k+1}-x)^2 \sum_{i=0}^{n} \frac{1}{(x-x_i)^2} \leq \frac{C}{n^2}.$$

To bound the second sum, we first use (4.21) to get

$$\begin{aligned}
\left| \sum_{\substack{j=0 \\ j\neq i}}^{n} \frac{(-1)^j v_j}{j-i} \right| &= \left| \sum_{\substack{j=0 \\ j\neq i}}^{n} \frac{(-1)^j}{j-i} \sum_{l=d}^{n} \binom{d}{l-j} \right| \\
&= \left| \sum_{l=0}^{d} \binom{d}{l} \sum_{\substack{j=d-l \\ j\neq i}}^{n-l} \frac{(-1)^j}{j-i} \right| \\
&\leq 2^d \max_{0\leq l\leq d} \left| \sum_{\substack{j=d-l \\ j\neq i}}^{n-l} \frac{(-1)^j}{j-i} \right|,
\end{aligned}$$

and since

$$\left|\sum_{\substack{j=d-l\\ j\neq i}}^{n-l}\frac{(-1)^j}{j-i}\right| = \begin{cases} \left|\displaystyle\sum_{j=d-l}^{n-l}\frac{(-1)^j}{j-i}\right|, & 0\le i<d-l,\\ \left|\displaystyle\sum_{j=1}^{i-(d-l)}\frac{(-1)^j}{j}-\sum_{j=1}^{(n-l)-i}\frac{(-1)^j}{j}\right|, & d-l\le i\le n-l,\\ \left|\displaystyle\sum_{j=d-l}^{n-l}\frac{(-1)^j}{i-j}\right|, & n-l<i\le n, \end{cases}$$

with

$$\left|\sum_{j=d-l}^{n-l}\frac{(-1)^j}{j-i}\right| \le \frac{1}{(d-l)-i}, \qquad 0\le i<d-l,$$

$$\left|\sum_{j=1}^{i-(d-l)}\frac{(-1)^j}{j}-\sum_{j=1}^{(n-l)-i}\frac{(-1)^j}{j}\right| \le \begin{cases} \dfrac{1}{i-(d-l)+1}, & d-l\le i\le \dfrac{n+d}{2}-l,\\ \dfrac{1}{(n-l)-i+1}, & \dfrac{n+d}{2}-l\le i\le n-l, \end{cases}$$

$$\left|\sum_{j=d-l}^{n-l}\frac{(-1)^j}{i-j}\right| \le \frac{1}{i-(n-l)}, \qquad n-l<i\le n,$$

we further have

$$c_i=\left|\sum_{\substack{j=0\\ j\neq i}}^{n}\frac{(-1)^j v_j}{j-i}\right| \le 2^d \begin{cases} 1, & 0\le i\le d,\\ \dfrac{1}{i-d+1}, & d\le i\le \dfrac{n}{2},\\ \dfrac{1}{(n-d)-i+1}, & \dfrac{n}{2}\le i\le n-d,\\ 1, & n-d\le i\le n. \end{cases}$$

Let us now assume that $d\le k<n/2-1$ and $x_k<x<x_{k+1}$. Then,

$$\sum_{i=0}^{k-1}\frac{c_i}{k-i}\le 2^d\left(\sum_{i=0}^{d-1}\frac{1}{k-i}+\sum_{i=d}^{k-1}\frac{1}{(k-i)(i-d+1)}\right)\le 2^d(d+1),$$

and

$$\frac{c_k}{x-x_k}\le\frac{2^d}{x-x_k}, \qquad \frac{c_{k+1}}{x_{k+1}-x}\le\frac{2^d}{x_{k+1}-x},$$

and

$$\begin{aligned}\sum_{i=k+2}^{n}\frac{c_i}{i-k-1} &\le 2^d\Bigg(\sum_{i=k+2}^{\lfloor n/2\rfloor}\frac{1}{i-k-1}\left(\frac{1}{i-d+1}-\frac{1}{n-d-i+1}\right)\\ &\qquad+\sum_{i=k+2}^{n-d}\frac{1}{(i-k-1)(n-d-i+1)}\\ &\qquad+\sum_{i=n-d+1}^{n}\frac{1}{i-k-1}\Bigg)\\ &\le 2^d\Bigg(\sum_{i=k+2}^{\lfloor n/2\rfloor}\frac{1}{(i-k-1)(i-d+1)}\\ &\quad+\sum_{i=1}^{n-d-k-1}\frac{1}{i(n-d-k-i)}+\sum_{i=n-d}^{n-1}\frac{1}{i-k}\Bigg)\\ &\le 2^d\left(\frac{\pi^2}{6}+1+d\right).\end{aligned}$$

Therefore,

$$\begin{aligned}\sum_{i=0}^{n}\frac{1}{|x-x_i|}\left|\sum_{\substack{j=0\\ j\neq i}}^{n}\frac{(-1)^j v_j}{x_j-x_i}\right| &\le n^2\sum_{i=0}^{k-1}\frac{c_i}{k-i}+n\frac{c_k}{x-x_k}\\ &\qquad+n\frac{c_{k+1}}{x_{k+1}-x}+n^2\sum_{i=k+2}^{n}\frac{c_i}{i-k-1}\\ &\le 2^d\Bigg(n^2(d+1)+\frac{n}{x-x_k}\\ &\qquad+\frac{n}{x_{k+1}-x}+n^2\left(\frac{\pi^2}{6}+1+d\right)\Bigg).\end{aligned}$$

Using (4.25) and (4.26), we finally obtain

$$(x-x_k)^2(x_{k+1}-x)^2\sum_{i=0}^{n}\frac{1}{|x-x_i|}\left|\sum_{\substack{j=0\\ j\neq i}}^{n}\frac{(-1)^j v_j}{x_j-x_i}\right|\le\frac{2^d(d+1)}{n^2}C.$$

The other cases $k<d$ and $k\ge n/2-1$ can be treated similarly. □

We are now ready to state our main result.

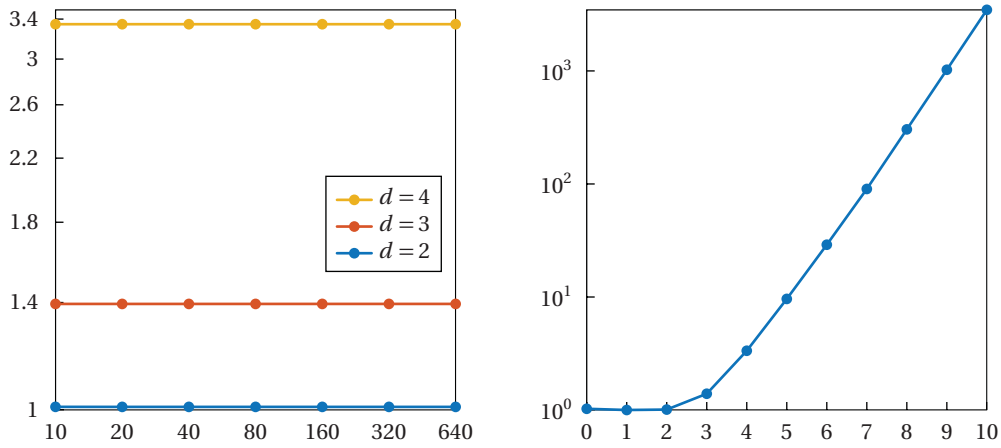

Figure 4.18. Left: log-log plot of $\Omega_{0,n}$ over n for different values of d. Right: semi-log plot of $\Omega_{0,n}$ over d for $n = 20$.

Theorem 4.13. The Lebesgue constant associated with Floater–Hormann Hermite interpolation with $m = 1$ at equidistant nodes satisfies

$$\Lambda_n \leq 4^d(d+1)C,$$

for some constant C that does not depend on d and n.

Proof. If $x = x_k$ for $k = 0, \ldots, n$, then

$$b_{i,0}(x) = \Big(1 - 2(x_k - x_i)b_i'(x_i)\Big)b_i(x_k)^2 = \delta_{i,k}, \qquad b_{i,1}(x) = (x_k - x_i)b_i(x_k)^2 = 0$$

and consequently $\Omega_{0,n}(x) = 1$ and $\Omega_{1,n}(x) = 0$. Otherwise, it follows from (4.24), Lemma 4.2, and Lemma 4.3, that there exists some constant C that does not depend on n and d, such that

$$\Omega_{0,n}(x) \leq 4^d(d+1)C, \qquad \Omega_{1,n}(x) \leq 4^d C.$$

The statement then follows from (4.13). □

4.5 Numerical results

We performed several experiments to confirm numerically that the upper bounds derived above are correct. Figure 4.19 shows $\Omega_{0,n}(x)$ and $\Omega_{1,n}(x)$ for Floater–Hormann Hermite interpolation at equidistant nodes in the interval $[0, 1]$ for several values of d and n. Note that $\Omega_{0,n}(x)$ dominates $\Omega_{1,n}(x)$ in all examples,

a behavior that we consistently observed in our experiments. Also note that the maxima $\Omega_{0,n}$ and $\Omega_{1,n}$ of both functions are obtained inside the first and the last sub-interval, except for $d = 0$, and that $\Omega_{0,n}$ is basically independent of n in all examples. This is confirmed by the plot in Figure 4.18 (left), which additionally shows that $\Omega_{0,n}$, although independent of n, seems to grow exponentially with d, as suggested by the upper bound in Lemma 4.3. This trend can also be observed in Figure 4.18 (right), where the same quantity is plotted for a fixed value of n and d between 0 and $n/2$.

A completely different result can be observed for non-equidistant nodes. For example, in the case of Chebyshev nodes, $\Omega_{0,n}$ grows quickly as n increases, except for $d = 0$, as shown in Figure 4.20. We therefore recommend to use Floater–Hormann Hermite interpolation for equidistant nodes, but to stick to polynomial Hermite interpolants for Chebyshev nodes. It remains future work to investigate other choices of interpolation nodes.

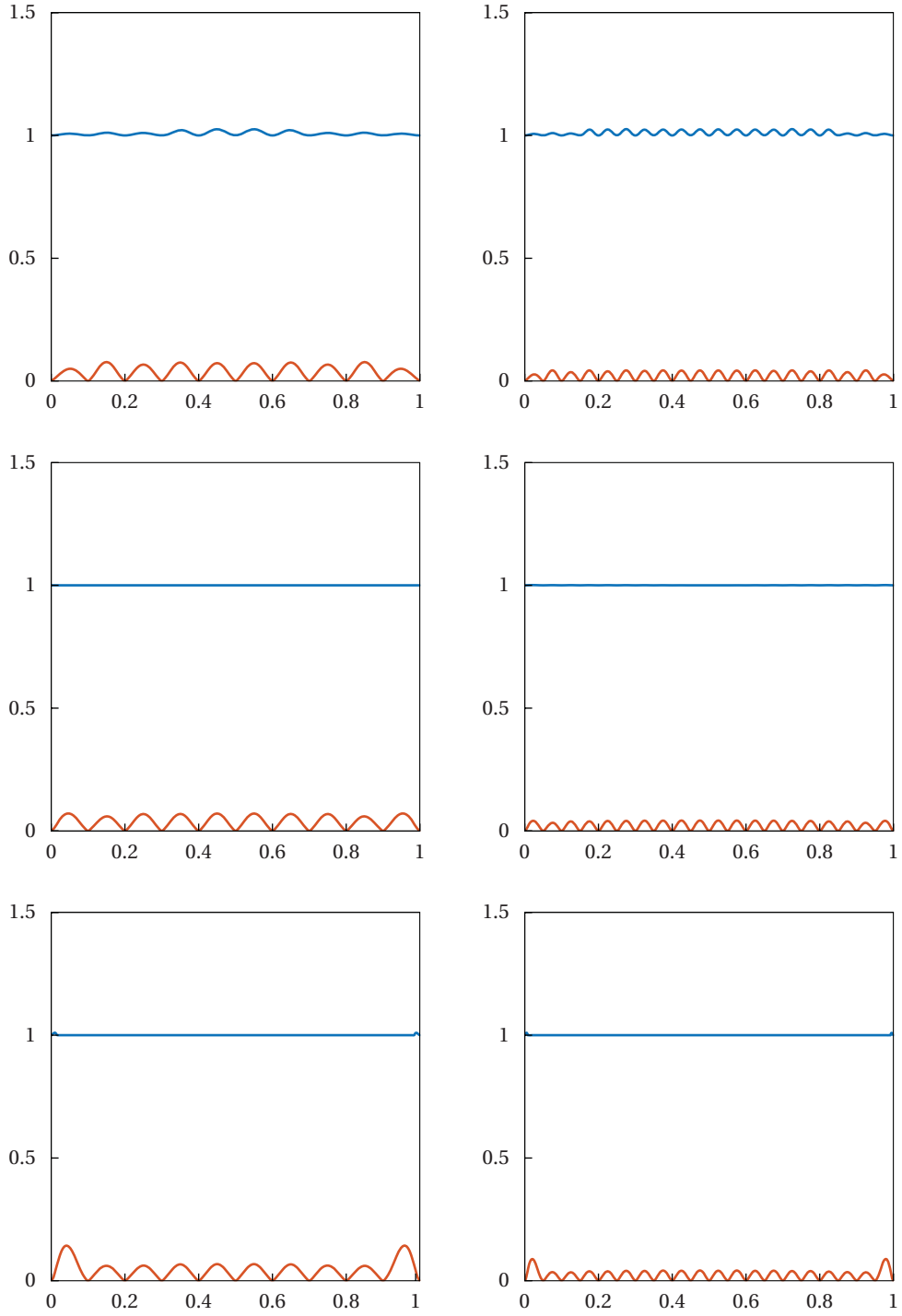

Figure 4.19. $\Omega_{0,n}(x)$ (in blue) and $\Omega_{1,n}(x)$ (in red) for $d = 0, 1, 2$ (from top to bottom) and $n = 10, 20$ (from left to right) and equidistant nodes in the interval $[0, 1]$.

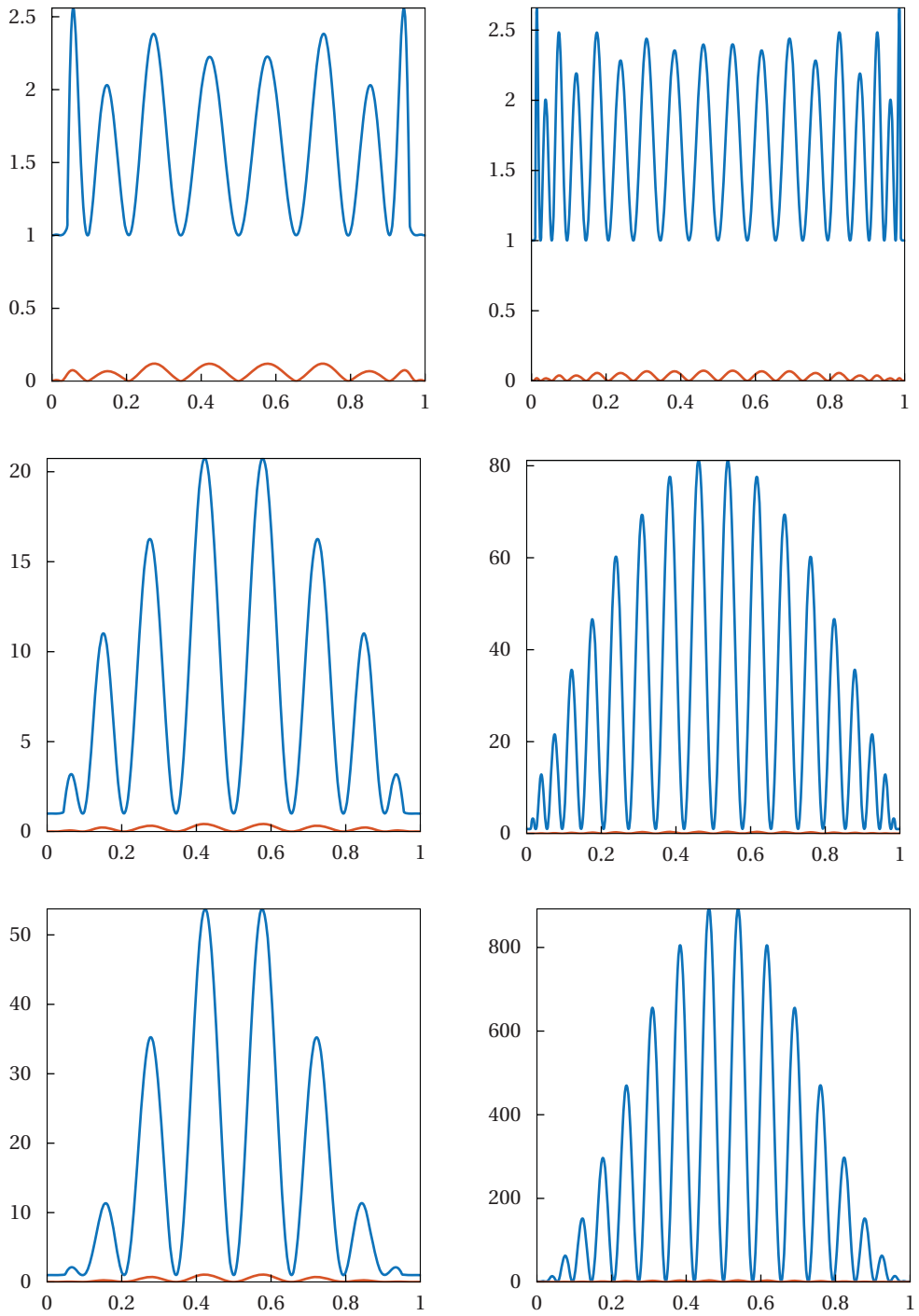

Figure 4.20. $\Omega_{0,n}(x)$ (in blue) and $\Omega_{1,n}(x)$ (in red) for $d = 0, 1, 2$ (from top to bottom) and $n = 10, 20$ (from left to right) and Chebyshev nodes of the second kind in the interval $[0, 1]$.

Conclusion and future work

Barycentric rational interpolants are nowadays recognised as a valid alternative to more classical interpolation methods thanks to their flexibility, robustness and favorable convergence rate. The use of Floater–Hormann weights (2.26) results in an extremely versatile tool for interpolation of univariate data, especially in the equispaced setting, where the Runge phenomenon and the unfavorable growth of the Lebesgue constant make polynomial interpolants basically useless. The convergence rate of the Floater–Hormann interpolants and the slow growth of the corresponding Lebesgue constants make these tools a state-of-the-art method for interpolation at equispaced nodes. The main goal of this dissertation was to investigate the use of the Floater–Hormann family in the context of approximation and interpolation of derivatives of a function, and to show that, also in this setting, these interpolants provide a good alternative to more classical interpolation methods.

In the context of the approximation of derivatives of a function at well-spaced nodes, we have shown that the k-th derivative of the error produced by Floater–Hormann interpolants converges as $O(h^{d+1-k})$, and that the error can be localised, meaning that $e(x)$ is strongly influenced by the subinterval in which x is located. This is a property that can be extremely useful when more accuracy is required in some parts of the interpolation interval, as it is sufficient to get more samples of the function in that region. Although this is an expected result, to the best of our knowledge, no other interpolation method enjoys such a theoretical bound. We proved this result for the so-called well-spaced nodes, a class of interpolation points that, despite being quite general, does not include all possible systems. Our extensive numerical tests suggest that $\|e^{(k)}\|$ converges to zero as $O(h^{d+1-k})$ for any set of nodes, but the localisation of the error is a special property related to well-spaced nodes. Bounding this quantity for general sets of nodes, so as to generalise Theorems 2.9 and 2.10 by Berrut et al. [2011], should still be considered as a potential future work.

As for the interpolation of the derivatives of a function we have presented

a new iterative method that allows us to obtain a Hermite interpolant starting from any Lagrange interpolant with sufficiently continuous basis functions. The divergence problems experienced by polynomials, also in this setting, make again barycentric rational interpolants a valid alternative for interpolation at equispaced points. When applied to the Floater–Hormann basis functions (2.31), our method results in a smooth barycentric rational Hermite interpolant with numerator and denominator of degree at most $(m+1)(n+1)-1$ and $(m+1)(n-d)$, respectively, with a convergence rate of $O(h^{(m+1)(d+1)})$. This iterative interpolant compares favorably with the ones proposed by Schneider and Werner [1991], Floater and Schulz [2009] and Jing et al. [2015] and represents one of the most valuable tools for Hermite interpolation at equispaced nodes. In this setting, it would be interesting to investigate the behavior of the derivatives of the iterative interpolant in the same way as Theorem 3.6, so as to understand how well the k-th derivative of f is approximated by $r_m^{(k)}$, $k = 0, \dots, m$.

In the last part of this thesis we analysed the behavior of the Lebesgue constant of the iterative rational Hermite interpolant for $m = 1$, at equispaced nodes. The comparison between Theorem 4.12 and Theorem 4.13 shows again that this interpolant should be strongly considered as one of the state-of-the-art interpolants in this setting. The extension of this result to the Hermite interpolants of higher order and different sets of interpolation nodes is still an important open question that we should consider in the future.

Finally, it would be extremely important to extend the Floater–Hormann construction to the interpolation of multivariate functions $f\colon \mathbb{R}^p \to \mathbb{R}^q$, with $p > 1$ and $q \geq 1$. A similar construction as the one proposed by Floater and Hormann have been proposed for bivariate functions by Little [1983], using linear polynomials interpolating f at the vertices of a triangle. Such a construction is guaranteed to converge quadratically for very general triangulations (Dell'Accio et al. [2016]), a similar behavior experienced by the univariate Floater–Hormann interpolants for $d = 1$. The extension of this approach to polynomials of higher degree is a challenging but yet intriguing task.

Bibliography

Atkinson, K. E. [1989]. *An Introduction to Numerical Analysis*, Wiley, New York.

Baltensperger, R., Berrut, J.-P. and Noël, B. [1999]. Exponential convergence of a linear rational interpolant between transformed Chebyshev points, *Math. Comput.* **68**(227): 1109–1120.

Bernstein, S. N. [1931]. Sur la limitation des valeurs d'un polynôme $p_n(x)$ de degré n sur tout un segment par ses valeurs en $(n+1)$ points du segment, *Bull. Acad. Sci. URSS* (1): 1025–1050.

Berrut, J.-P. [1988]. Rational functions for guaranteed and experimentally well-conditioned global interpolation, *Comput. Math. Appl.* **15**(1): 1–16.

Berrut, J.-P., Baltensperger, R. and Mittelmann, H. D. [2005]. Recent developments in barycentric rational interpolation, *in* D. H. Mache, J. Szabados and M. G. de Bruin (eds), *Trends and Applications in Constructive Approximation*, Birkhäuser, Basel, pp. 27–51.

Berrut, J.-P., Floater, M. S. and Klein, G. [2011]. Convergence rates of derivatives of a family of barycentric rational interpolants, *Appl. Numer. Math.* **61**(9): 989–1000.

Berrut, J.-P. and Mittelmann, H. D. [1997]. Lebesgue constant minimizing linear rational interpolation of continuous functions over the interval, *Comput. Math. Appl.* **33**(6): 77–86.

Berrut, J.-P. and Trefethen, L. N. [2004]. Barycentric Lagrange interpolation, *SIAM Rev.* **46**(3): 501–517.

Bos, L., De Marchi, S. and Hormann, K. [2011]. On the Lebesgue constant of Berrut's rational interpolant at equidistant nodes, *J. Comput. Appl. Math.* **236**(4): 504–510.

Bos, L., De Marchi, S., Hormann, K. and Klein, G. [2012]. On the Lebesgue constant of barycentric rational interpolation at equidistant nodes, *Numer. Math.* **121**(3): 461–471.

Bos, L., De Marchi, S., Hormann, K. and Sidon, J. [2013]. Bounding the Lebesgue constant for Berrut's rational interpolant at general nodes, *J. Approx. Theory* **169**: 7–22.

Brutman, L. [1978]. On the Lebesgue function for polynomial interpolation, *SIAM J. Numer. Anal.* **15**: 694–704.

Brutman, L. [1984]. A note on polynomial interpolation at the Chebyschev extrema nodes, *J. Approx. Theory* **42**: 283–292.

Brutman, L. [1997]. Lebesgue functions for polynomial interpolation—a survey, *Ann. Numer. Math.* **4**: 111–127.

Bulirsch, R. and Rutishauser, H. [1968]. Interpolation und genäherte Quadratur, *in* R. Sauer and I. Szabó (eds), *Mathematische Hilfsmittel des Ingenieurs*, Springer Berlin Heidelberg, pp. 232–319.

Cheney, E. W. and Light, W. [2000]. *A course in approximation theory*, Vol. 114, Brooks/Cole publishing company.

Claessens, G. [1978]. On the Newton-Padé approximation problem, *J. Approx. Theory* **22**: 150–160.

Davis, P. J. [1975]. *Interpolation and approximation*, Dover publications, inc., New York.

Dell'Accio, F., Tommaso, F. D. and Hormann, K. [2016]. On the approximation order of triangular Shepard interpolation, *IMA J. Numer. Anal.* **36**: 359–379.

Deng, C., Zhang, S., Li, Y., Jin, W. and Zhao, Y. [2016]. A tighter upper bound on the Lebesgue constant of Berrut's rational interpolant at equidistant nodes, *Appl. Math. Lett.* **59**: 71–78.

Dyn, N., Levin, D. and Gregory, J. A. [1987]. A 4-point interpolatory subdivision scheme for curve design, *Comput. Aided Geom. Des.* **4**(4): 257–268.

Erdős, P. [1961]. Problems and results on the theory of interpolation. II, *Acta Math. Acad. Sci. Hung.* **12**: 235–244.

Faber, G. [1914]. Über die interpolatorische darstellung stetiger funktionen, *Jahresber. der Deutschen Math. Ver.* **23**: 190–210.

Floater, M. S. and Hormann, K. [2007]. Barycentric rational interpolation with no poles and high rates of approximation, *Numer. Math.* **107**(2): 315–331.

Floater, M. S. and Schulz, C. [2009]. *Rational Hermite interpolation without poles*, chapter 9, pp. 117–139.

Fousse, L., Hanrot, G., Lefèvre, V., Pélissier, P. and Zimmermann, P. [2007]. MPFR: A multiple-precision binary floating-point library with correct rounding, *ACM Trans. Math. Softw.* **33**(2): Article 13, 15 pages.

Gautschi, W. [1997]. *Numerical Analysis An Introduction*, Birkhäuser.

Grünwald, G. [1942]. On the theory of interpolation, *Acta Math.* **75**: 219–245.

Henrici, P. [1982]. *Essentials of Numerical Analysis with Pocket Calculator Demonstrations*, John Wiley & Sons Inc., New York.

Higham, N. J. [2004]. The numerical stability of barycentric Lagrange interpolation, *IMA J. Numer. Anal.* **24**(4): 547–556.

Hoppe, R. [1845]. *Theorie der independenten Darstellung der höhern Differentialquotienten*, Johann Ambrosius Barth.

Hormann, K. [2014]. Barycentric interpolation, *Approximation Theory XIV: San Antonio 2013*, Vol. 83 of *Springer Proceedings in Mathematics & Statistics*, Springer, New York, pp. 197–218.

Hormann, K., Klein, G. and De Marchi, S. [2012]. Barycentric rational interpolation at quasi-equidistant nodes, *Dolomites Res. Notes Approx.* **5**: 1–6.

Hormann, K. and Schaefer, S. [2016]. Pyramid algorithms for barycentric rational interpolation, *Comput. Aided Geom. Des.* **42**: 1–6.

Ibrahimoglu, B. A. and Cuyt, A. [2016]. Sharp bounds for Lebesgue constants of barycentric rational interpolation, *Exp. Math.* **25**: 347–354.

Isaacson, E. and Keller, H. B. [1966]. *Analysis of Numerical Methods*, Wiley, New York - London - Sidney.

Jing, K., Kang, N. and Zhu, G. [2015]. Convergence rates of a family of barycentric osculatory rational interpolation, *Appl. Math. Comput.* pp. 1–13.

Johnson, W. P. [2002]. The curious history of Faà di Bruno's formula, *Am. Math. Mon.* **109**(3): 217–234.

Klein, G. [2012]. *Applications of Linear Barycentric Rational Interpolation*, PhD thesis, University of Fribourg.

Klein, G. and Berrut, J.-P. [2012]. Linear rational finite differences from derivatives of barycentric rational interpolants, *SIAM J. Numer. Anal.* **50**(2): 643–656.

Little, F. F. [1983]. Convex combination surfaces, *in* R. E. Barnhill and W. Boehm (eds), *Surfaces in Computer Aided Geometric Design*, North-Holland, pp. 99–107.

Manni, C. [1993]. Lebesgue constants for Hermite and Fejér interpolation on equidistant nodes, *Calcolo* **30**(3): 203–218.

Mascarenhas, W. F. and de Camargo, A. P. [2014]. On the backward stability of the second barycentric formula for interpolation, *Dolomites Res. Notes Approx.* **7**: 1–12.

Natanson, I. P. [1965]. *Constructive Function Theory*, Vol. III of *III, Constructive Function Theory, Interpolation and Approximation Quadratures*, Frederick Ungar, New York.

Platte, R. B., Trefethen, L. N. and Kuijlaars, A. B. J. [2011]. Impossibility of fast stable approximation of analytic functions from equispaced samples, *SIAM Rev.* **53**(2): 308–318.

Rivlin, T. J. [1974]. *The Lebesgue constant for polynomial interpolation*, Springer Verlag Berlin Heidelberg New York, pp. 422–437.

Rivlin, T. J. [1981]. *An Introduction to the Approximation of Functions*, Dover Publications.

Runge, C. [1901]. Über empirische funktionen und die interpolation zwischen äquidistanten ordinaten, *Z. Math. Phys.* **46**: 224–243.

Rutishauser, H. [1990]. *Lectures on Numerical Mathematics*, Vol. 1, Birkhäuser Boston.

Salzer, H. E. [1972]. Lagrangian interpolation at the Chebyshev points $x_{n,\nu} = \cos(\nu\pi/n), \nu = 0(1)n$; some unnoted advantages, *Comput. J.* **15**: 156–159.

Schneider, C. and Werner, W. [1986]. Some new aspects of rational interpolation, *Math. Comput.* **47**(175): 285–299.

Schneider, C. and Werner, W. [1991]. Hermite interpolation: The barycentric approach, *Comput. J.* **46**: 35–51.

Schönhage, A. [1961]. Fehlerfortpflanzung bei interpolation, *Numer. Math.* **3**: 62–71.

Shi, Y. G. [2000]. On Hermite interpolation, *J. Approx. Theory* **105**: 49–86.

Stoer, J. and Bulirsch, R. [1993]. *Introduction to Numerical Analysis*, Vol. 12, Springer.

Szabados, J. [1993]. On the order of magnitude of fundamental polynomials of Hermite interpolation, *Acta Math. Hung.* **61**: 357–368.

Tietze, H. F. F. [1917]. Eine Bemerkung zur Interpolation, *Z. Angew. Math. Phys.* **64**: 74–90.

Trefethen, L. N. [2011]. Six myths of polynomial interpolation and quadrature, *Math. Today* .

Trefethen, L. N. [2013]. *Approximation Theory and Approximation Practice*, SIAM.

Trefethen, L. N. and Weideman, J. A. C. [1991]. Two results on polynomial interpolation in equally spaced points, *J. Approx. Theory* **65**: 247–260.

Zhang, R.-J. [2014]. An improved upper bound on the Lebesgue constant of Berrut's rational interpolation operator, *J. Comput. Appl. Math.* **255**: 652–660.

Zhang, R.-J. [2017]. Optimal asymptotic Lebesgue constant of Berrut's rational interpolation operator for equidistant nodes, *Appl. Math. Comput.* **294**: 139–145.

Zhao, Q., Hao, Y., Yin, Z. and Zhang, Y. [2010]. Best barycentric rational hermite interpolation, *Proceedings of the 2010 International Conference on Intelligent System Design and Engineering Application*, IEEE, pp. 417–419.